4

Part One: Environmental Chemical Impact of Recycled Plastic Timbers Used as Construction Material in Tiffany Street Pier, South Bronx, New York

Part Two: Chiral Separation of Dansyl-DL-Amino Acids by Counterflow Capillary Electrophoresis

by

Yili K. Xie

A dissertation submitted to the Graduate Faculty in Chemistry in partial fulfillment of the requirements for the degree of Doctor of Philosophy, The City University of New York

1998

This manuscript has been read and accepted for the Graduate Faculty in Chemistry in satisfaction of the dissertation requirement for the degree of Doctor of Philosophy.

4 September 97
Date

David C. Lorde
Chair of Examining Committee

October 21, 1997
Date

Richard Pike
Executive Officer

Ronald H Baker

Arthur D Baker
Supervisory Committee

THE CITY UNIVERSITY OF NEW YORK

Abstract

Part One: Environmental Chemical Impact of Recycled Plastic Timbers Used as Construction Material in Tiffany Street Pier, South Bronx, New York

Part Two: Chiral Separation of Dansyl-DL-Amino Acids by Counterflow Capillary Electrophoresis

by

Yili K. Xie

Advisor: Professor David C. Locke

In 1994-95 the New York City Department of General Services designed and managed construction of a 11,390 ft^2 pier to replace a decaying wooden recreational pier in the East River at the foot of Tiffany Street, the South Bronx. The new pier was constructed almost entirely of post-consumer recycled plastic (PCRP), which is immune to damage by marine boring organisms. In order to assess the environmental impact of the pier on water quality in the East River, we carried out a leaching study using simulated East River water to leach organic and inorganic species from the plastic used in the construction, and compared with similar leaching of CCA wood. The organic and metallic compounds in the leachates were characterized quantitatively. In addition, the odor from the

constructing recycled plastic was trapped using a headspace device and analyzed qualitatively. From the data collected, we concluded that the recycled plastic will not add appreciably to the pollutant load of the East River.

The chiral separation of twelve pairs of chiral dansyl-DL-amino acids were carried out by using quaternary ammonium β-cyclodextrin (Q-CD) as chiral selector with a coated capillary, which enabled a true counterflow between Q-CD and the enantiomers. Baseline separations of all the enantiomers were obtained with 0.2 - 1 mM Q-CD in the buffer solutions. The fundamentals of chiral separation were studied based on our experimental data. The effects of the concentration of Q-CD, buffer pH, applied voltage and temperature on the chiral selectivities were evaluated. In addition to the conventional capillary electrophoresis, a new partial-filling method was developed. A major advantage of this method is that it could eliminate the possible detection interference from chiral selectors.

Acknowledgments

More than four years of graduate study has come to the end. There are several people to whom I would like to give my sincere gratitude.

First, I must thank my mentor Dr. David C. Locke, not only for his numerous valuable advise and guidance during the research, but also for his constant support and understanding through my graduate career no matter whether I was up or down. Next, I would like to thank my dissertation committee members, Dr. Arthur D. Baker and Dr. Ronald L. Birke for their valuable suggestions for my research.

I acknowledge Supelco, Inc. (Bellfonte, PA) for their kind donation of CELect-N coated capillary and Cerestar USA, Inc. (Hammond, IN) for the free sample of quaternary ammonium β-cyclodextrin.

At last, I would like to express my deepest thank to my parents. Even though they are thousands of miles away, their love and encouragement have always been with me through these years of my study. I would also like to give my hearty thanks to my wife, Ning Wu, for her belief in me and her patience.

Table of Contents

List of Tables

Lists of Figures

Part One:

Environmental Chemical Impact of Recycled Plastic Timbers Used as Construction Material in Tiffany Street Pier, South Bronx, New York

1.1. Introduction

Wood has been used traditionally for the construction of piers, docks and bulkheads. For such structures, wood is vulnerable to decay and attack by boring organisms, and therefore methods have been devised to preserve the wood [1,2]. Creosote and pentachlorophenol were the most popular wood preservatives but concern over health effects of these chemicals has reduced their popularity [3]. The most common wood preservative at present is chromated copper arsenate (CCA), which is a combination of chromium (VI) oxide (47%, w/w), copper (II) oxide (19%), and diarsenic pentoxide (34%), pressurized into the wood at high temperatures (a process known by the trade name "Wolmanizing") [4]. While the amount of CCA retained in the wood varies, the standards for marine use specify retention of 1.5 or 2.5 pounds per cubic foot.

Ganapati and Nagabhushanam [5] reported on the toxic effects of CCA to wood-destroying marine organisms. But at the same time, the diffusion of the heavy metal from CCA-treated wood have apparently negative effects on aquatic environment. Arsenic is readily taken up by phytoplankton and enters food webs [6]. There is evidence that inorganic arsenic compounds are skin and lung carcinogens in humans [7]. Chromium exists in the environment as chromate, which can be taken up by fish from aquatic environment. If consumed, it can produce a wide variety of harmful effects on human organs [8]. All three elements are listed as USEPA "priority pollutants" and are recognized toxicants at trace levels. The necessity for alternative construction material is

demanding.

As water quality has improved dramatically in recent years in the waters surrounding New York City, boring organisms have returned and are causing widespread damage to piers and other marine structures of commercial and recreational importance. Neither creosote- nor CCA-treated timber has long-term resistance to marine boring organisms such as shipworms (*Teredo navalis* and *Bankia gouldi*) and gribbles (*Limnoria tripunctata*), and both leach potentially toxic materials into the marine environment [9]. One line of defense that New York City has taken recently is to wrap important vulnerable pier pilings with high density polyethylene, which is an expensive and impermanent solution [10]. In 1994-95 the New York City Department of Real Property of the Department of General Services designed and managed construction of a 11,390 ft^2 pier to replace a decaying wooden recreational pier in the East River at the foot of Tiffany Street, the South Bronx. The new pier was constructed almost entirely of postconsumer recycled plastic (PCRP), principally high and low density polyethylene and polyethylene terephthalate, plus 4-6% miscellaneous materials. Approximately 700 tons of PCRP were used in fabricating piles, pile caps and rangers, and decking, at a total material cost of about $900,000. Construction materials for a comparable wooden pier would have been about $1.2 million. But disposing the CCA-treated wood from the collapsed pier costed New York City about twice the amount as building a new one.

Currently plastics account for about 9% by weight (16.2 million tons) of the municipal

solid waste stream in US, and consume 21% of the Nation's landfill space by volume. Discarded plastic packaging amounted to 6.7 million tons in 1990, or 4.1% of all U.S. municipal solid waste. Approximately 2% of all plastics thrown away in the United States are recovered for recycling. 15% of all plastic bottles and containers were recycled in 1992 [11]. At the present time, most recycling programs that collect plastics request only unpigmented High-Density Polyethylene (HDPE) milk and food jugs and Polyethylene Terephthalate (PET) soft drink bottles from among the plastic containers. These comprise 80% of the mixed plastics at curbside for recycling, leaving 20% as a potential commingled feedstock referred as "tailings", which comprises the containers for household cleaners, cooking oils, foods, motor oils, cosmetics and the like [12,13]. These are the source of commingled plastics. The exact polymeric composition of the tailings, which consist principally of polyolefins, naturally varies from one municipality to another and from year to year as collecting and sorting practices change. Essentially, the tailings consist predominately of HDPE(about 80%) and small amounts of other thermoplastics including Low-density Polyethylene (LDPE), Polypropylene (PP), Polystyrene (PS), Polyvinyl Chloride (PVC), and PET together with ferrous and nonferrous metals, foodstuff, dirt, paper, adhesive and plastic labels [12,13].

The complicated sources of the commingled plastic lumber generate the difficulties of chemical evaluation of its potential environmental impact. Very little research has been done on this subject [12, 13], although the utilization of commingled plastics as an alternative construction material has been climbing. Kells and Solomon [6] studied the

leachability of pesticides from the products made with recycled pesticide container plastics under dry and damp conditions. Levels of pesticides dislodged ranged from 0.18 μg / 100 cm^2 to 4.18 μg / 100 cm^2 for all plastics tested.

In our study, simulated leaching of commingled plastic lumber and conventional CCA-treated wood by artificial sea water was carried out through sequential leaching intervals. The total leaching times were 92 days for the wood and 116 days for the plastics. The leachate solution from each leaching interval was extracted using methylene chloride. Sample analysis was done by GC-MS following concentration of the extract. Chemical characterization of two different kinds of leachate and their parallel comparison were performed. The leaching mechanisms of wood and plastic were interpreted based on the data collected. The potential environmental impact of commingled plastic lumber as an alternative construction material was evaluated. In order to provide a chemical baseline for assessing the impact of the use of commingled plastic lumber for pier construction, it is also necessary to determine what chemical species are already present in the water column at the construction sites. Chemical evaluation of water matrix of East River at Tiffany Street, the South Bronx was also completed using GC-MS. The Concentrations of arsenic, chromium and copper ion in the East River water samples and wood and plastic leachates were determined by ICP-AES.

1.2. Experimental Section

1.2.1. Chemical Characterization of Water Quality in the East River at Tiffany Street.

1.2.1.1. Samples

Water samples were obtained from the East River at Tiffany Street, the South Bronx. The sampling was carried out at three sites: (1) the shore end of the pier (called "0 meter") (2) 100 meters offshore and (3) outside of the pier's footprint at the embankment east of the pier using buckets and ropes. The water samples were stored in a 4 ^{0}C cold room and extracted within a maximum of seven days. The temperature in our laboratory was maintained at 26 ^{0}C ± 2 ^{0}C. All the water used in the leaching study was distilled and was purified using a Millipore Milli-Q system (Milipore Corp., Bedford, MA).

1.2.1.2. Organics extraction.

One liter of each water sample was filtered through a 0.45 μm Millipore filter. Dissolved organics were extracted by passing the samples through a C_{18} solid phase extraction (SPE) disc (Spec Division of Ansys., Inc, Irvine, CA), and recovered by flushing the SPE disc with 15 mL of HPLC grade methylene chloride (Fisher Scientific, Springfield, NJ) three times. The extracts were combined and concentrated to 2 mL using a Kuderna-Danish (K-D) sample concentrator (Supelco Inc., Bellefonte, PA). The extracts were evaporated to 100 μL under gentle stream of nitrogen gas. The recoveries of spiked surrogates were found between 70% and 90%.

1.2.1.3. Instrumental conditions and compound quantitation.

One μL aliquots were injected into a Hewlett-Packard 5890GC-5972MS system. The GC column was a 30 m x 0.25 μm id. HP-5 MS (crosslinked 5% phenyl methyl siloxane) fused silica capillary, 0.25 μm film thickness. The initial temperature of the GC oven was set at 40 ^{0}C with splitless injection, held for 2 minutes, then raised to 250 ^{0}C at the rate of 8 ^{0}C/min. The final temperature was kept at 250 ^{0}C for 20 minutes to ensure all the compounds in the samples were carried through the column. Detection temperature was set at 280 ^{0}C. Compound identification was achieved by comparing the experimental mass spectrum of an unknown compound with the standard mass spectra in the Wiley 138k Mass Spectral Database library in the Hewlett Packard Chemstation software.

10 μL of a 1000 parts per million (ppm) solution of three deuterated external standards (n-hexadecane-d_{34}, pyrene-d_{10} and di-n-octyl phthalate-d_4) purchased from Cambridge Isotope Laboratories (Andover, MA) were added into each leachate before the extraction. Semiquantitative estimates were obtained by comparing the peak areas of the organics in the leachate with the peak areas of the deuterated standards according to the compound characteristics. Peak areas of nonaromatic hydrocarbons, and aromatic compounds and phenols in the analytes were compared with those of hexadecane-d_{34} and pyrene-d_{10}, respectively. The quantitation of oxygenated compounds including phthalates, esters, aldehydes, fatty acids and alcohols were based on comparison of peak areas with that of

di-n-octyl phthalate-d_4.

1.2.1.4. Analysis of heavy metals.

Filtered samples (50 mL) were placed in autosampler tubes and run on a Spectro Modula ICP-Atomic Emission Spectrometer (AES) (Spectro Analytical Instruments, Fitchburg, MA) using a Spectro ultrasonic nebulizer. For quantitation, peak intensities were compared with those of standards prepared by dilution of 1000 ppm ICP-grade standards (CPI, Santa Rosa, CA) with water purified with a Milli-Q system (Millipore, Bedford, MA), using the Evolution software package supplied with the instrument.

1.2.2. Leaching Characteristics of the CCA-Treated Wood

1.2.2.1. Samples.

Pressure-treated 1x6 in pine boards were purchased from R&R Lumber (Brooklyn, NY) and cut into bars 1x1x8 in using a radial arm saw.

1.2.2.2. Leaching solution.

So as not to introduce complicating factors into an already chemically complex system, leaching experiments of both the CCA-treated wood and the plastic were carried out

using clean artificial sea water, rather than the water from the East River. The formula of the artificial sea water used is given in Table 1.1, based on the formula of Lyman and Fleming [16] but scaled down to match the salinity of the water sample from the East River, 21 parts per trillion (ppt) [17].

1.2.2.3. Leaching procedure.

The apparatus used for the leaching experiment for the CCA-treated wood is shown in Figure 1.1. A wood bar (1x1x8inches) was attached to the metal arm of a mechanical stirrer and suspended in a 1 liter glass graduated cylinder containing 1 liter of artificial sea water. The cylinder cap was drilled with a hole for the stirrer arm. The bar was rotated at about 60 rpm to provide agitation and facilitate dissolution of the extractable organic components into the water. The time periods of the leaching are given in Table 1.2. After each leaching period, the leaching solution containing the leachate was removed and a liter of new artificial sea water was added to continue leaching the same piece of wood.

1.2.2.4. Organics extraction.

Each leachate sample was extracted using the SPE discs and concentrated to 100 μL using the same method described in 1.2.1.2.

Table 1.1. Formula For Artificial Sea Water

Salt	g/kg
NaCl	14.298
$MgCl_2$	3.033
$MgSO_4$	2.385
$CaCl_2$	0.671
KCl	0.404
$NaHCO_3$	0.117
KBr	0.058
H_3BO_3	0.016
$SrCl_2$	0.015
NaF	0.002
Total	21.000

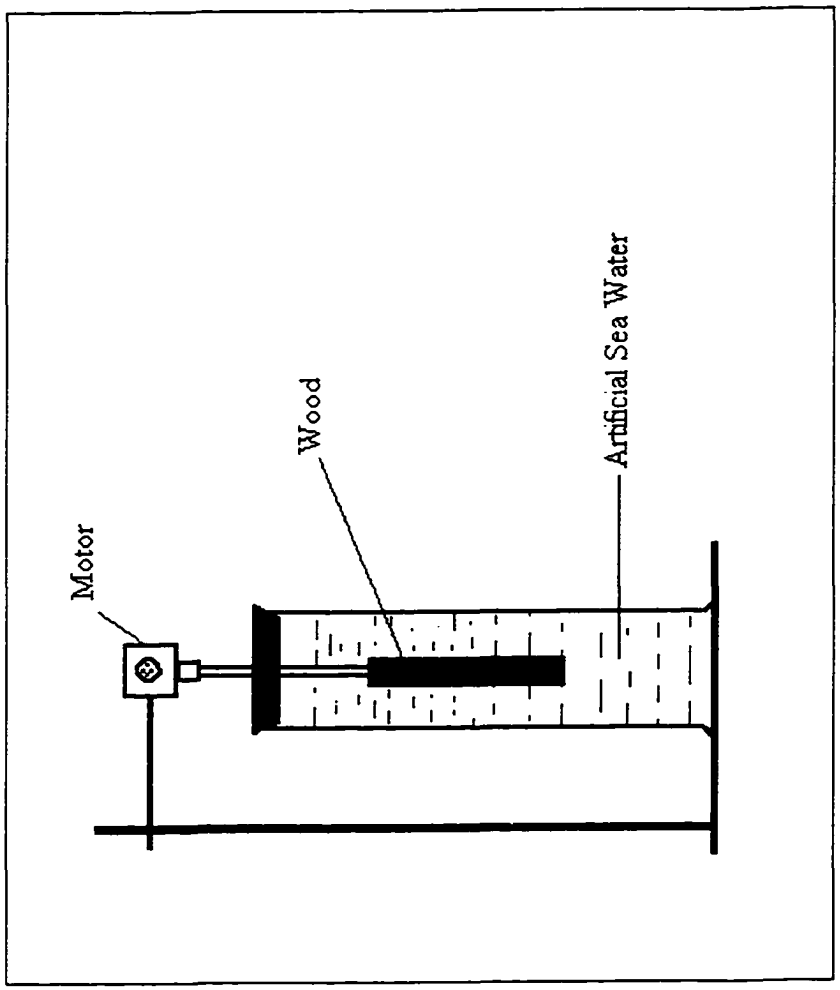

Figure 1.1. Apparatus Used For Leaching CCA-Treated Wood.

Table 1.2. Leaching periods for CCA-Treated Wood and Plastic Lumber.

Leaching Event	1	2	3	4	5	6	7	8	9	10	11
Time Interval (day)	1-2	3-8	9-20	21-32	33-44	45-56	57-68	69-80	81-92	93-104	105-116

1.2.2.5. Instrumental conditions and compound quantitation.

Same as 1.2.1.3.

1.2.2.6. Analysis of heavy metals.

Same as 1.2.1.4.

1.2.3. Leaching Characteristics of the Plastic Timber.

1.2.3.1. Samples.

Samples of the lumber used to construct the Tiffany Street pier were provided from the construction site by the Department of General Services of the City of New York. The material appears gray. The cross-sectional profile of the plastic "lumber" pieces shows that they are solid around the perimeter of a cross section, while the area around the center (core) contains numerous pores or voids, varying in size. There are small metal pieces (Cu, Al, etc.) incorporated into the lumber from the source material. Also, the plastic has an odor reminiscent of laundry detergent or fabric softener.

Initially the lumber was cut into 1x1x8 in bars, but the amount of organic compounds leached was undetectable. To increase the leaching contact surface area, the plastic

lumber was cut into bars 0.25 x 0.25 x 8 in.

1.2.3.2. Leaching solution.

Same as 1.2.2.2.

1.2.3.3. Leaching procedure.

40 pieces of plastic bar (0.25x0.25x8inches) were leached in a 1 liter glass graduated cylinder containing 1 liter of clean artificial sea water. Due to the buoyancy of the water, the bars were lifted to the top of container. Agitation was achieved by using a magnetic stirring bar at the bottom of the graduated cylinder. The apparatus for the leaching of the plastic lumber is shown in Figure 1. 2. The leaching periods were the same as those for the wood sample in the Table 1.2. A liter of new artificial sea water replaced the leachate from the previous period.

1.2.3.4. Organics extraction

Two methods of extracting the organics from the leachate solutions were evaluated for recovery, SPE and solvent extraction using methylene chloride or hexane. Extraction with 3-60 mL portions of methylene chloride gave the highest recoveries (70%-90%) of the deuterated standards spiked into the leachate. The 3 x 60 mL of methylene chloride

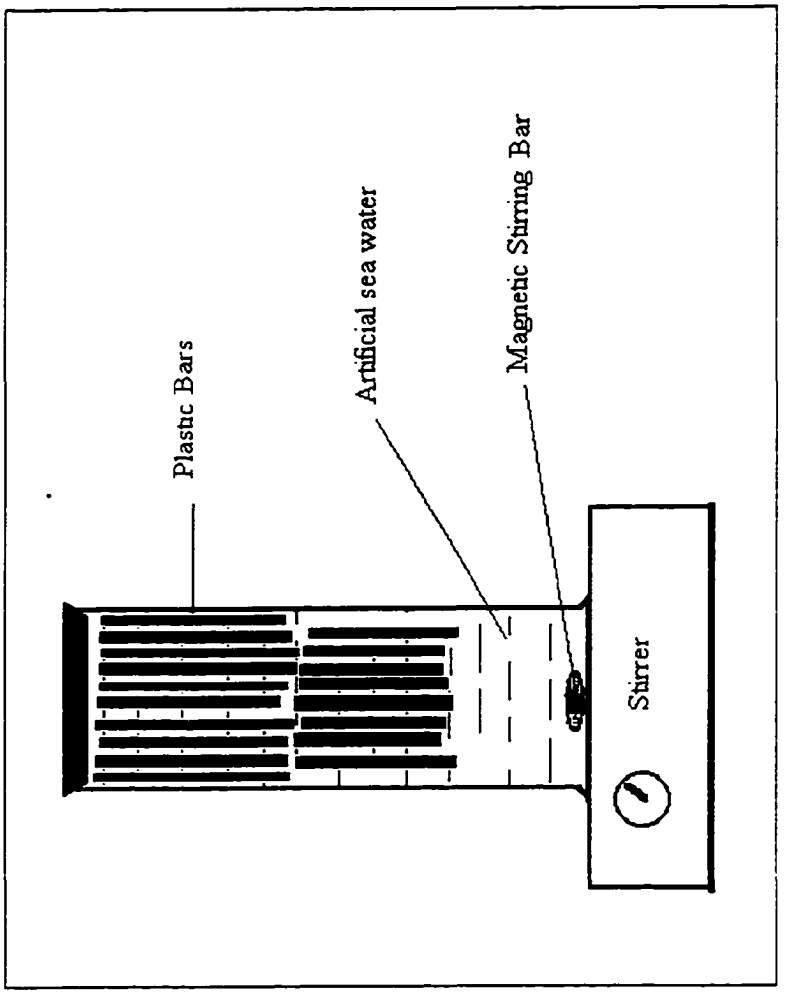

Figure 1.2. Apparatus Used for Leaching Plastic.

extracts were combined, concentrated to 4 mL in a 500 mL K-D sample concentrator. This was evaporated to 100 μL under a stream of nitrogen gas.

1.2.3.5. Instrumental conditions and compound quantitation.

Same as 1.2.1.3.

1.2.3.6. Analysis of heavy metals.

Same as 1.2.1.4.

1.2.4. Headspace Analysis of Volatile Organics from Plastic Timber.

1.2. 4.1. Samples.

As mentioned before, the plastic sample appeared gray and had the kind of soapy odor. In order to trap the volatile organic compounds which contributed to the odor, headspace collection was used. The apparatus is depicted in Figure 1.3. The Airchek air sampler pump, the charcoal tube and the Tenax tube were from SKC Inc. (Eighty Four, PA). The air flowrate was set to 1 liter per minute and the sampling time was 115 minutes. When the vacuum pump was on, air was sucked into the container through the charcoal filter and carried the volatiles from the plastic bars to the Tenax cartridge which absorbed the

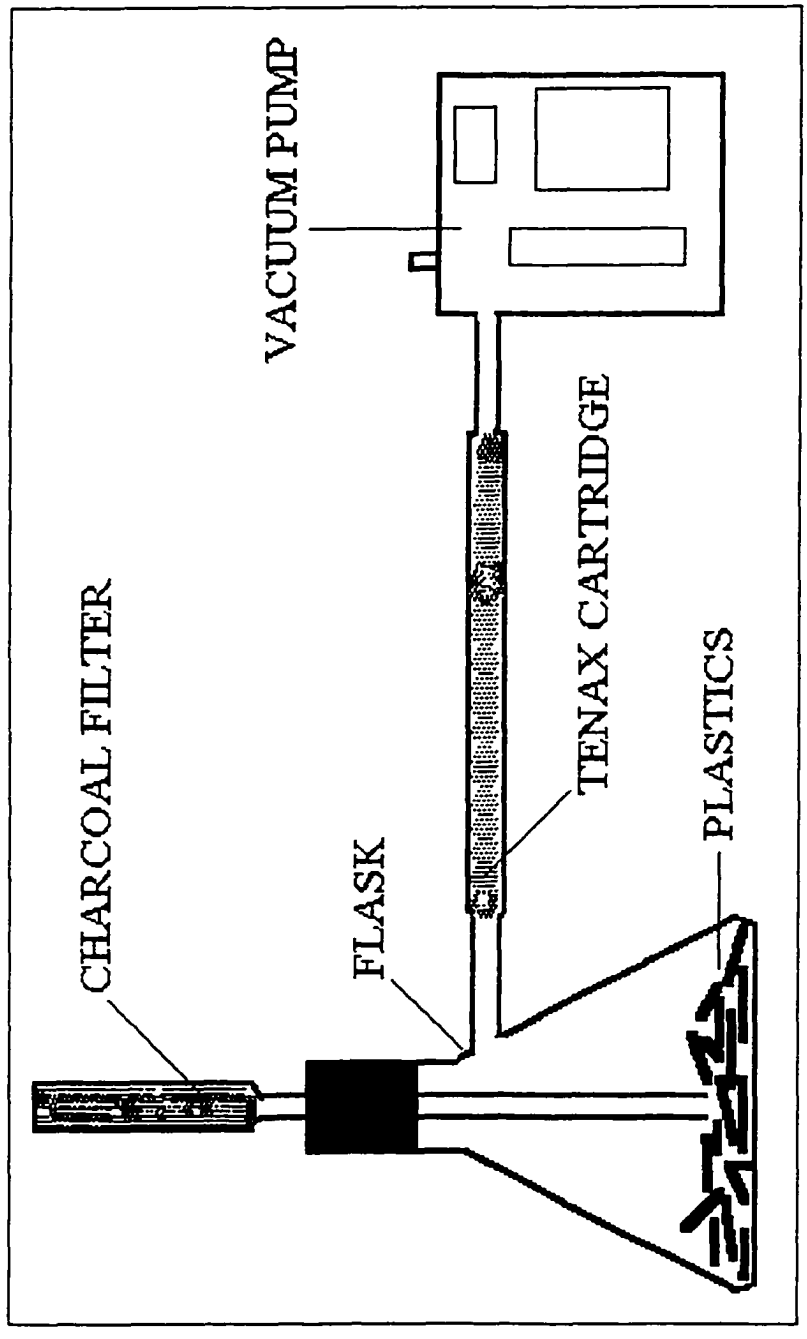

Figure 1.3. Headspace analysis of volatiles from plastic timber.

volatiles After the sampling, the Tenax resin was rinsed by 0.5 mL methanol to elute the organics. One μL methanol elutent was injected into the GC/MS for analysis.

1.2.4.2. Instrumental conditions and compound quantitation.

Same GC-MS condition as described in 1.2.1.3. Qualitative analysis was performed.

1.3. Results and Discussion

1.3.1. East River Water Quality at Tiffany Street

1.3.1.1. Organic analysis.

The compounds identified at the three sampling sites are listed in Table 1.3. Many common organic species are found including hydrocarbons, fatty acids, phenols, amines and phthalates. Their concentrations in the leachate are in the parts per billion (ppb) range. The hydrocarbons range from C_{11} to C_{29}, and could come from diesel fuel from street runoff and atmospheric inputs. The fatty acids may result from the natural process of biological decomposition. 2,6-bis-(1,1-dimethylethyl)-4-methoxyphenol (BHA) and 2,6-bis(1,1-dimethylethyl)-4-methylphenol (BHT) are widely used as preservatives for food, pharmaceutical and industrial products [18]. Nonylphenol is one of the metabolites or breakdown products of nonylphenol polyethoxylates, which constitute a major class of

Table 1.3. Water Quality of the East River at Tiffany Street, South Bronx, New York. (Concentration Units: ppb)

Compound ID.	100 m	0 m	Off F.
Aromatic Hydrocarbons			
Benzene, ethyl-			0.6
Benzene, 1-(1,1-dimethy(ethyl)-4-ethoxy	11.0	8.0	19.0
Phenols			
Phenol, 2,6-bis(1,1-dimethylethyl)-4-methoxy	7.0	10.0	10.0
Phenol, 2,6-bis(1,1-dimethylethyl)-4-methyl	3.1	2.2	3.5
Phenol, nonyl-	3.8	5.3	
Hydrocarbons			
Octane, 2,3,3-trimethyl-	0.8		
Decane, 3-methyl	0.8		
Undecane	11.2	1.2	1.4
Pentadecane	7.0	3.2	4.5
Docosane	6.0	2.0	8.0
Tricosane	3.0	8.0	6.0
Tetracosane	5.0	9.0	9.0
Pentacosane	11.0	9.0	13.0
Heptacosane	2.3	4.6	3.9
Octacosane	13.0	8.9	4.3
Nonacosane	5.3	7.3	0.1
Alcohols, Ketones and Aldehydes			
2-Cyclohexen-1-ol	2.6	5.0	2.4
2-Cyclohexen-1-one	1.2	3.4	2.3
2,6-Di-t-Butyl-4-methylene-2,5-cyclohexadiene-1-one			1.0
Cyclohexanol, 2-chloro-,trans-	3.0	3.9	7.5
Nonanal	3.0	7.0	6.4
Decanal	1.1	1.9	
Amines			
Formamide, N,N-dibutyl-	3.4	1.2	2.0
Cyclohexanamine, N-cyclohexyl-N-methyl-		3.0	

Table 1.3 Cont.

Fatty Acids			
Propanoic acid, 2-isopropyl, 3-hyroxyhexyl			0.4
Tetradecanoic acid	2.4	2.0	4.0
Hexadecanoic acid	12.1	6.3	9.1

Esters			
Phosphoric acid, trimethyl ester	0.5		0.3
Phthalate, diethyl-	7.7	4.2	5.4
Phthalate, dibutyl	12.3	13.3	7.0
Phthalate, Butyl-phenylmethyl	9.6	2.1	6.0
Phthalate, dioctyl-	52.8	46.4	72.4

Miscellaneous			
Benzothiazole	1.2		0.3
Pyridine, 2-tridecyl-	4.8		

non-ionic surfactants used in industrial applications (i.e., emulsifiers, detergents, wetting and dispersing agents, radical inhibitors, etc.) and in household products [19]. Cyclohexenone is popular industrial solvent for resins, rubber and cellulose. Tridecylpyridine is one of the starting materials in surfactant manufacture. The phthalates are common plasticizers for polymers [20]. It is not surprising that these industrial byproducts are retrieved in the water matrix of an urban area. The commonalties of compound species and their quality at three different sampling sites are apparent.

1.3.1.2. Heavy metals analysis.

From Table 1.6, the concentrations of all heavy metals analyzed are in low ppb level in the water sampled from three sites.

1.3.2. The Leaching Characteristics of the CCA-treated Wood

1.3.2.1. Organic analysis.

There are two major chemical components in wood: Lignin (18%-35%) and carbohydrate(65%-75%) which comprises celluloses and the hemicelluloses. Both lignin and carbohydrate are complex, polymeric materials and strongly water insoluble. Minor extraneous materials, mostly in the form of organic extractives and inorganic minerals

Table 1.6. Heavy metals detected. (Units:ppb)

	Water Samples of East River			Wood Leaching		Plastic leaching	
	0 m	100 M	Off F.	Period 1	Period 2	Period 1	Period 2
As	9	-	-	647	1328	20	20
Cd							
Cr	13	12	11	144	126	7	7
Cu	61	31	8	195	105	186	85
Mn	16	36	7.4	633	1020	20	37
Mo	6	6.1	8.4	-	1.7	1.8	5.4
Ni	7.8	10	6.6	3	0.2	6.7	8.2
Pb	14	-	3.3	.5	-	-	6.6
Se	-	6.2	-	131	188	67	76
Zn	210	140	85	39	33	75	36

- Not detected.

(ash), are also present in wood (usually 4%-10%) [21]. The extraneous components (extractives and ash) in wood do not contribute to the cell wall structure. Extractives are a variety of organic compounds including fats, waxes, alkaloids, proteins, simple and complex phenolics, glycosides, saponins, pectins, mucilages, gums, resins, terpenes, starches, simple sugars, and essential oils. The volatile compounds detected in the leachate should contain the components of extractives such as phenolics, terpenes and essential oils [22].

Because the organics are leached gradually from the whole volume of the wood pieces, we express the quantity of leached compounds as μg per 100 $inch^3$ of wood. The distribution of the total organic content in the leachate is shown at Fig. 1.4. Ketones, alcohols and fatty acids combined make up more than half of the total organic matter. Most of these organic compounds, such as bicycloalcohols, bicycloketones and fatty acids are wood extractives, together with carveol, sobrerol, myrtenol, etc. [22]. The group of hydrocarbons is relatively unusual. Possibly the wood sample was contaminated by diesel fuel during the processing or transportation of the lumber. The organic compounds identified in wood leachate are listed in Table 1.4 and Fig. 1.5 plots the amount of organics vs. leaching fractions. In Fig. 1.5, the quantity of most of the organics reached its apex at leaching fraction 1, which was the first a couple of days of the leaching. It is most likely attributed to the diffusion of the organics from the exterior of the wood. The quick diffusion of these organics then produced the dramatic decline of the organic quantity from fraction 1 to 2. After fraction 2, the organic species from the interior of

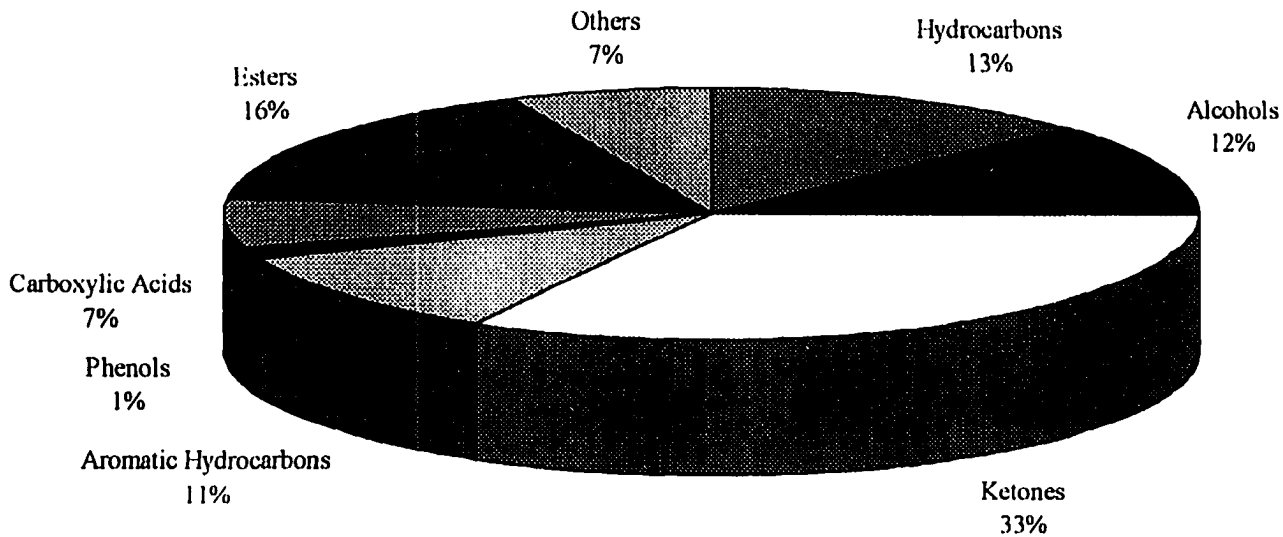

Fig. 1.4. Distribution of types of organics detected in wood leachate.

Table 1.4. Organic Compounds Identified In Wood Leachates. (Units: μg / 100 in^3 of Wood Bar).

	Leaching period No.								
Compound ID	**1**	**2**	**3**	**4**	**5**	**6**	**7**	**8**	**9**
Hydrocarbons									
Decane		8	31						
Nonane, 3,7-dimethyl-	20								
Octane, 6-ethyl-2-methyl	52	20							
Decane, 4-methyl-	111	11	24						
Undecane	372	75	228	246					
Undecane, 3,9-dimethyl-	44	51							
Hexadecane	28	17							
Heptadecane		3							
Octadecane	224	35							
Nonadecane		5							
Eicosane	38	6							
Dococane	36								
Tricosane	31								
Heptacosane	25								
1,2,3,3,4-Pentamethyl-cyclopentene	16								
Cyclopentane, 2-isopropyl-1,3-dimethyl-	227	5							
1,7-Octadiene, 2,3,3-trimethyl-		57							
Cis-Carveol	302	55	351	76	36	8	18	15	14

Table 1.4. Cont.

Alcohols									
1-Hexanol	359	46							
1-Hexanol, 2-ethyl-		5	11						
Ethanol,2-butoxy-	151	10							
Ethanol, 2-(2-butoxyethoxy)-			143	63	44	32			
Ethanol, 2-chloro-, phosphate			195						
Benzenepropanol, 4-methoxy	107	12							
Myrtenol			131						
Trans-Sobrerol	208	662	371						
Bicyclo[2.2.1]heptan-2-ol, 2,6,6-trimethyl-			113						

Ketones									
Methanone, diphenyl-	25	9	35						
Ethanone, 1-(3-methylphenyl)-	74	21	41						7
Ethanone, 1-(4-methylphenyl)-	189	23							
Ethanone, 1-(4-hydroxy-3-methoxyphenyl)-			28	32	21	20	18	17	49
1-Propanone, 1-anisyl-	82	17	42	38	22	19	17	18	36
2-Heptanone, 5-methyl-	36	7							
2(3H)-Furanone, dihydro-5-pentyl-	290								
8-Hydroxycarvotanacetone		68	60						
Bicyclo[3.1.0]hex-3-en-2-one, 4-methyl-1-(1-methylethyl)			46	50					
Bicyclo[3,1,1]hept-3-en-2-one, 4,6,6-trimethyl-	1985	625	1161	606	531	224	201	144	94
2-Cyclohexan-1-one, 2-methyl-5-(1-methylethenyl)-	120	39	146	49	28	7	15	13	10

Aromatic Hydocarbons									
Benzene, 1-methoxy-4-(1-propenyl)-	907	58	134	54	26	10	33	27	22
Benzene, 1-(1,1-dimethylethyl)-4-ethoxy-	454	33	134	164	64	21			

Table 1.4. Cont.

Phenols									
Phenol, 2,6-bis(1,1-dimethylethyl)-4-methyl-	195	5	29						
Phenol, 2,2'-methylenebis[6-(1,1-dimethylethyl)]-	51	4							
Carboxylic Acids									
Nonanoic acid	589								
Tetradecanoic acid	39	21	39						
Hexadecanoic acid	170	53	87						29
Octadecanoic acid	38								
Benzenepropanoic acid, .beta.-dimethyl-			20						
1-Phenanthrenecarboxylic acid	179	125	105						
Esters									
Sabinyl acetate			165	128	76	17	52	41	47
Benzoic acid, ethyl ester	138	69							
Phosphoric acid, tributyl ester			23		11	2			
Benzaldehye propylene glycol acetate			45						
Phthalate, dimethyl-			33						
Phthalate, diethyl-	422	8	347	65		33	12		
Phthalate, bis(2-methylpropyl)-			39						
Phthalate, dibutyl-	107	7	143	41	23		11	19	16
Phthalate, butyl phenylmethyl -	63	81	266	147	35	64	51	38	42
Phthalate, bis(2-ethylhexyl)-	221	176	152	33	76	45	22	27	19

Table 1.4. Cont.

Miscellaneous									
3-Methoxycinnamaldehyde	338								
1,3-Benzenedicarbonitrile, 2,4,5,6	414								
Furan, 2-pentyl-	624	19	10						

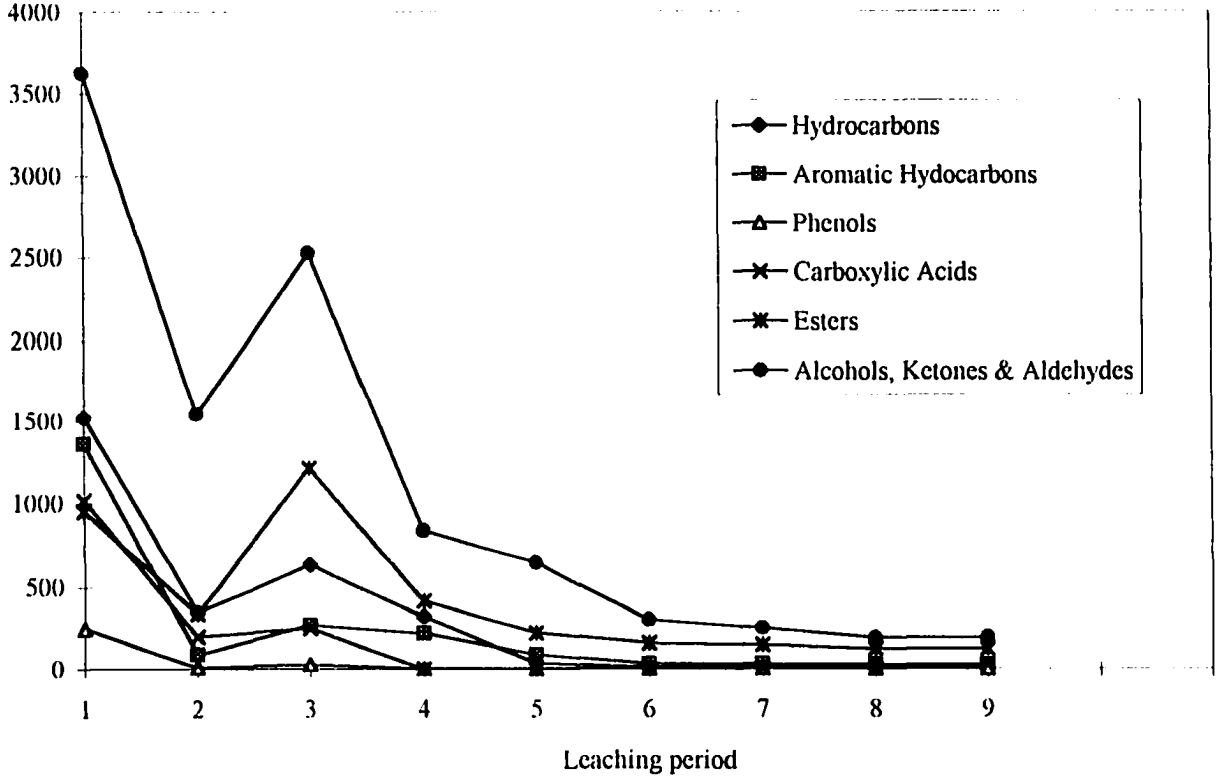

Fig. 1.5. Organics detected in wood leachate vs. leaching periods. (Unit: $\mu g/in^3$)

wood such as the woody constituents started to spread to the leachate solution, which created a substantial growth at leaching fraction 3. The abundance of all kinds of organics drop constantly afterwards. The amounts leached range from 10 to 2 x 10^3 μg/100 in^3 of wood. This produces concentration in the leachate water of 8 x 10^{-4} ppb to 0.2 ppb.

1.3.2.2. Heavy metals analysis.

From Table 1.6, about 2 mg of arsenic and magnesium was detected in the total of 2 liters of leachate in 8 days, while chromium, copper and selenium had about 0.2~0.3 mg.

1.3.3. The Leaching Characteristics of the Plastic Lumber

1.3.3.1. Organics analysis.

Unlike the case of the wood sample, the compounds found in the non-porous plastic leachate are derived mainly from the surface of the impermeable plastic pieces. Therefore the amount of organic matter leached from the plastic sample was expressed as μg per 100 $inch^2$ of plastic. The distribution of the types of organics is shown in Fig. 1.6. Esters, mainly phthalate esters, comprise more than one-third of the total amount of organics leached off the plastic pieces. As noted above, phthalates are widely used commercial plasticizers. Dioctyl phthalate is the most widely used in vinyl chloride

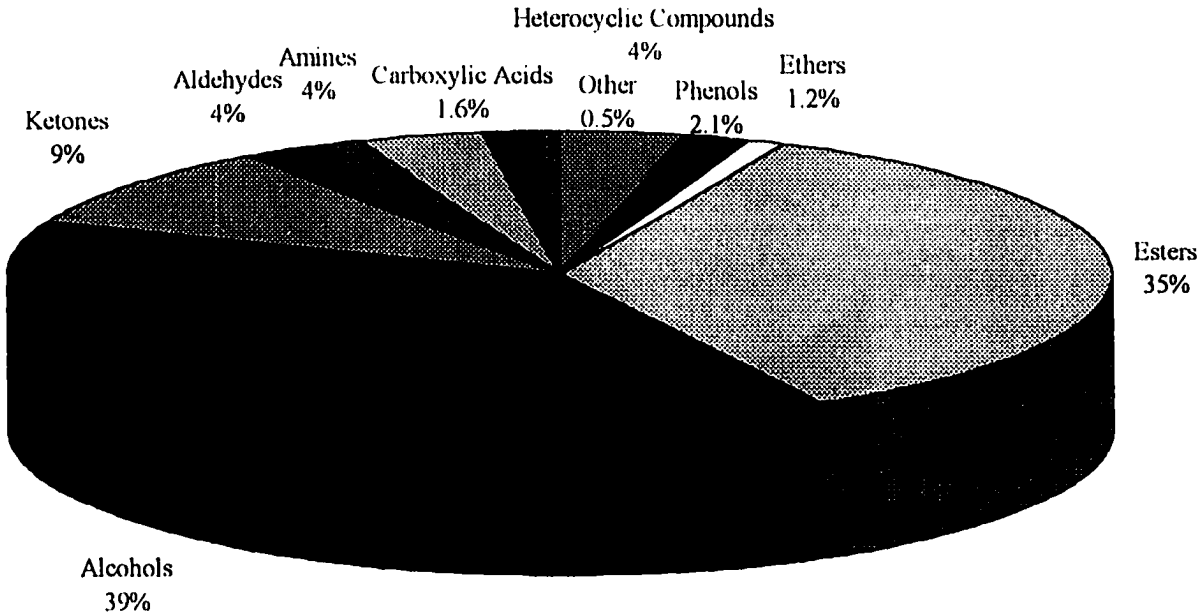

Fig. 1.6. Distribution of types of organics detected in plastic leachate.

resins, where they are preferred because they offer a good compromise with respect to a wide range of properties: satisfactorily low volatility, good compatibility, fair low-temperature flexibility, and moderately low cost [23]. The lower alkyl phthalates are generally employed in resins other than polyvinyl chloride. Dibutyl phthalate is used chiefly in nitrocellulose lacquers and polyvinyl acetate adhesives; diethyl and dimethyl phthalates are used in cellulose acetate [23]. Even though the dioctyl is used more extensively than other phthalates, lower alkyl phthalates are present in much larger amounts than dioctyl phthalate in the leachate. This can be attributed to the lower water solubility of dioctyl phthalate, which leads to its low leachability. Besides phthalates, dioctyl adipate is another common plasticizer. It leads the field for its low-temperature flexibility and efficiency in vinyl [23]. It is not surprising that these plasticizers are present in the leachate in significant amount.

Table 1.5 lists the amounts of the organic compounds detected in every leaching fraction. The possible kinds of residues left in the bottles are probably the source of most of the organics besides the plasticizers. These bottles were used for food, cleaning reagents, oils etc., are were often not rinsed clean during the recycling process. Natural products have a substantial fraction of alcohols, fatty acids, ethers and ketones. They include linallool, borneol, menthol, terpineol, and camphor. These natural products represents approximately over one-third of the total amount of listed in Table 1.5. Some of them are the constituents of essential oils. They are widely used as flavoring compounds in beverages, foodstuffs and oral medicines. They are somewhat water soluble and because

Table 1.5. Organic Compounds Identified In Plastic Leachates. (Units: μg / 100 in^2)

	Leaching fraction No.										
Compound ID	1	2	3	4	5	6	7	8	9	10	11
Heterocyclic Compounds											
Pyrazine, methyl-	16	2									
Pyrazine, ethyl-	20	12									
Pyrazine, 2-ethyl-6-methyl-	16										
Pyrazine, 2,6-diethyl-	12										
Pyridine, 3,5-dimethyl-	18	4									
Pyridine, 3-(1-methyl-2-pyrolidinyl)-	18		3								
Pyridine, 2-butyl,1-oxide	12		2								
Thiophene, 2,5-bis(2-methylpropyl)-	160	29	29	16	14	5	7	3	2	1	3
3,4-Dihydroisoquinoline	20										
Pseudoephedrine,(+)-	8										
Phenols											
Phenol, 2-(1,1-dimethylethyl)-6-methyl-	72	12	8	2	8			1	1		
Phenol, 4,4'-(1-methylethylidene)bis-			10								
Phenol, (1,1-dimethylethyl)-4-methoxy-	102	11	6	7	5	3	2	1	1		
Ethers											
Isocineole	106	11	2								
1,8-Cineole		21									

Table 1.5 Cont.

Esters											
Endo-Bornyl Acetate	44		1								
Benzoic acid, 2-amino, methyl ester	142	25									
Acetic acid, phenylmethyl ester	248	63	4								
Phthalate,dimethyl-	92	19	5	3	1						
Phthalate, diethyl-	221	394	402	101	15	44	1				
Phthalate, dibutyl-	13		3	5	1	25	1	2	1	1	1
Phthalate, dioctyl-	21	11	23	58	31	1	1	3	1	2	2
Hexanedioic acid, dioctyl ester				184	51	18	6	3	2	3	1

Alcohols											
2-Propanol, 1-butoxy-	4	2	4								
2-Propanol, 1-[1-methyl-2(2-	276	61	34	4	2	1	1				
Benzenemethanol	370										
Benzenepropanol,.alpha.,.alpha.-dimethyl-	48	8	2								
1,8-Nonanediol, 8-methyl-	376	24	6								
1-Hexanol, 2-ethyl-	408	60	16	3	2	1					1
3-Octanol, 3,6-dimethyl	351	78	15								
Ethanol. 2-(2-butoxyethyoxy)-			12	9		4	1	2			
Ethanol, 2-phenoxy-	112	9									
Ethanol,2-[2-(2-butoxyethoxy)ethoxy]	76	21	4								
3-Cyclohexen-1-ol, 4-methyl-1-(1-methylethyl)-	86	33	2								
Dicyclopentadiene alcohol	76	19	34		11	14	5	1	3	3	
Linallool	244	61	10								
Endo-Borneol	52										
Menthol	52		1								
1-Terpineol	147	147	12								

Table 1.5. Cont.

Ketones											
Cyclohexanone	34	3									
Cyclohexanone, 2-ethyl	96	11	2								
Methanone, diphenyl-	136	49	38	13	4	7	3	4	3	2	3
Ethanone, 1-phenyl-	54	2									
2-Hydroxy-2-methyl-1-phenyl-1-propanone	48	9									
2H-Benzopyran,-2-one	44	19	4								
2H-1-Benzopyran-2-one, 7-(ethylamino)-		8									
Fenchone	54										
Camphor	130	34	16	7		1	1				
2H-Azepine-2-one, hexahydro-	234	26	28								
Aldehydes											
Benzaldehyde	384	36	4								
Benzaldehyde, 4-hydroxy-3-methoxy-	21										
Amines											
Benzeamine, 2-Chloro-	34	4									
Benzenamine, 4-propyl-			4								
Benzamide, N,N-diethyl-3-methyl-	44		9	4	1	2	1	1	1		
2-Toluenesulfonamine	84	29	36	9		1	0	2	1		3
1,3,5-Triazine-2,4-diamine,6-chloro-	10		6								
Acetamide, 2-chloro-N-(2-ethyl-6-methyl)-	108		36		4	8	5	5	4		3
Carboxylic Acids											
Decanoic acid	24	3									
Dodecanoic acid	102								0		

Table 1.5. Cont.

Octadecanoic acid		22							0		
Propanoic acid, 2-methyl-3-hydroxy-2,4-	34	8	1			3	1				0
Miscellaneous											
Pentane, 2,4-dimethyl-	8		1								
Benzene, (2,2-Diethyoxyethyl)-	8	8	2								
Benzoic Acid, 4-hydroxy-	20		1								

of their high volatility, they are easily detected by gas chromatography. The various sources of recycled plastic bottles might also account for some of the industrial byproducts in the leachate. For instance, toluenesulfanamine is used in the dye and pharmaceutical industries; 2,6-bis(1,1-dimethylethyl)-4-methoxyphenol (BHA) and 2,6-bis(1,1-dimethylethyl)-4-methylphenol (BHT) are common antioxidants used in food products, and these food products may also be responsible for some of the fatty acids found in the leachate. 4,4'-(1-methylethylidene)bisphenol (bisphenol A) is one of the popular reagents in the epoxy resins [24]. The breakdown of epoxy polymeric materials could account for the appearance of bisphenol A in the leachate.

The amount of organics detected vs. the leaching fraction are plotted in Fig. 1.7. The quantity of organics leached from the plastic pieces drops dramatically in the first several days of leaching. Only one-third of the organics are still present at trace level after the third leaching fraction. This justifies our assumption that the organics are leached only from the surface of the plastic lumber.

1.3.3.2. Heavy metals analysis.

As is clear from Table 1.6, all heavy metals detected in plastic leachate are at trace levels. They should come from the metal pieces incorporated into the plastic timbers during the recycling process.

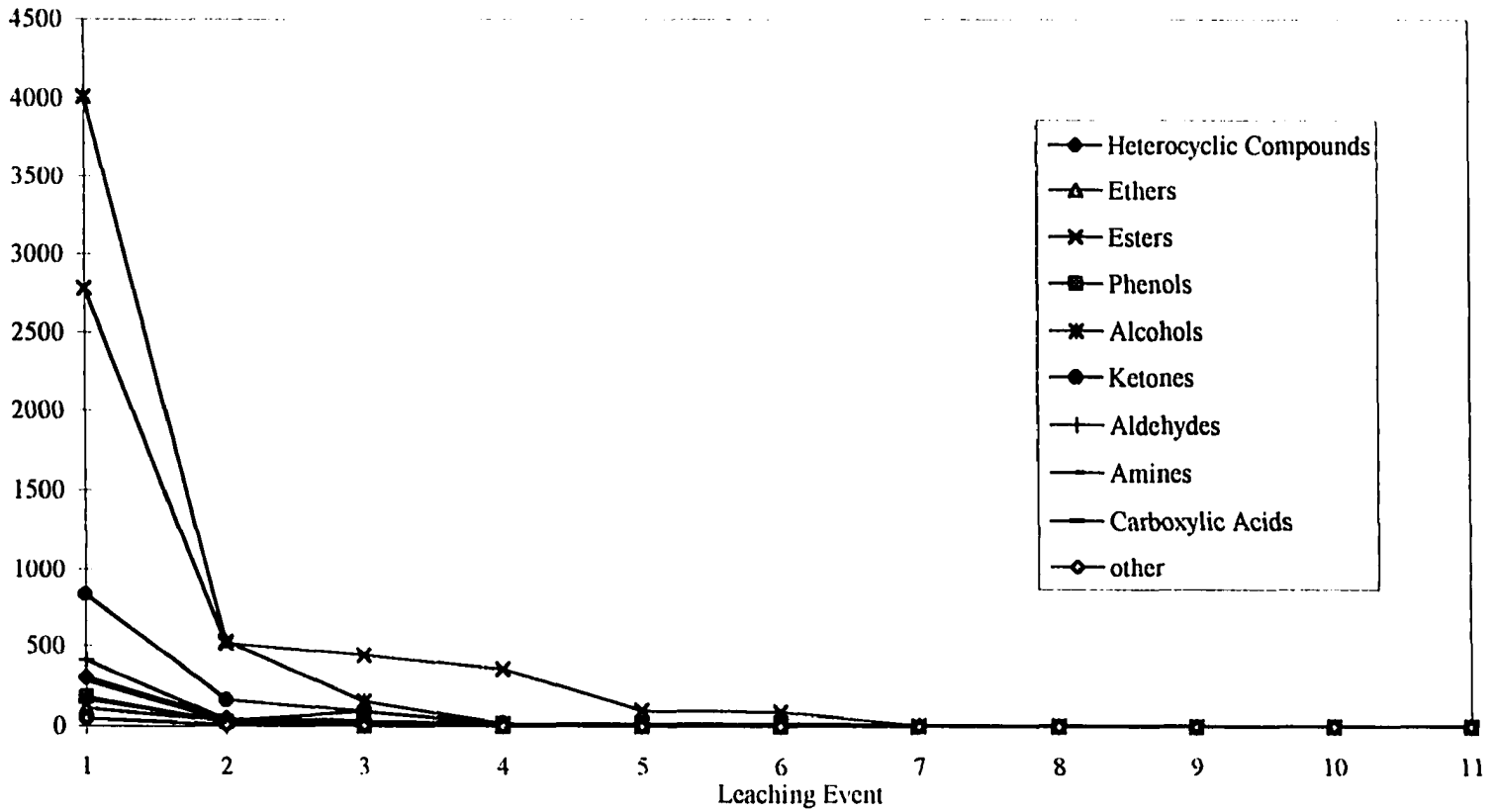

Fig. 1.7. Organics detected in plastic leachate vs. leaching periods. (Unit: $\mu g/in^2$)

Table 1.7. Compounds Identified in Headspace Volatiles of Recycled Plastic Timber

Terpinoids	**Hydrocarbons**	**Miscellaneous organics**
Limonene	1-Ethyl-2,4-dimethyl benzene	Benzaldehyde
α-Pinene	Undecane	Nonanal
α-Terpinene	1-Dodecene	2-(2-butoxy ethoxy) ethanol
Geranyl acetate	Tridecane	Benzyl acetate
Neryl acetate	Tetradecene	2-Hydroxy benzoic acid methyl ester
Farnesene	Tetradecane	Undecanone
α-Cedrane	Pentadecane	Benzophenone
	Hexadecane	2-Amino benzoic acid methyl ester
	Octadecene	Hexadecanol
	Octadecane	2.6-bis(1,1-dimethyl ethyl) phenol
	1,4-bis(1 methylethyl)benzene	2-Hydroxy--3-methyl benzoic acid
Phthalates		Tetradecanoic acid
		Hexadecanoic acid
Diethyl phthalate		
Dibutyl phthalate		
Dioctyl phthalate		

1.3.4. Organic Analysis of Volatile Compounds from Plastic Timber.

Table 1.7 lists all the organic compounds detected in the headspace trap. These are mainly terpinoids, low molecular hydrocarbons and phthalates. The soapy odor from the plastic should come from the group of terpinoids even though it is very difficult to tell which ones makes larger contribution. The source of this terpinoids should also be the product residues in the plastic bottles such as detergent bottles.

1.4. Conclusion

Comparing the total organics detected in the wood leachate with those from the plastic leachate in Fig.1.8, there are comparable amount of organics leached. Organics detected in the wood leachate are mainly natural woody constituents which usually will not harm the marine environment. On the other hand, the phthalate esters which make up a large portion of total organics in the plastic leachate are ubiquitous environmental pollutants. Phthalates can be taken up by fish, and induce toxic effect on human livers after they eat contaminated seafood [25]. Some of the amines, ketones and aldehydes are also threatening factors to both the environment and human health. Have we reached the conclusion that commingled plastic lumber is a environmentally hazardous construction material? Not too soon! Despite the potential hazard of some of the organic compounds leached from the plastic, we have to consider a very important factor in environmental safety, the dosage. These organic compounds could be considered hazardous only when

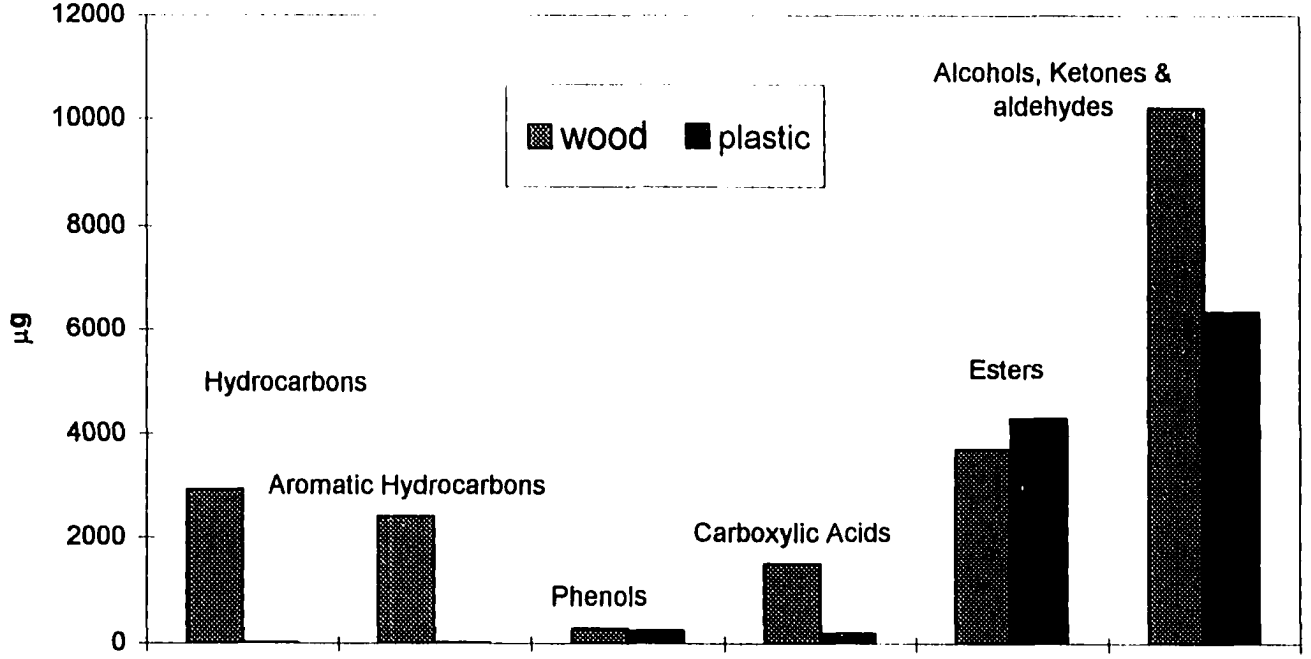

Fig. 1.8. Comparison of total organics detected in wood and plastic leachate.

their concentrations exceed certain limits. During the 116 days of leaching, the cumulative amount of each organics from the 40 pieces of plastic bar ranges from 10.3 mg (diethylphthalate) to 0.026 mg (2,4-dimethylpentane). In the aquatic environment, they will be well mixed and rapidly diluted so that these compounds would be even undetectable by existing analytical instruments if we assume that the plastic lumber was the sole source of these contaminants. Compared with the existing East River water quality, the contamination from the plastic timbers is negligible.

As mentioned above, in the leachate of CCA-treated wood there are relatively small quantities of hazardous organic compounds left besides the natural wood extractives, which possess insignificant environmental impact. But when we study Fig. 1.9, which gives parallel comparison of the total amount of arsenic, copper and chromium detected in the existing water matrix of the East River, the wood leachate and the plastic leachate. It is clear that CCA-treated wood attributes much more heavy metals than the plastic material does. For instance, there is about 2000 ppb of arsenic found in the wood leachate, while only 40 ppb from the plastic. Arsenic, copper and chromium have been shown to be easily dislodged from CCA-treated wood into the marine environment [26,27]. The study by Weis [15], showed that leachate from CCA-treated wood depressed animal regeneration, reduced sea urchin fertilization, and totally inhibited larval development of those that were fertilized.

Based on our experimental results, there is no indication so far that using plastic lumber

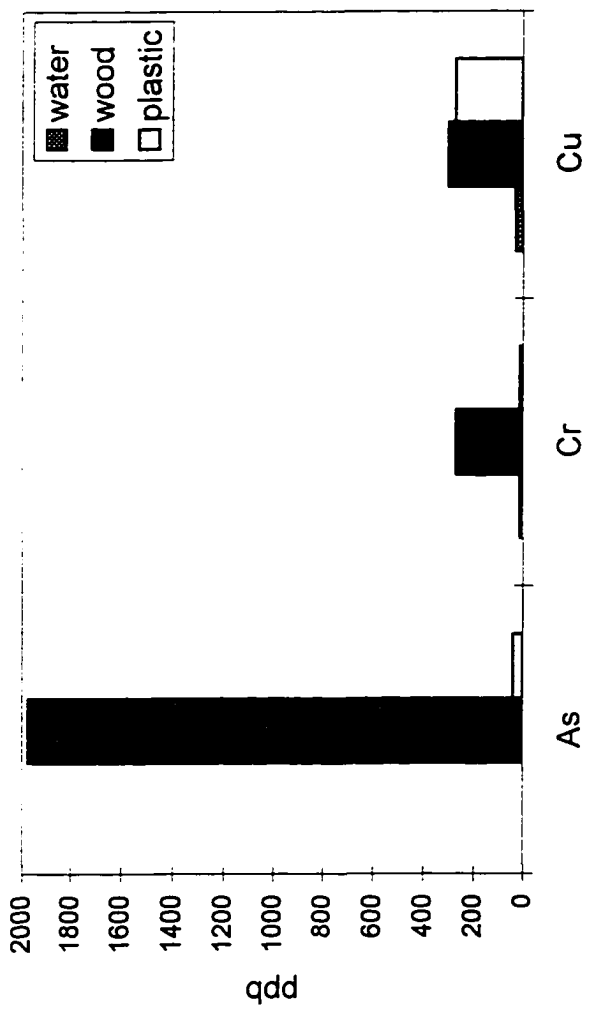

Fig 1.9. Heavy metals detected in East River water, wood and plastic leachate.

for construction will have any noticeable environmental impact. It will serve as a cheaper, safer and longer lasting alternative construction material for the coastal waterfront development than conventional construction materials.

At the end, it has to be stressed that GC-MS, which the main detection tool for the organic matter in our leaching study, is not capable of analyzing all the existing organics in water samples, although it enables a convenient separation and structure determination for many organic components of interest. Complete resolution and determination of organic constituents in environmental samples are extremely difficult, it not impossible. The better our analytical methods, the more we recognize the complexity of the mixtures present. For instance, the electron capture detector would have given us excellent sensitivity for PCBs, pesticides and herbicides; the flame ionization detector would have provided better detectability for hydrocarbons. Derivatization and high-pressure liquid chromatography could widen the scope of our organic analyses. Moreover, for evaluating potential health hazards and ecological impacts of organic chemicals, the direct interrelation between chemical structure and biological activity should be taken into the consideration.

1.5. Postscript.

Despite the fact that plastic lumber is a non-conductor of electricity, in August 1996 the gazebo on the pier was struck by lightning. The plastic did not burn, but rather the

lightning melted or vaporized about a third of the decking. According to the New York City Fire Department, had it been constructed of wood, the entire pier would have burnt to the water. Plastic melts rather than sustains combustion, which is what saved most of the pier. The City plans to replace the damaged part of the pier, this time with a lightning rod installed.

Part Two:

Chiral Separation of Dansyl-DL-Amino Acids by Counterflow Capillary Electrophoresis

2.1. Introduction

2.1.1. The significance of chiral separations

Many chemical compounds used in pharmaceutical formulations possess one or more asymmetric centers responsible for optical activity, that can strongly influence their pharmacological properties. Of 1327 totally synthetic drugs marketed worldwide in 1990, 528 are chiral, capable of existing as two or more optical isomers depending on the number of asymmetric centers [1]. But only 61 of the 528 chiral synthetic drugs are marketed as single enantiomers, while the other 467 are sold as racemates. Most often, only one enantiomer is responsible for a compound's activity, while the antipode is either less or inactive. Examples of drugs in which one of the two enantiomers possesses a different pharmacological activity are well documented, e.g. (-)-epinephrine and (-)-terbutaline are 10- and 4-times more potent than their (+)-antipode, respectively [2], (-)-propranolol is 100-fold more potent than (+)-propranolol. In some cases, the antipode is even toxic. The antihistaminic racemic terfenadine causes side effects of dizziness and dry mouth, while (s)-terfenadine, does not suffer these drawbacks [3]. (s)-(-)-Thalidomide has a teratogenic effect [4]. As our understanding of the biological action of drugs with respect to their stereochemistry has improved, it is necessary for chemists to investigate the pharmacological and toxicological properties of individual drug enantiomers. For example, Janssen Pharmaceutica (Piscataway, NJ) developed nebivolol as a β-blocker for hypertension. But whereas (+)- is a β-blocker, (-)-nebivolol is not but

is a vasodilating agent. Thus by alleviating hypertension by two different mechanisms, the racemate may be superior to either enantiomer [4]. The same scenario occurs with xenobiotics such as pesticides and herbicides in the agricultural field. Based on these factors, the demand for analytical methods with high resolution power and high efficiency has increased dramatically recently for the purposes of chiral drug purity control, pharmacokinetic and pharmacodynamic studies, etc.

Most chiral analysis is currently carried out employing chromatographic techniques including gas chromatography (GC) [5-9], supercritical fluid chromatography (SFC) [10,11], thin-layer chromatography (TLC) [12-14] and high-performance liquid chromatography (HPLC) [15-26]. Capillary GC and SFC have been well developed with different stationary phases such as optically active polymers and modified cyclodextrins [5-11]. Their applications, however, are limited to relatively volatile compounds. HPLC can accommodate large as well as small molecules. Series of chiral stationary phases such as Pirkle columns [15-18] and cyclodextrin columns [19-23] have been successfully developed to separate various compounds. But the main drawback of this technique is its relatively inadequate efficiency due to its pressure driven flow profile, and the high cost of the specialty chiral columns.

2.1.2. Introduction to capillary electrophoresis and its application to chiral separations

Capillary electrophoresis (CE) is a recently developed powerful analytical technique widely applied in different areas of research. e.g., pharmaceutical, biological, and environmental. It was first introduced by Mikker *et al.* [27], and Jorgenson and Lukas [28] about two decades ago.

Like conventional electrophoresis, CE is a process for separating charged molecules based on their movement through a fluid under the influence of an applied electric field. A basic schematic of a capillary electrophoresis apparatus is shown in Fig. 2.1, where the two ends of a capillary, which is usually made of fused silica, are submerged into two identical buffer solutions on both sides. Once a high voltage is applied across the capillary, analytes injected will be driven by the electric field. Different analytes will migrate through the capillary at different velocities, which are called electrophoretic mobilities, expressed as [29]:

$$\mu_{ep} = q/6\pi\eta r \qquad (1)$$

where q is the net charge of the analyte, r is its ionic radius and η is the buffer viscosity, i.e. mobility is related to the ion's charge to size ratio.

One of the unique features of CE is electroosmotic flow, depicted in Fig. 2.2. As mentioned, the capillary is made of fused silica. There is a layer of silanol groups present

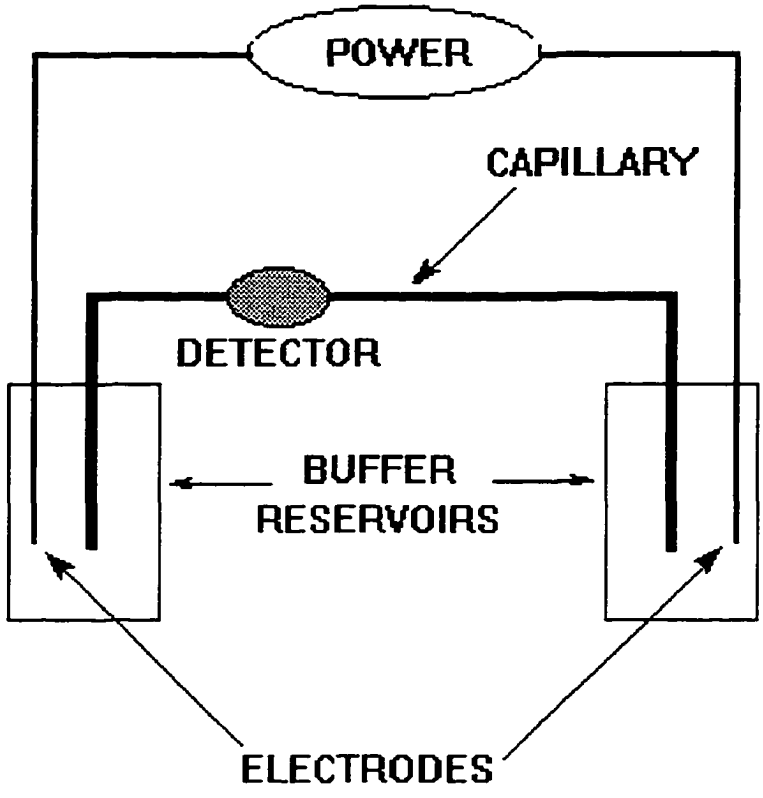

Fig. 2.1. The schematic of capillary electrophoresis.

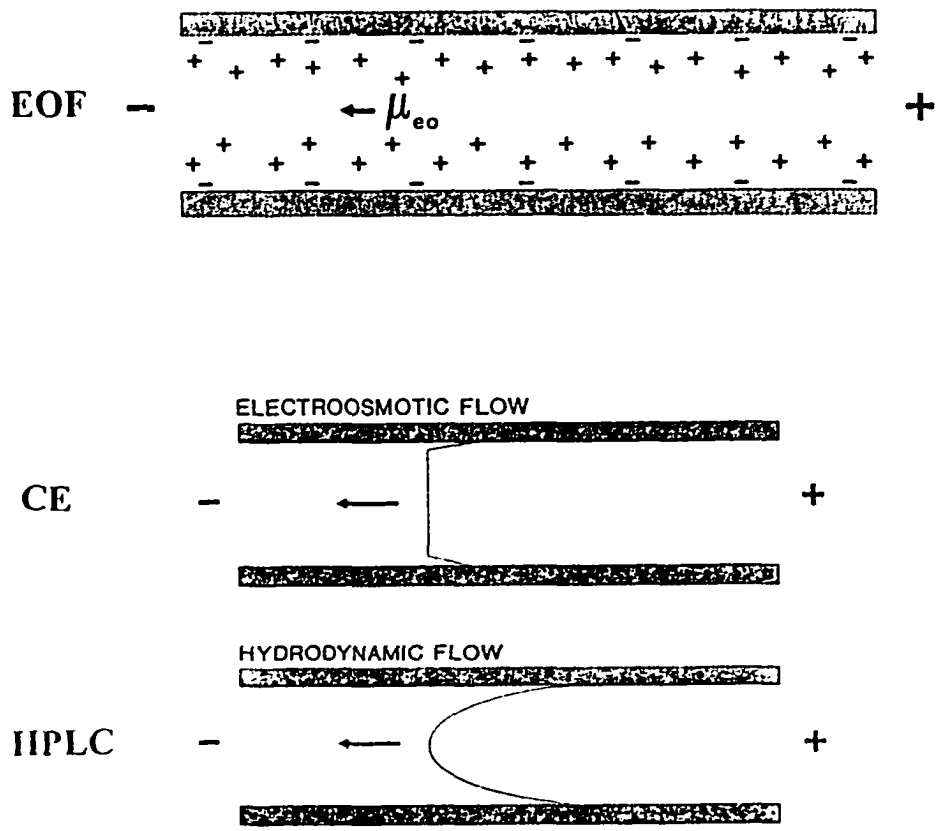

Fig. 2.2. The origin of electroosmotic flow (upper), and the comparison of flow profile between CE and HPLC (lower).

on the inner surface of the capillary. For pH > 2, these silanol groups are at least partially deprotonated, and generate negative charge on the inner surface of the capillary. Anions in buffer solution are repelled from the negatively charged wall region, whereas cations are attracted as counterions. This double layer phenomenon was described by Gouy and Chapman in 1910 and 1913 [29]. When a voltage is applied, the mobile positive charges migrate in the direction of the cathode. Since ions are solvated by water, the fluid in the buffer is mobilized as well and dragged along by the migrating charge. This phenomenon is called electroosmotic flow (EOF), and is the main driving force in CE. The electroosmotic flow velocity as defined by Smoluchowski in 1903 is given by [29],

$$V_{eo} = \varepsilon\zeta E/\eta, \qquad (2)$$

where ε is the dielectric constant, η is the viscosity of the buffer. E is the electric field strength, and ζ is the zeta potential of the liquid-solid interface which occurs because of the surface charge of capillary. Then the electroosmotic mobility is:

$$\mu_{eo} = \varepsilon\zeta/\eta \qquad (3).$$

Because EOF is uniformly generated across the capillary, the flow profile has a flat front. By comparison, HPLC, whose flow is produced by pump, suffers from mass transfer resistance, which leads to a parabolic flow profile. The difference of flow profile between CE and HPLC is the key that CE exhibits much higher efficiency than HPLC.

The separation of a mixture of ionic analytes by CE can be easily obtained by taking advantage of different mass/charge ratio of ionic analytes, which leads to different electrophoretic mobilities under the electric field. As a result, individual ionic analytes migrate at different velocities in the capillary and form separated moving zones. This mode is called capillary zone electrophoresis (CZE). CZE is not applicable to the separation of neutral compounds, since in that case the only driving force is electroosmotic flow, which is identical for all analytes. This problem was solved by the introduction of micellar electrokinetic capillary chromatography (MEKC) by Terabe and coworkers [30-31]. In MEKC, a pseudostationary phase, micelles, which usually are ionic surfactants, is introduced into the buffer solution. If the different neutral analytes have different degree of association with the charged moving ionic micelle under the influence of the electric field, they will travel with different mobilities in the capillary. A schematic representation of CZE and MEKC is given in Fig. 2.3.

Besides the two most popular modes, CZE and MEKC, several other CE techniques have also been developed for various applications. Those techniques include capillary isotachophoresis (CITP) [32-33], capillary gel electrophoresis (CGE) [34-35] and capillary isoelectric focusing (CIF) [36-37].

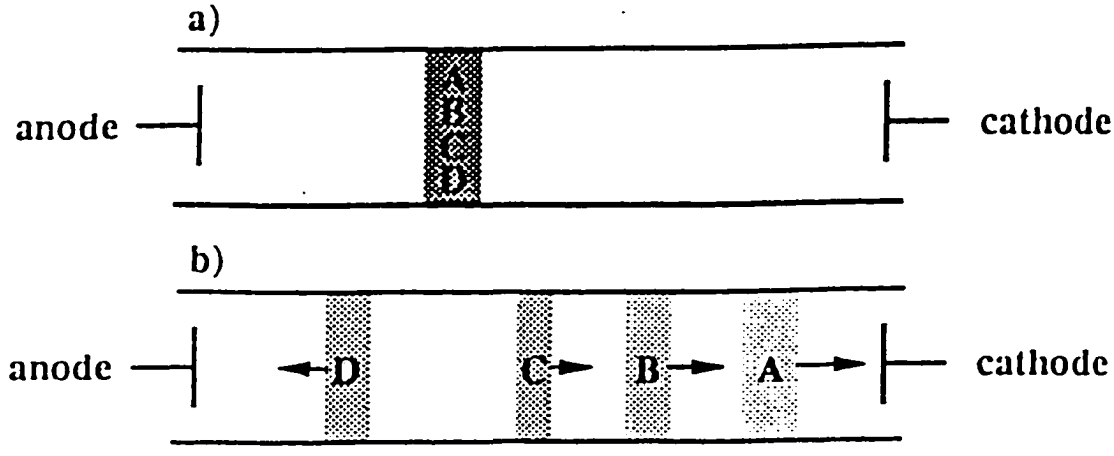

CZE

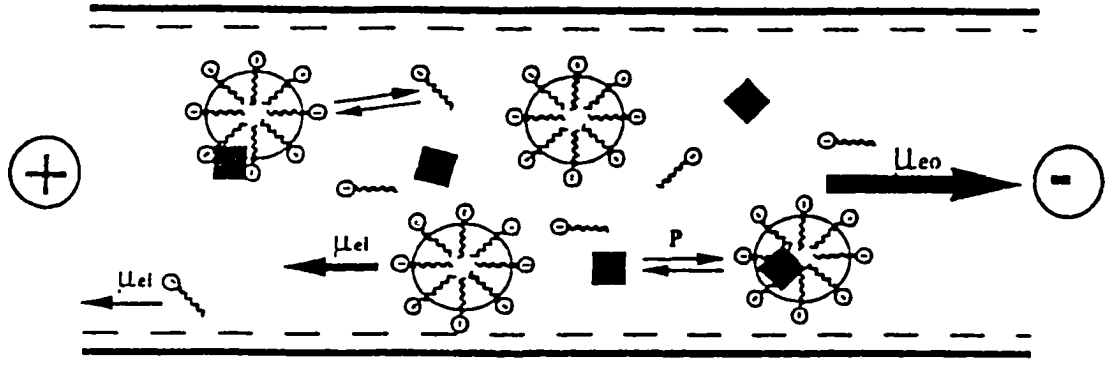

MEKC

Fig. 2.3. The schematic of capillary zone electrophoresis(CZE) and micellar electrokinetic chromatography(MEKC).

The separation of enantiomers is a difficult task in CE because the two enantiomers themselves possess identical electrophoretic mobilities in a free solution. Most of the approaches to chiral separations by CE have been borrowed from HPLC. There are two possible ways to resolve enantiomers in CE, direct chiral separation and indirect chiral separation. The latter involves derivatization of the enantiomers with chiral reagents to form diastereomers. Obviously direct separation is a more convenient technique, and it has been the main focus of attention in CE. Direct enantiomeric separation in CE can be achieved through modification of the buffer solution with a chiral additive, which forms transient diastereomeric pairs with analytes. Chiral separations in CE are achieved through various molecular interactions between the enantiomers and chiral selectors including hydrogen bonding, hydrophobic interactions, electrostatic attraction, dipole-dipole interactions and steric hindrance. A difference in stability of transient diastereomeric complexes can lead to a successful enantioseparation. The selection of appropriate chiral selectors and the suitable mode of capillary separations are the keys to the solution of difficult chiral separations. Although discovery of a universal chiral selector should be the ultimate goal for CE chiral separations, a variety of chiral selectors have been demonstrated to be quite satisfactory for specific applications. Among them, various native cyclodextrins (CDs) and their derivatives have been by far the most extensively used group of chiral selectors in CE enantiomeric separations.

In our study, we used quaternary ammonium β-cyclodextrin(Q-CD) as a chiral selector to

separate enantiomers of twelve dansyl-DL-amino acids. To elininate the electrostatic attraction between the Q-CD and the negatively charged capillary inner surface, a coated capillary was used in the study. The effects of various parameters, including Q-CD concentration, organic modifiers, temperature, field strength and buffer pH on the chiral separation were studied in some detail. In addition to the separation in the conventional CE condition that both injection and detection sides of buffer solution contain Q-CD as the chiral selector, a partial-filling method were also examined. In this method, a small amount of buffer with Q-CD is filled into the capillary as a moving zone to achieve the chiral recognition, while neither side of the buffer contains Q-CD.

2.2. Chiral selectors and mechanisms used in CE

2.2.1. The use of cyclodextrins.

Cyclodextrins are cyclic oligosaccharides prepared by hydrolytic degradation of starch using the microorganism *Bacillus macerans*. Their structures are depicted in Fig. 2.4. They are cyclic macromolecules composed of six or more D(+)-glucose residues joined by α-(1-4) glycosidic linkages. α-, β- and γ-CDs, which contain 6, 7 and 8 D-glucose units, respectively, are used as chiral selectors (shown in Fig. 2.5). The wider side of the truncated CD cone is formed by the secondary 2- and 3-hydroxyl groups and the narrow side by the primary 6-hydroxyl groups. Thus the location of the hydrophilic hydroxyl

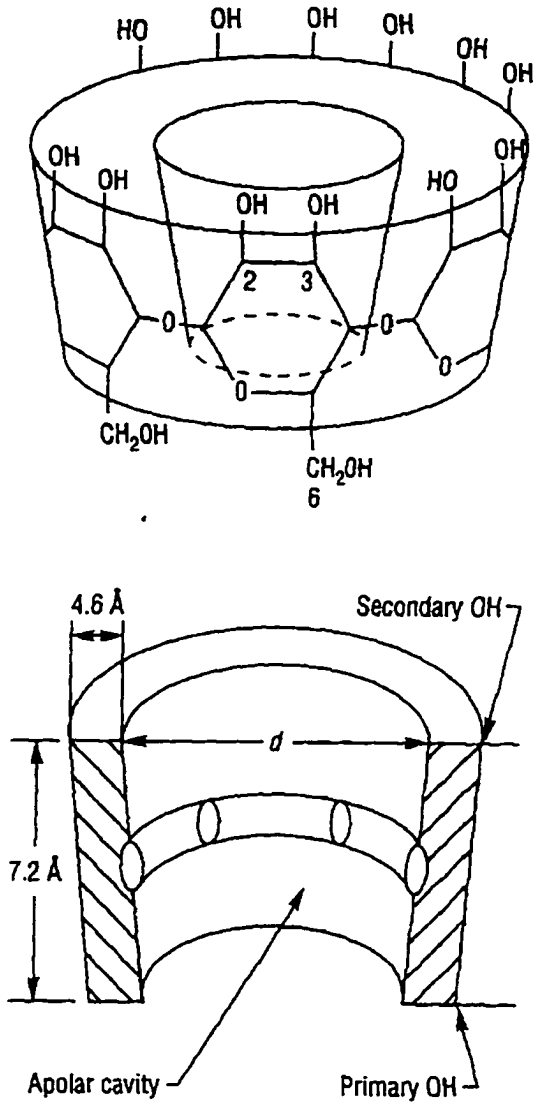

Fig. 2.4. β-Cyclodextrin structures showing the relative approximate cavity size.

(d = 0.78 nm)

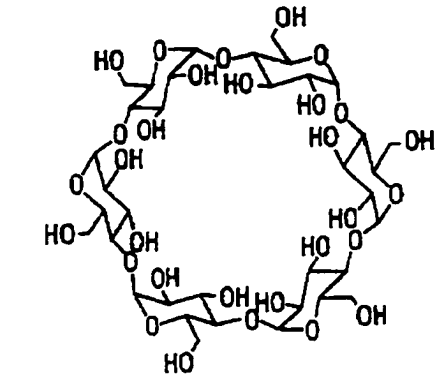

α-Cyclodextrin

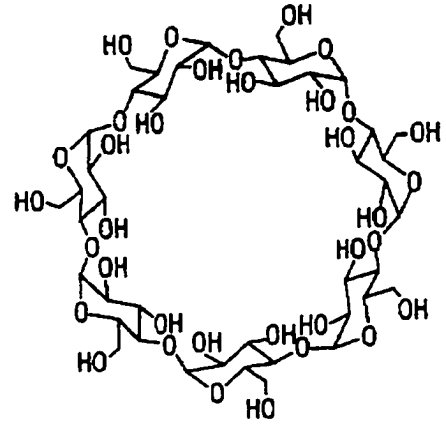

β-Cyclodextrin

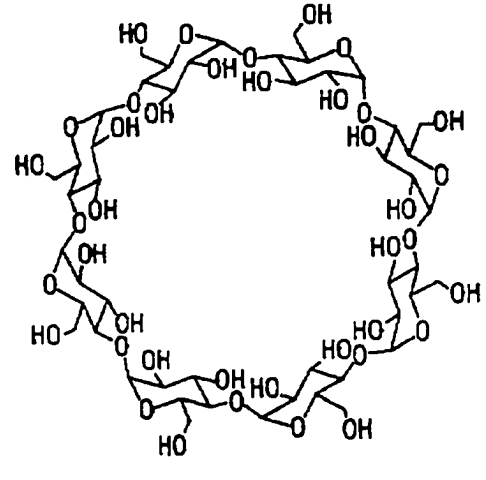

γ-Cyclodextrin

Fig. 2.5. Molecular models of α, β, γ–cyclodextrin.

groups on the outer CD rims determines their solubility in water. The inner rim of the CD cavity is lined by hydrogen atoms and the glycosidic oxygen bridges. The nonbonding electron pairs of the glycosidic oxygen are directed towards the inside of the cavity. As a result, the CD cavity is relatively hydrophobic. Intermolecular hydrogen bonds formed between the 2-hydroxyl and the 3-hydroxyl groups of adjacent glucose units maintain the remarkably rigid structure of the CDs. In addition, each D-glucose unit in the CD structure contains five chiral carbon atoms and as a result the CD macrocycle is chiral. The unique structure of CDs leads to the properties such as solubility in aqueous media, hydrophobicity of the cavity, rigid structure and chirality which are of crucial importance for this application of CDs. The ability of CDs to bind stereoselectively to chiral organic molecules has led to widespread applications in analytical science, especially for enantioseparations in GC, HPLC, SFC and CE [8,9,19-23,38]. Since the first chiral separation using CDs was accomplished by Fanali's group in CZE in 1989 [39], chiral separations using native CDs and derivatized CDs have achieved tremendous success. A wide range of chiral organic compounds have been separated using neutral CDs [39-43], charged CDs [44-47], and immobilized CDs [48-50] in various modes (CZE, MEKC, CEC, etc.) of CE.

2.2.2. Other chiral selectors used in CE

2.2.2.1. Ligand exchange

The first CE separation by ligand exchange was reported by Zare *et al.* [51] in 1985. They used an optically active copper (II) complex of L-histidine as buffer additive to separate dansyl amino acids. Later they used a copper (II) - aspartame complex system for the separation of same class of compounds [52]. There are other applications of chiral separation by ligand exchange [53,54]. The mechanism of ligand exchange can be credited to different formation or stability constants of diasteromeric complexes formed between enantiomers with identical mobility and chiral ligand.

2.2.2.2. Micellar systems

The addition of various cationic, anionic, or neutral surfactant molecules to buffer media in CE can have different beneficial effects. When the concentration of surfactant reaches the critical micelle concentration (CMC), they aggregate into micelles, and provide the primary sites of solute interaction. The micelles can act either as the major site of interaction for chiral recognition, or they can host other chiral selectors added to the separation medium. The popular chiral micelle selectors include bile salts and saponins, long alkyl chain chiral surfactants and high molecular mass chiral surfactants. A more complicated micelle system is a mixed micelle, which involves common micelle-forming surfactants used in conjunction with chiral surfactants or cyclodextrin derivatives.

Various uses of micelle systems for enantiomer separation were recently reviewed by Nishi [55].

2.2.2.3. Crown ethers

A macrocyclic ether (chiral 18-crown-tetracarboxylic acid) was used to resolve several chiral amines and aminoalcohols [56,57]. The interaction between primary amines and the crown ether cavity is based on the bonding between the hydrogen atoms of the amine group and the oxygen dipoles within the polyether ring. Chiral recognition is achieved through electrostatic interactions of the host and guest molecules.

2.2.2.4. Proteins

The idea of enantiomeric separations using proteins as chiral selectors was brought from their great success in HPLC. A protein is charged and migrates according to its electrophoretic mobility in CE. Chiral solutes, both ionic and neutral, can form transient diasteromeric complexes with the protein in dynamic equilibrium. The difference in the formation constants between the diastereomeric pair causes the difference in effective electrophoretic mobility between the enantiomers. Various proteins have been employed for the separation of enantiomers, such as bovine serum albumin (BSA), α_1-acid glycoprotein(AGP), human serum albumin, and avidin [58-60].

2.2.2.5. Macrocyclic antibiotics

Recently, several macrocyclic antibiotics and their derivatives have been shown to have good potential for chiral separations. Vancomycin, Rifamycin B, *A82846B*, and Ristocetin A have been used as chiral selectors to separate various chiral drugs [61,62]. Each of these has a glycone portion comprising fused macrocyclic rings that forms a characteristic basket shape, numerous functional groups such as hydroxyl, carboxyl and amine, and various pendant sugar moieties. Each molecule usually has many chiral centers; e.g., Ristocetin A has 38 chiral centers. The varieties of functional groups and abundance of chiral centers make macrocyclic antibiotics promising chiral selectors in CE enantiomeric separations.

2.3. Experimental section

2.3.1. Materials

2.3.1.1.Quaternary Ammonium β-Cyclodextrin (Q-CD)

Building on the success of native CDs for chiral separations, various CD derivatives such

as methylated, hydroxypropylated and hydroxyethylated CDs have been synthesized and used as chiral selectors [40-47,63]. These derivatives possess short alkyl, hydroxylalkyl, or ionic substitutents attached directly to the CD rim or connected with it via a short alkyl chain to modify the solubility and cavity dimensions to improve their chiral selectivity. Among these, the ionic CDs have attracted a great deal of attention. Ionic CDs have much higher aqueous solubility than neutral CDs, which makes it possible to use higher concentrations of chiral selectors. In addition, charged CDs migrate under the high electric fields so that the counterflow can be realized when the enantiomers carry a charge opposite to that of the CD. Static attraction can enable a stronger binding between charged CDs and chiral solutes and contribute to chiral recognition together with other molecular interactions such as hydrogen bonding and hydrophobic interaction. Mono-2-O-carboxymethyl-β-CD was used as the moving pseudostationary phase by Terabe *et al.* [64] more than ten years ago. Since then, anionic CDs have received much more attention than cationic CDs. Smith [44] described the enantioseparation of some chiral analytes using carboxymethyl-β-CD (CM-β-CD) as a chiral selector at pH 12.4. A more detailed study of carboxylated CDs as chiral selectors in CE was performed by Engelhardt and Schmidt [45,46]. Recently sulfated- and alkyl sulfated-β-CDs have been used as chiral selectors for enantiomeric separations [65]. Compared with the success of anionic CDs, the potential of cationic CDs has not yet been explored. Few papers have been published [66-68]. Among them, Fanali *et al.* [67] separated some chiral 2-hydroxy acids by using methylamino and dimethylamino-β-CDs with pH 5-7 buffers and 2-hydroxylpropyl alcohol as buffer modifier in a coated capillary. Gareil *et al.* [68] used a

mono(6-amino-6-deoxy)-β-CD as chiral selector to separate a group of chiral mandelic acid compounds in the acidic buffers and an untreated capillary. The obstacle to wide application of cationic CDs in CE chiral separation is adsorption of cationic CDs on the negatively charged capillary wall, which distorts the double layer in the capillary. As a result, the electroosmotic flow is not generated uniformly cross the capillary, and the flat flow profile is distorted. The separations lose efficiency and resolution.

In our study, we chose quaternary ammonium β-cyclodextrin (Q-CD) as the chiral selector to separate dansyl-DL-amino acids (Dns-DL-AAs). The Q-CD was kindly provided by Cerestar USA, Inc. (Hammond, IN). Its structure is given in Fig. 2.6, in which the protons on the hydroxyl groups at 2,3 and 6 positions are randomly substituted by trimethyl-2-hydroxylpropyl-amine groups with the propyl chain linked to oxygens. Because it is a quaternary amine, the Q-β-CD carries positive charges at virtually all pH values and moves electrophoretically towards the cathode in a capillary under an applied electric field. This characteristic is convenient for us to optimize the buffer pH over a wide range without having to worry about the ionization of the chiral selector. To prevent the possible adsorption of Q-β-CD on the capillary wall, we used a coated capillary which had a layer of hydrophilic polymer coated onto the inner surface of capillary. The coating polymer covers the silanol groups on the inner surface of capillary and eliminates the electroosmotic flow.

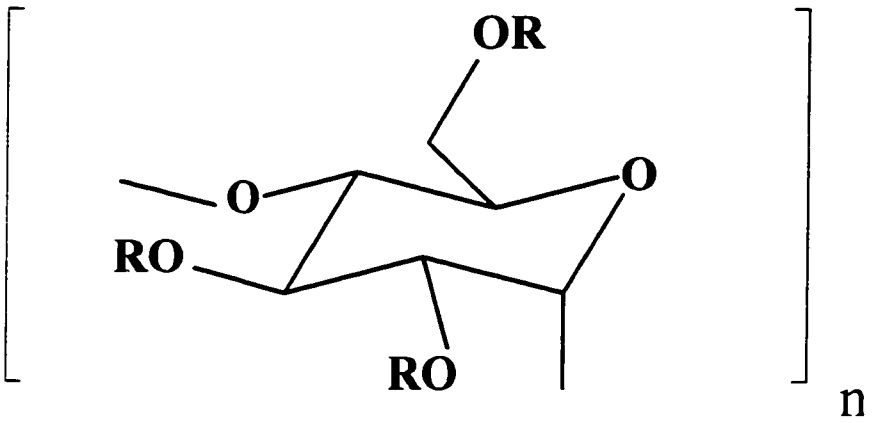

R = H or $CH_2CH(OH)CH_2N(CH_3)_3Cl$

Random substitution with average degree of substitution 3.5.

Fig. 2.6. Molecular structure of Quaternary Ammonium β-Cyclodextrin (Q-CD)

2.3.1.2. Coated capillary

The first description of a capillary with a hydrophilic coating was given by Hjerten [69]. He first used organosilane reagents such as methacryoxypropyltrimethoxysilane to react with the silanol groups on the capillary wall, then acrylamide was added to form a non-crosslinked polyacrylamide monolayer covalently bound to the capillary wall. Several analytical chemists adopted this method with minor modifications to coat capillaries for various purposes [70-71]. So far it still remains as the most common and popular coating method. The biggest the drawback of this coating is that it is not stable at high pH since Si-O-C bond is hydrolyzed in basic solution. In 1990 Novotny [72] reported an alternative coating procedure to make the coating strong enough to stand basic solution. The reactions involved three steps: (1) chlorination of the silica surface through a reaction of thionyl chloride with surface silanol groups; (2) reaction of Grignard reagent, vinyl magnesium bromide, with the chlorinated silica, resulting in direct attachment of the vinyl moiety to the silica surface; and (3) reaction of the bonded vinyl group with acrylamide, which polymerizes in a non-crosslinked manner to yield the linear polyacrylamide coating. The resulting coating with Si-C bond was reported to be stable over pH 2 - 10 [72].

During our study, we first followed Hjerten's method [35] and ran the coating reaction by

using a microsyringe to flush the reactants through the capillary. After testing our coated capillaries, we found the EOF was substantially suppressed but not totally eliminated. We then carried out the Grignard reaction described by Novotny [36]. The both ends of the capillary were inserted into sealed vials. One vial was connected to pressurized nitrogen at 100 psi, while the vial at the other end was connected to a vacuum. The coating materials were added in the vial using a microsyringe. But once we added the Grignard reagent in step 2, we found the capillary was immediately plugged. The cause might be the salt byproduct (magnesium chloride) produced from the Grignard reaction since it is insoluble in the solvent (THF). After repeated attempts we abandoned these procedures.

Throughout this study the capillaries used were kindly donated by Supelco, Inc. (Bellefonte, PA). The CElect-N column with 75 μm id from Supelco is coated with a hydrophilic layer and reported to be stable at pH 2-10.

2.3.1.3. Dansyl-DL-Amino Acids (Dns- DL-AAs)

Twelve chiral dansyl-DL-amino acids were purchased from Sigma (St. Louis, MO). They are produced by reacting native amino acids with dansyl chloride. Their structures are given in Table 2.1. Every amino acid has at least a carboxyl groups and an amine group

Table 2.1. Molecular structures of 12 Dansyl-DL-Amino Acids and their assigned peak numbers on the electropherograms

Name	Abbrev.	Peak #	Structure
Dns-DL-Aspartic Acid	Asp	1,1' (L,D)	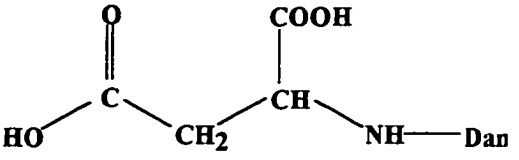
Dns-DL-α-Amino-n-Butyric Acid	Abu	2, 2' (L,D)	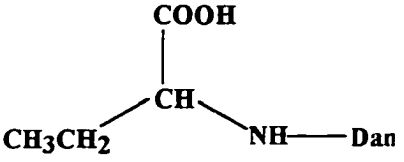
Dns-DL-Norvaline	Norval	3, 3' (L,D)	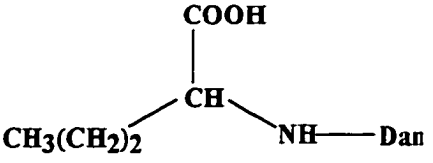
Dns-DL-Glutamic Acid	Glu	4, 4' (L,D)	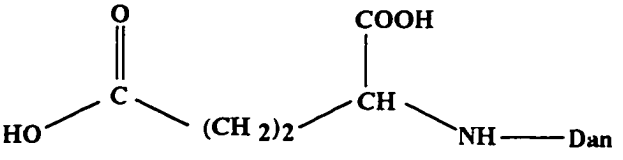
Dns-DL-Serine	Ser	5, 5' (L,D)	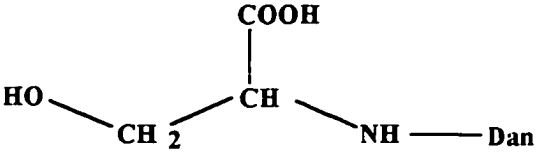
Dns-DL-Methionine	Met	6, 6' (L,D)	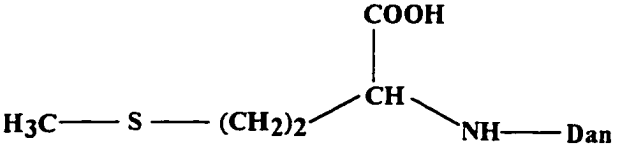
Dns-DL-Norleucine	Norleu	7, 7' (L,D)	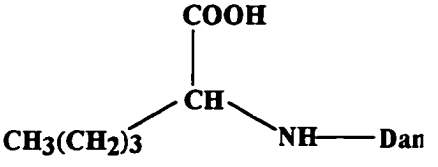

Table 2.1. Cont.

Dns-DL-Theronine	Thr	8, 8 (L,D)'	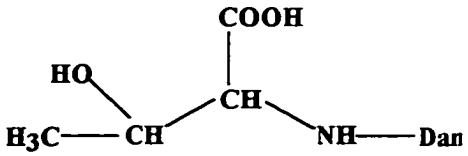
Dns-DL-Valine	Val	9, 9' (L,D)	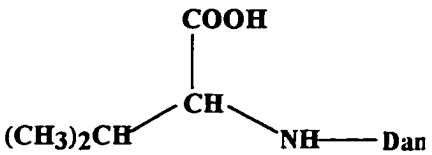
Dns-DL-Leucine	Leu	10, 10' (L,D)	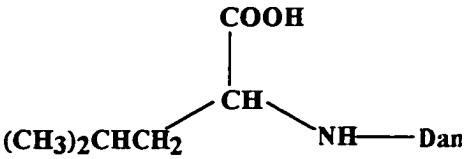
Dns-DL-Phenylalanine	Phe	11, 11' (L,D)	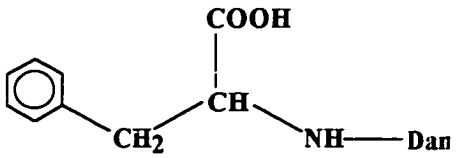
Dns-DL-Tryptophan	Trp	12, 12' (L,D)	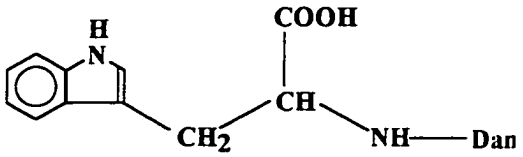
Dansyl group	Dns		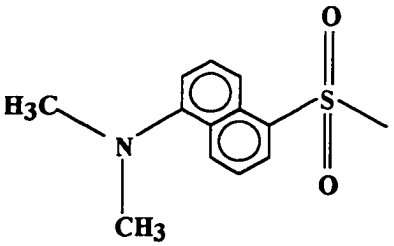

as well as possible other functional groups such as aromatic and hydroxyl group, which are common functional groups for pharmaceutical organics. Amino acids can act as either bases or acids in aqueous solution. In addition, as zwitterions, amino acids can be either cations or anions depending on the buffer pH. Dns-DL-AAs have been resolved using different chiral selectors or buffer systems in CE [73-78]. Tananka *et al.* [73] used neutral CDs such as heptakis-β-CD and methylated-β-CD (>10 mM) as chiral selectors to separate the same group of Dns-DL-AAs we chose, using an uncoated capillary and a pH 9.0 buffer solution. Baseline separations were obtain only for DL-asparic acid and DL-glutamic acid, and some of the other amino acids were partially separated. Karger *et al.* [75] resolved twelve pairs of Dns-DL-AAs by using 100 mM native β-CD in a polyacrylamide gel-filled capillary.

2.3.2. Apparatus and experimental

All separations were performed using a Perkin-Elmer Applied Biosystems 270A-HT capillary electrophoresis system (Foster City, CA) with forced air temperature control. Data was acquired and analyzed using Perkin-Elmer Turbochrom software on a Dell Dimension P133v computer via a PE Nelson 900 interface and 600 LINK. The maximum run time for each run is set to 100 minutes by the manufacturer. As mentioned before, the coated capillaries were provided by Supelco (Bellefonte, PA) and cut to 48 cm

total length with 27.5 cm between injector and detector except as noted otherwise. The detection window was formed by burning off a small portion (about 1 cm) of polyimide coating of the capillary using a low flame. 30 mM phosphate buffer was prepared by dissolving sodium hydrogen phosphate (J.T. Baker, Phillipsburg, NJ) in deionized water and adjusting the pH to 7 using 12 M hydrochloric acid. 30 mM acetate buffer was prepared by dissolving sodium acetate (Fisher Scientific, Springfield, NJ) in deionized water and adjusting the pH to 5 using glacial acetic acid (EM Science, Gibbstown, NJ). Quaternary-ammonium-β-CD was a gift from Cerestar, USA (Hammond, IN), and was used as supplied. All buffers were filtered through 0.45 μm syringe filters (Chromacol, Trumbull, CT) and degassed in an ultrasonicator before use. All Dns-DL-AA standards were purchased from Sigma (St. Louis, MO) and dissolved in 1 mM phosphate buffer to approximately 10-20 ppm. Vacuum injection time was 1 s at 5 mm Hg. The detection wavelength was set at 254 nm. All separations were performed at 30 °C and 15 kV reversed polarity unless noted otherwise. The capillary was flushed with acetonitrile, deionized water and the running buffer consecutively for three minutes each between runs. The experimental conditions are summarized in Table 2.2.

Since there is no electroosmotic flow in a coated capillary, the apparent mobility is the same as the effective mobility, and was calculated from:

$$\mu = Ll/tV \qquad (4)$$

Table 2.2. Experimental conditions of capillary electrophoresis

Capillary	Supelco CElect-N column;
	total length = 48 cm; effective length = 27.5 cm
Applied voltage	-15 kV
Buffer	30 mM phosphate at pH 7
Injection	vacuum injection at 5 mm Hg; injection time 1 s
Detection	UV detection; detection wavelength = 254 nm
Temperature	30 °C

where L is the total length of the capillary, l is the length between the injection and detection window, t is the migration time and V is the applied voltage.

Adding Q-CD changes the viscosity of the background electrolyte (BGE), which affects the effective electrophoretic mobility of the analytes. The corrected value of the mobility, μ_c, can be obtained by using equation [85,92]:

$$\mu_c = \mu\eta_c/\eta_o, \qquad (5)$$

where μ is the measured effective electrophoretic mobility, η_c and η_o are the viscosities of the BGE with and without the chiral selector, Q-CD. To obtain the viscosity ratio, different approaches have been carried out experimentally, such as using the ratio of currents of BGE [79,88], using a mobility standard [93], measuring the change of electroosmotic flow [94], and using a viscometer [81,95]. In our study, the viscosity correction was performed by using the method described by Fanali and Bocek [96]. Buffers having various concentrations of Q-CD were sucked into an empty vial in the detection side buffer for 30 min by maintaining a constant vacuum of 20 mm Hg at 30 °C. The volumes of the solution collected were calculated from the weight (W) of the solutions, which were determined by weighing the vial before and after sampling. The corrected mobilities are then calculated as follows:

$$\mu_c = \mu\eta_c/\eta_o = \mu V_o/V_c = \mu(W_o/W_c)(\rho_c/\rho_o), \qquad (6)$$

where W and ρ stand for weight and density of BGE respectively.

The resolution, R_S, was calculated using the following equation:

$$R_S = 2\Delta t/(W_D + W_L), \quad (7)$$

where Δt is the migration time difference of two enantiomers, and W_D and W_L are the peak widths measured at the baseline.

2.4. Theory

Although chiral separations by capillary electrophoresis has received a great deal of attention, the theoretical aspects of the separation are not very clear. Several models have been proposed [79-91]. The model of Wren and Rowe [79-83] was intended to cover a simple situation where a freely soluble analyte interacts on a 1:1 basis with a single chiral selector. The model is summarized below:

$$R + C \xleftrightarrow{K_R} RC \quad (8)$$

$$S + C \xleftrightarrow{K_S} SC \quad (9)$$

where R and S represent a pair of enantiomers and C is the chiral selector. K_R and K_S are the equilibrium association constants. Because the binding between each enantiomer and chiral selector is a dynamic equilibrium, the apparent electrophoretic mobility of each

enantiomer can be expressed as:

$$\mu_R = \frac{[R]}{[R]+[RC]}\mu_R^o + \frac{[RC]}{[R]+[RC]}\mu_{RC}^o \qquad (10)$$

$$\mu_S = \frac{[S]}{[S]+[SC]}\mu_S^o + \frac{[SC]}{[S]+[SC]}\mu_{SC}^o \qquad (11)$$

where μ_R and μ_S are apparent electrophoretic mobilities (the measured mobilities which are controlled by electrophoretic and electroosmotic mobilities), superscript ^{o} represents the solution without chiral selector C ($\mu_R^o = \mu_S^o = \mu^o$), and μ_{RC} and μ_{SC} are the electrophoretic mobilities of the enantiomer-chiral selector complex. Assuming the *RC* and *SC* complexes have the same molecular size and shape in free solution, then

$$\mu_{RC} = \mu_{SC} = \mu_C \qquad (12)$$

The apparent mobility difference between the two enantiomers is:

$$\Delta\mu = \frac{[C](\mu'' - \mu_C)(K_R - K_S)}{1 + [C](K_R + K_S) + K_R K_S [C]^2} \qquad (13)$$

From equation (13), we see chiral separation will not take place if the enantiomers and enantiomer-chiral selector complex have the same mobilities, or if the equilibrium constants of two enantiomers are same.

The above model of Wren and Rowe can help one understand the key point of chiral separations by CE, which is the dynamic differential binding equilibrium between the enantiomers and chiral selector. When the concentration of chiral selector is too low, the equilibrium will be driven to the free enantiomer side so that both μ_D and μ_L will be close to μ^o. When the concentration of chiral selector is too high, the equilibrium will be driven to the enantiomer-chiral selector complex side and both μ_D and μ_L will be close to μ_C. At an intermediate condition, successful chiral separation may be achieved. From equation (6), w can find the optimum concentration of chiral selector by taking the derivative of $\Delta\mu$ with respect to *[C]* and setting it equal to zero, then

$$[C]_{opt} = \sqrt{\frac{1}{K_R K_S}} \qquad (14)$$

It is extremely important to choose appropriate concentration of chiral selector to obtain the chiral selectivity. From equation (14), we can easily find the optimum concentration for chiral selector once we know its binding constant for each enantiomer.

One of assumptions of Wren and Rowe's model is that a single enantiomer can exist in only one form which interacts with the chiral selector. But in cases where molecules undergo proton transfer, their dissociated and undissociated forms can coexist and can interact differently with the chiral selector. Rawjee and Vigh [89-91] took into account the effects of both pH and chiral selector concentration. They pointed out that both factors played important roles on chiral selectivity for weak acids and weak bases.

Considering the case of a pair of Dns-DL-AA , two enantiomers, *HD* and *HL*, dissociate as follows:

$$HD + H_2O \longleftrightarrow H_3O^+ + D^- \quad (15)$$

$$HL + H_2O \longleftrightarrow H_3O^+ + L^- \quad (16)$$

During chiral separation, quaternary ammonium β-cyclodextrin ($Q\text{-}CD^+$) complexes with both the protonated and the deprotonated forms of the enantiomers as follows:

$$D^- + nQCD^+ \xleftrightarrow{K_D} D^-(QCD^+)_n \quad (17)$$

$$L^- + nQCD^+ \xleftrightarrow{K_L} L^-(QCD^+)_n \quad (18)$$

$$HD + n'QCD^+ \xleftrightarrow{K'_D} HD(QCD^+)_{n'} \quad (19)$$

$$HL + n'QCD^+ \xleftrightarrow{K'_L} HL(QCD^+)_{n'} \quad (20)$$

Where K'_D and K'_L are the binding constants of protonated enantiomers with Q-CD, and K_D and K_L are the binding constants of deprotonated enantiomers with Q-CD. Taking these factors into consideration, the total concentrations of two enantiomers of a Dns-DL-AA, are

$$C_D = [D^-] + [D^-QCD^+_n] + [HD] + [HD^-QCD^+_{n'}] \quad (21)$$

$$C_L = [L^-] + [L^-QCD^+_n] + [HL] + [HLQCD^+_n] \quad (22)$$

Although the pK_as of Dns-DL-AAs are not available, it was proved by our experiments that all the Dns-DL-AAs carry negative charges and migrate anodically under electric field when buffer pH is higher than 5. Therefore At pH 7, virtually all the Dns-DL-AAs exist as deprotonated forms, $[D^-] >> [HD]$. In this case, it is reasonable to make the approximation that Q-CD interacts only with the deprotonated enantiomers, $[D^-QCD^+] >> [HDQCD^+]$. Then at pH7. C_D can be simplified as:

$$C_D = [D^-] + [D^-QCD^+_n] \quad (23)$$

and

$$C_L = [L^-] + [L^-QCD^+_n] \quad (24)$$

The effective electrophoretic mobility of each enantiomer can be expressed as the sums of the mole fraction-weighted ionic mobility of the respective species:

$$\mu_D = \mu^\circ_D \alpha_D + \mu_{DQ}\alpha_{DQ} \quad (25)$$

where μ_{DQ} is the mobility of enantiomer-QCD complex, μ°_D is the mobility of the enantiomer in free solution, and

$$\alpha_D = [D^-] / ([D^-]+[D^-QCD^+_n]) = 1/(1+K_D[QCD]^n) \quad (26)$$

$$\alpha_{DQ} = [D^-QCD^+_n]/([D^-]+[D^-QCD^+_n]) = K_D[QCD]^n/(1+K_D[QCD]^n) \quad (27)$$

By combining equations (25)-(27), we have:

$$\mu_D = \frac{\mu_D^{\circ} + \mu_{DQ} K_D [QCD]^n}{1 + K_D [QCD]^n} \tag{28}$$

In the same fashion, μ_L can be determined as:

$$\mu_L = \frac{\mu_L^{\circ} + \mu_{LQ} K_L [QCD]^n}{1 + K_L [QCD]^n} \tag{29}$$

The chiral separation selectivity can be expressed as the ratio of the effective mobility of two enantiomers, $A_{D/L} = \mu_D / \mu_L$ as follow:

$$A_{\frac{D}{L}} = \frac{1 + \frac{\mu_D}{\mu^{\circ}} K_D [QCD^+]^n}{1 + \frac{\mu_L}{\mu^{\circ}} K_L [QCD^+]^n} \cdot \frac{1 + K_L [QCD^+]^n}{1 + K_D [QCD^+]^n} \tag{30}$$

where $\mu^{\circ} = \mu^{\circ}_D = \mu^{\circ}_L$.

To determine the binding constants and the mobilities of enantiomer-QCD complex, we can rearrange equation (28) and obtain:

$$\mu_D = \frac{1}{K_D} \left(\frac{\mu_D^{\circ} - \mu_D}{[QCD^+]^n} \right) + \mu_{DQ} \tag{31}$$

If we assign the part in the parenthesis to be X, we can plot μ_D as a function of X to get

K_D from the slope and μ_{DQ} from the intercept. These values can be plugged into equation (30) to calculate the mobility ratio, $A_{D/L}$, which can be compared with the experimental mobility ratio.

2.5. Results and discussion

2.5.1. Effect of Q-CD concentration

The enantiomers of the 12 dansyl-DL-amino acids were studied at pH 5 and 7 by free solution capillary electrophoresis with various amounts of Q-CD. At both pHs the carboxyl groups of all the Dns-DL-AAs are dissociated and thus the Dns-DL-AAs migrate anodically in the absence of electroosmotic flow. With no Q-CD added, none of the enantiomers were resolved in accordance with the fact that the enantiomers possess identical physico-chemical properties and electrophoretic mobilities. Glu and Asp (see Table 2.1 for abbreviations) migrated with faster velocities than the others did since they have two carboxyl groups, which provides a higher charge/mass ratio. In the presence of Q-CD, the migration of Dns-DL-AAs is retarded due to their binding with the cyclodextrin derivative. Based on the literature results [75,97], the D enantiomer of a dansyl amino acid experiences stronger complexation neutral β–CD than the L enantiomer does. By the structural analogy between native β –CD with our Q-CD, we think it is reasonable to

believe that the L enantiomer elutes faster than the D enantiomer. The plots of electrophoretic mobility of Dns-DL-AAs vs. the concentration of Q-CD ([Q-CD]) in 30 mM phosphate buffer at pH 7 is given in Figs. 2.7a - 2.7i. The mobility of all the Dns-DL-AAs decreased substantially with increasing [Q-CD]. For instance, the mobility of Dns-DL-Aspartic Acid (Asp) drops from 27.8 x 10^{-5} cm^2/sV with no Q-CD present in the buffer to 3.7 x 10^{-5} cm^2/sV for the second eluted enantiomer (D-Asp) with 3 mM Q-CD. With 4 mM Q-CD,only two (Asp and Thr) of the twelve Dns-DL-AAs eluted within 100 minutes. At higher concentrations of [Q-CD], the mobility of Dns-AAs is extremely low, and some of them are carried by the Q-CD to the cathode.

Fig. 2.8a-c shows the electropherograms of the Dns-DL-AAs at Q-CD concentrations over the range of 0.2-3.0 mM. Fig. 2.9 shows the relationship between resolution and [Q-CD], where baseline resolution is indicated by $R_S > 1$. All the enantiomers are well resolved ($R_S > 1$) in the presence of 1 mM Q-CD, and the resolution gradually increases with [Q-CD]. Baseline chiral resolution of all 12 pairs of Dns-DL-AAs were obtained with [Q-CD] = 1 mM or lower. The significantly greater chiral selectivity of quaternary ammonium β-cyclodextrin (Q-CD) over native cyclodextrin and other CD derivatives in counterflow capillary electrophoresis can be credited to two factors. First, the electrostatic attraction between cationic Q-CD and anionic Dns-DL-AAs not only allows the enantiomers easy landing on the CD derivative to trigger the molecular interactions, but provides a strong point of molecular interaction needed to achieve chiral recognition.

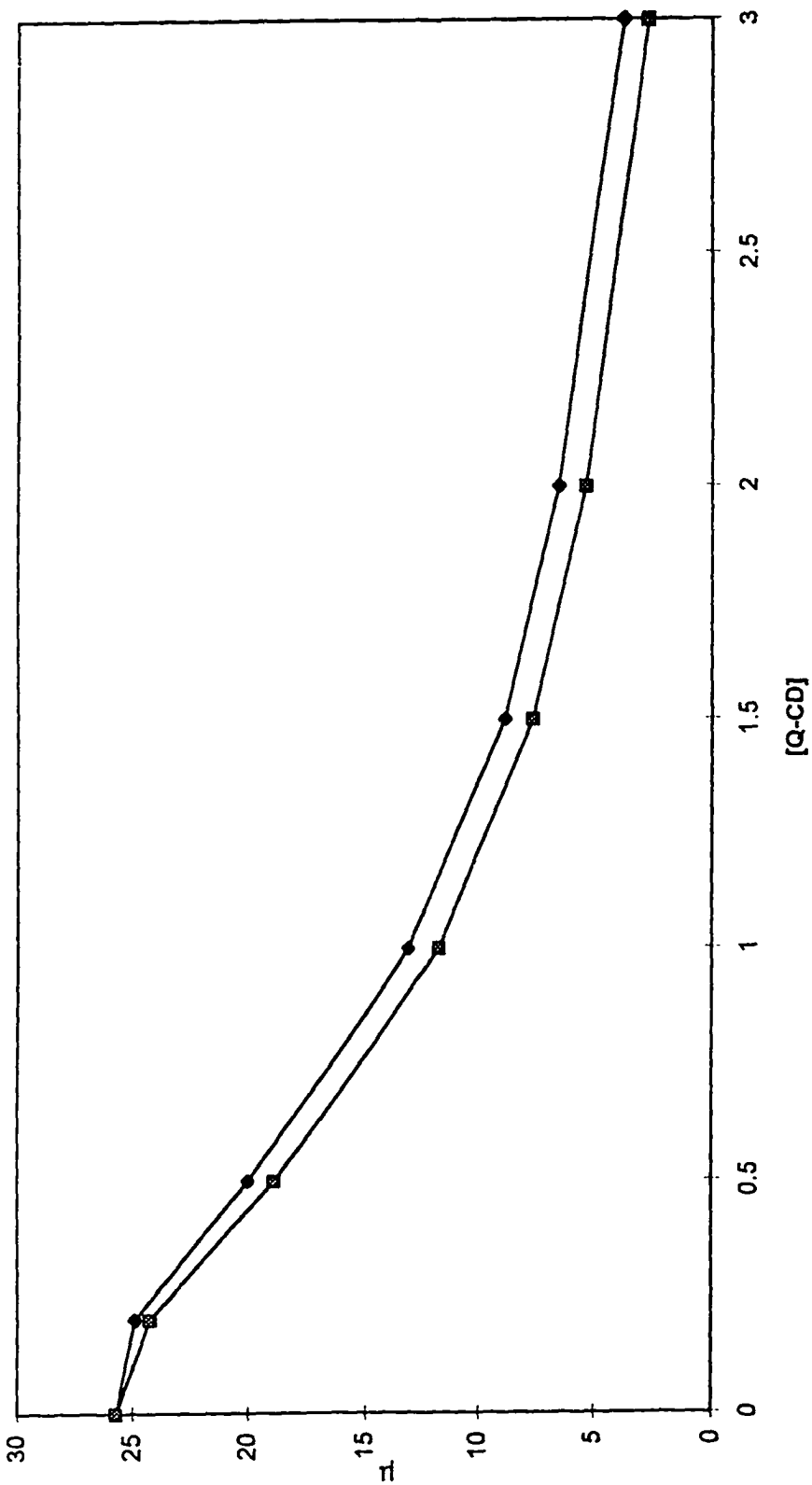

Fig. 2.7a. Mobilities (10^{-5} cm^2 S^{-1} V^{-1}) of Dns-DL-Aspartic Acid(upper line: L; lower line: D) vs. the concentration of Q-CD (mM). The experimental conditions are in Table 2.2.

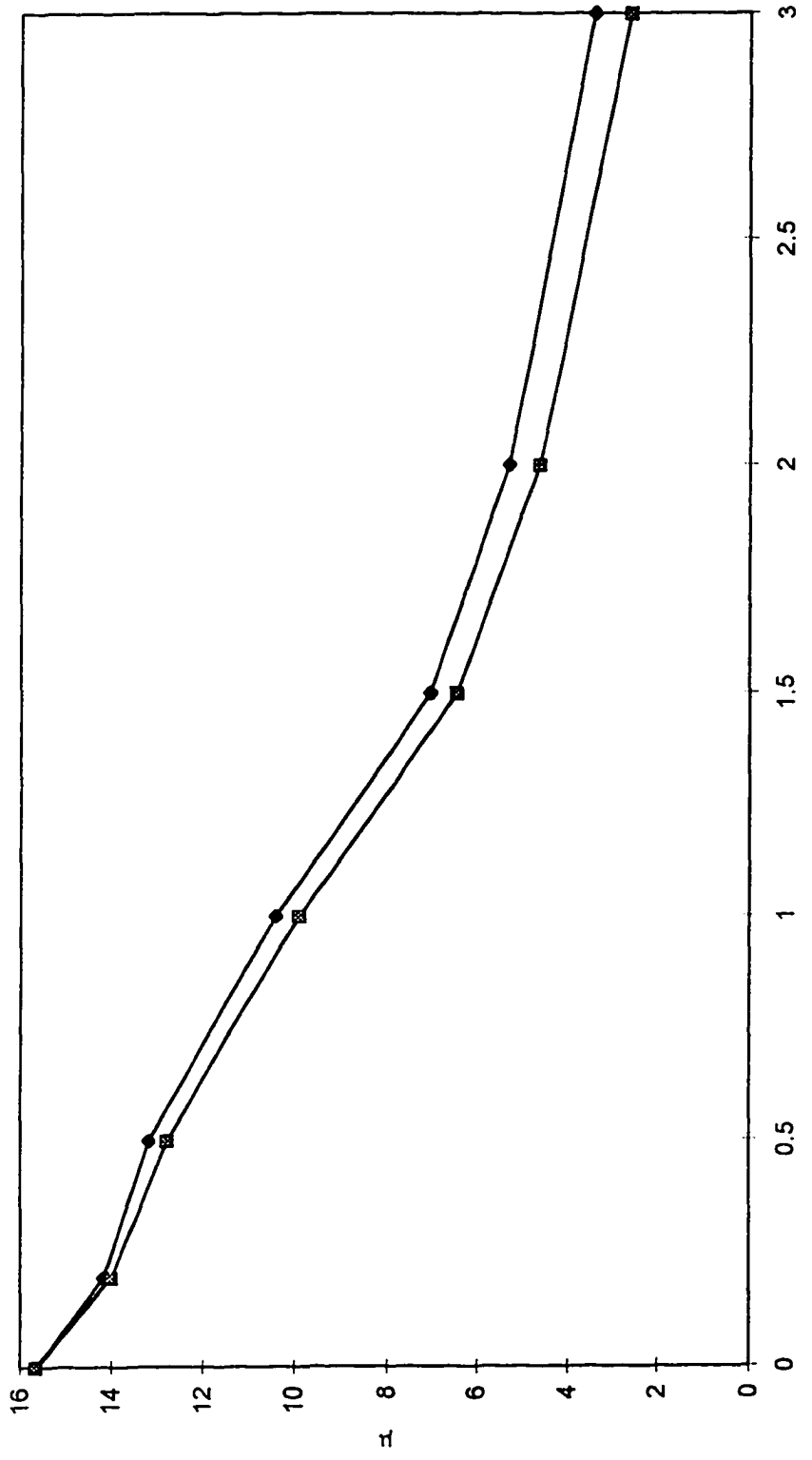

Fig. 2.7b. Mobilities (10^{-5} cm^2 S^{-1} V^{-1}) of Dns-DL-α-Amino Butyric Acid(upper line: L; lower line: D) vs. the concentration of Q-CD (mM). The experimental conditions are in Table 2.2.

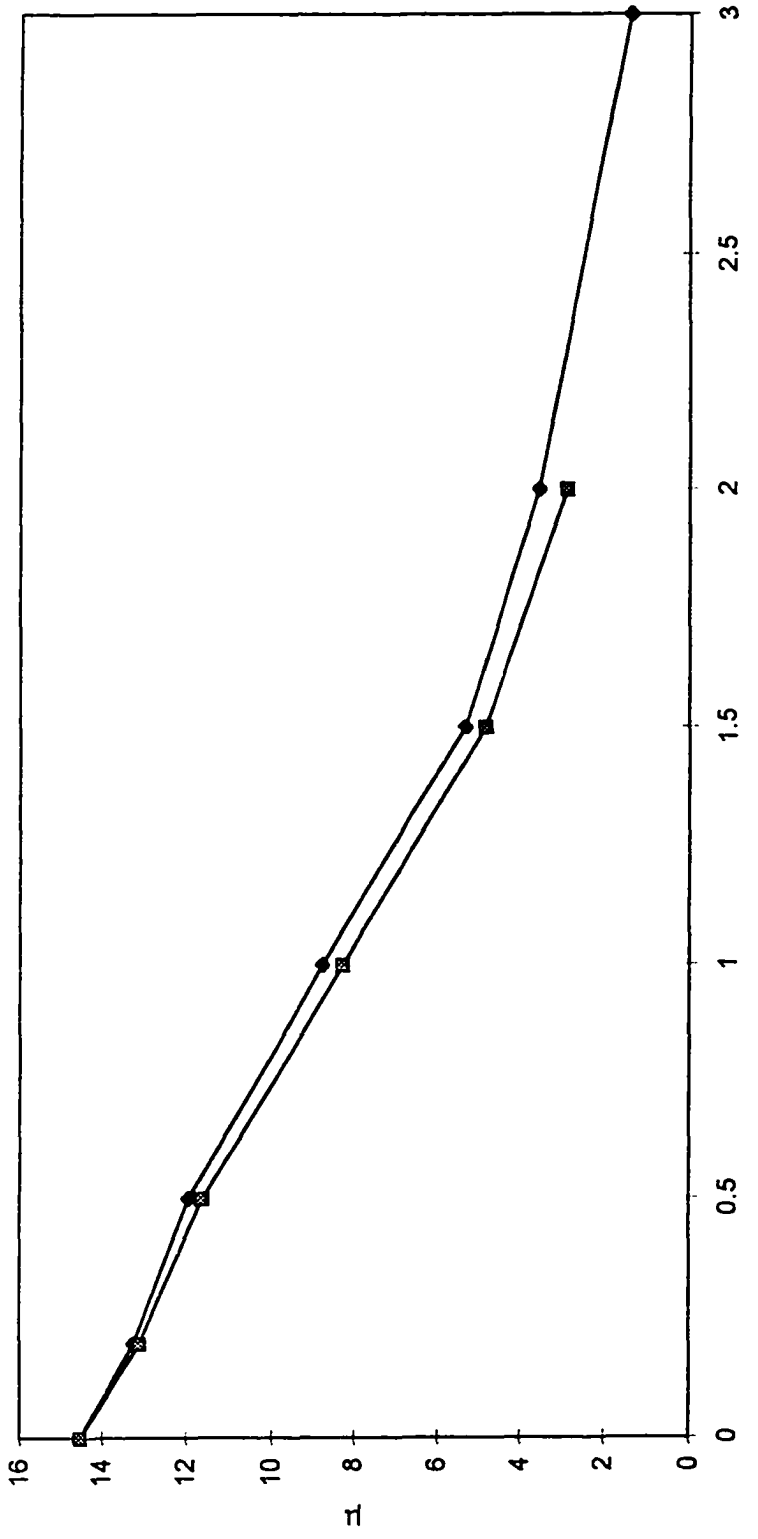

Fig. 2.7c. Mobilities (10^{-5} cm^2 S^{-1} V^{-1}) of Dns-DL-Norleucine(upper line: L; lower line: D) vs. the concentration of Q-CD (mM). The experimental conditions are in Table 2.2.

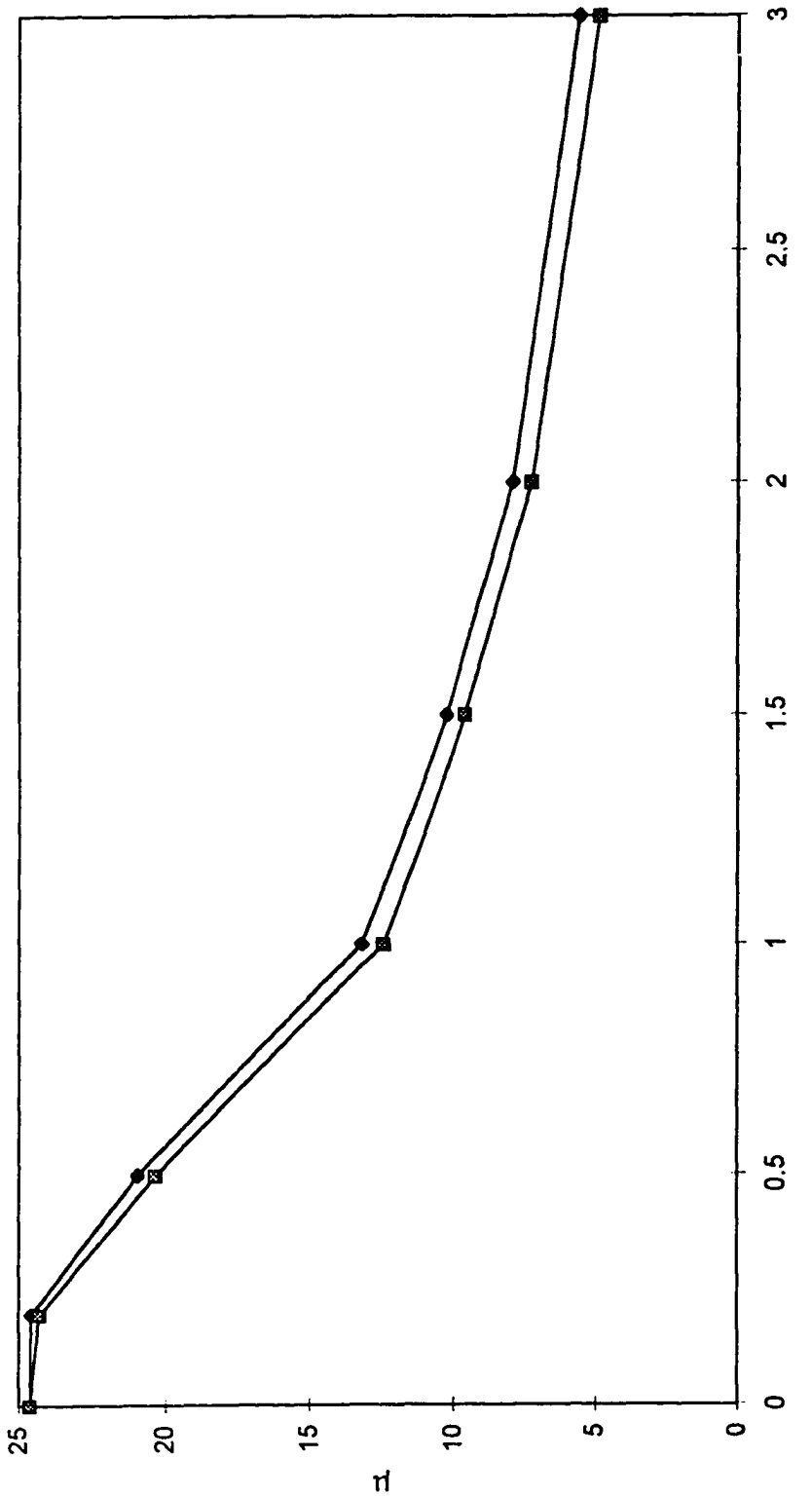

Fig. 2.7d. Mobilities (10^{-5} cm^2 S^{-1} V^{-1}) of Dns-DL -Glutamic Acid(upper line: L; lower line: D) vs. the concentration of Q-CD (mM). The experimental conditions are in Table 2.2.

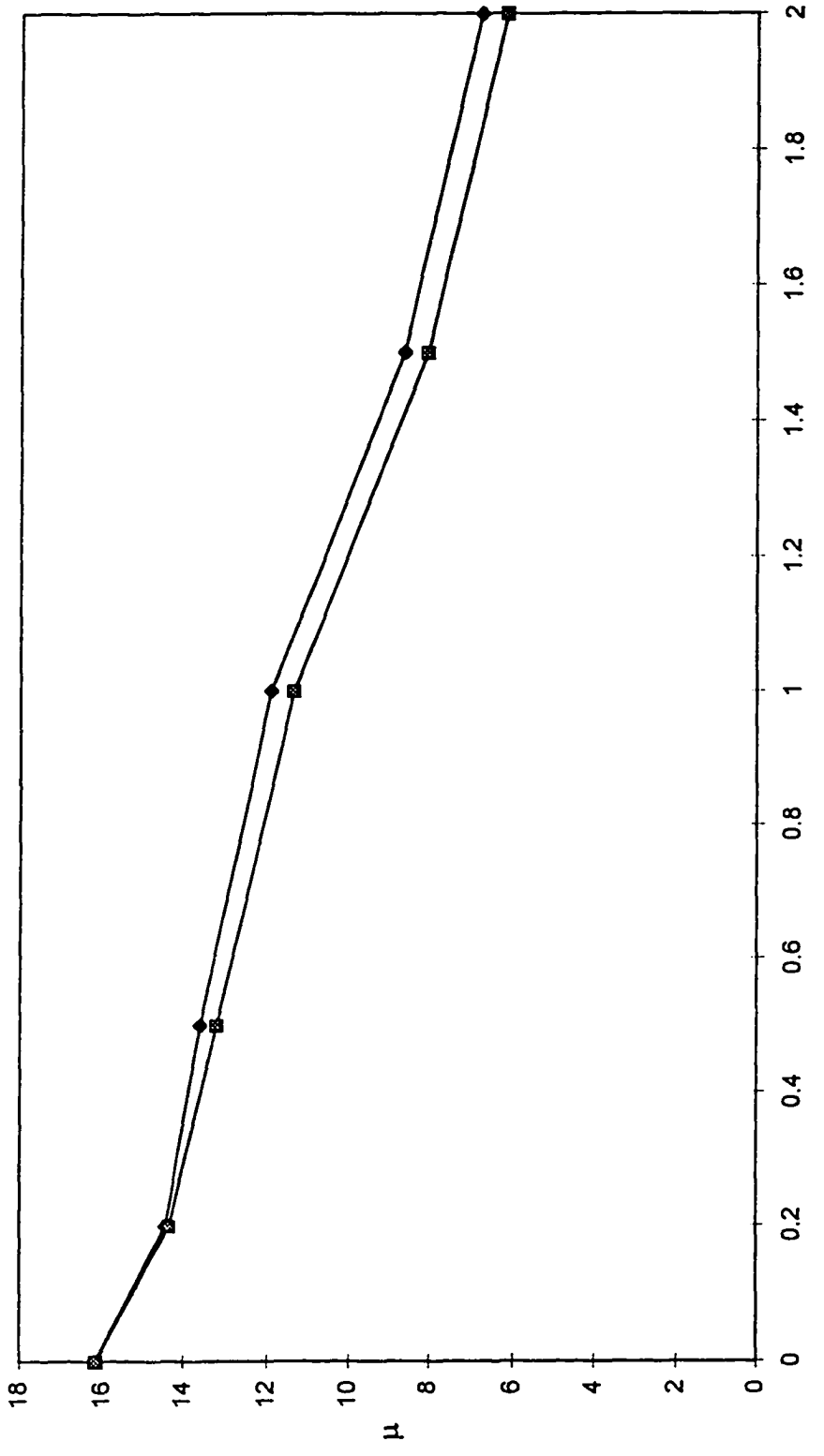

Fig. 2.7e. Mobilities (10^{-5} cm^2 S^{-1} V^{-1}) of Dns-DL-Serine(upper line: L; lower line: D) vs. the concentration of Q-CD (mM). The experimental conditions are in Table 2.2.

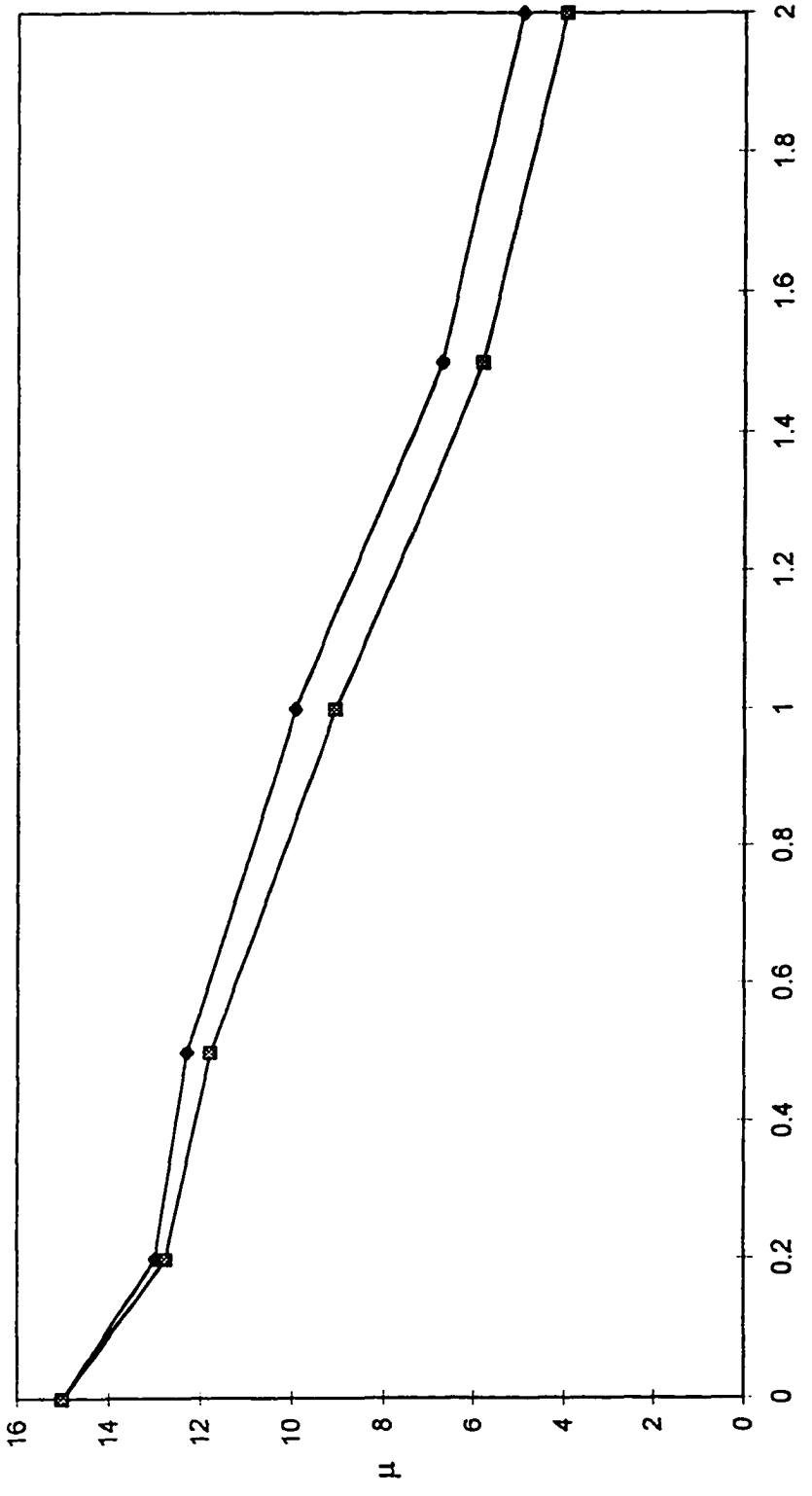

Fig. 2.7f. Mobilities (10^{-5} cm^2 S^{-1} V^{-1}) of Dns-DL-Methionine(upper line: L; lower line: D) vs. the concentration of Q-CD (mM). The experimental conditions are in Table 2.2.

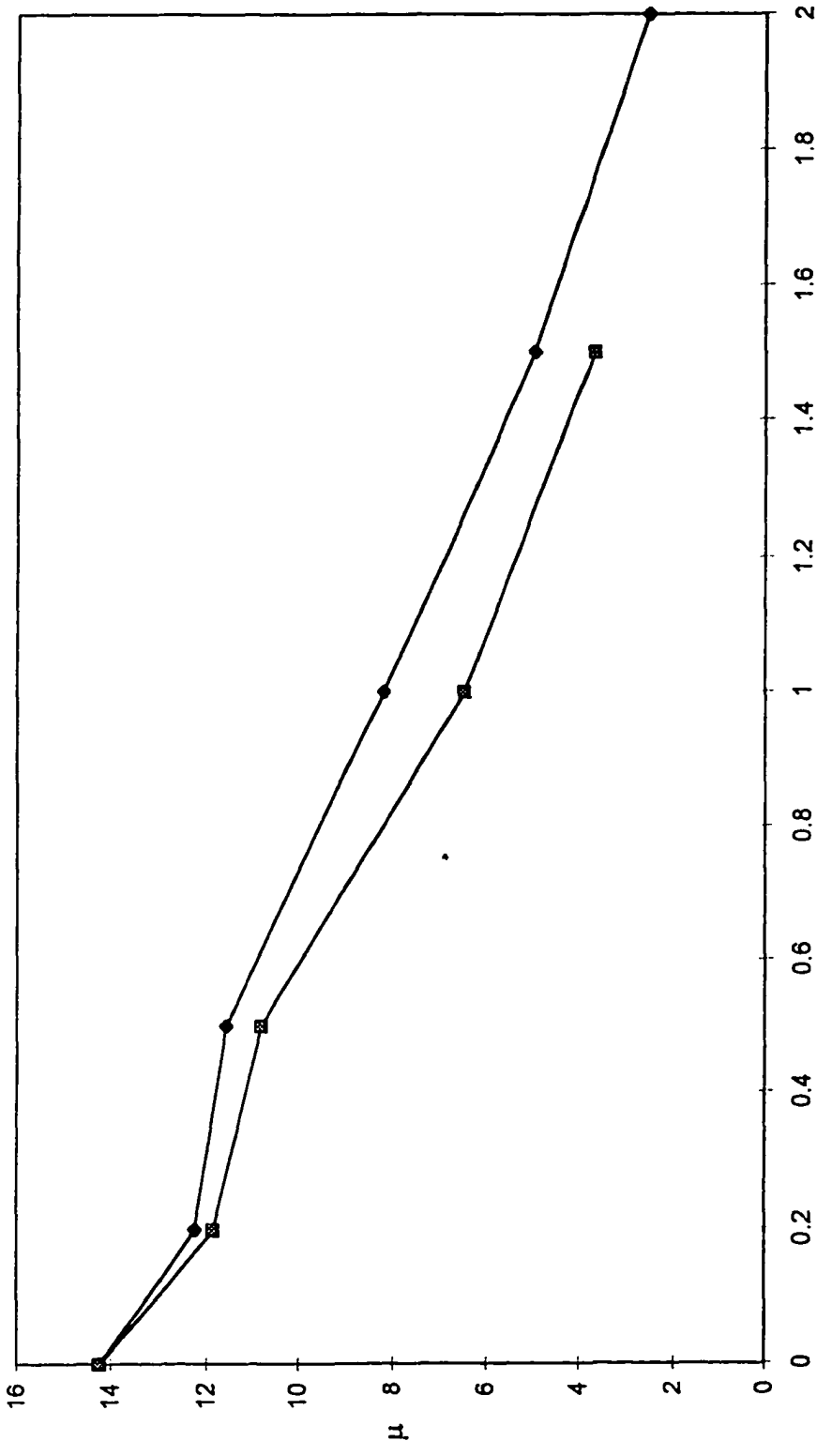

Fig. 2.7g. Mobilities (10^{-5} cm^2 S^{-1} V^{-1}) of Dns-DL-Norvaline(upper line: L; lower line: D) vs. the concentration of Q-CD (mM). The experimental conditions are in Table 2.2.

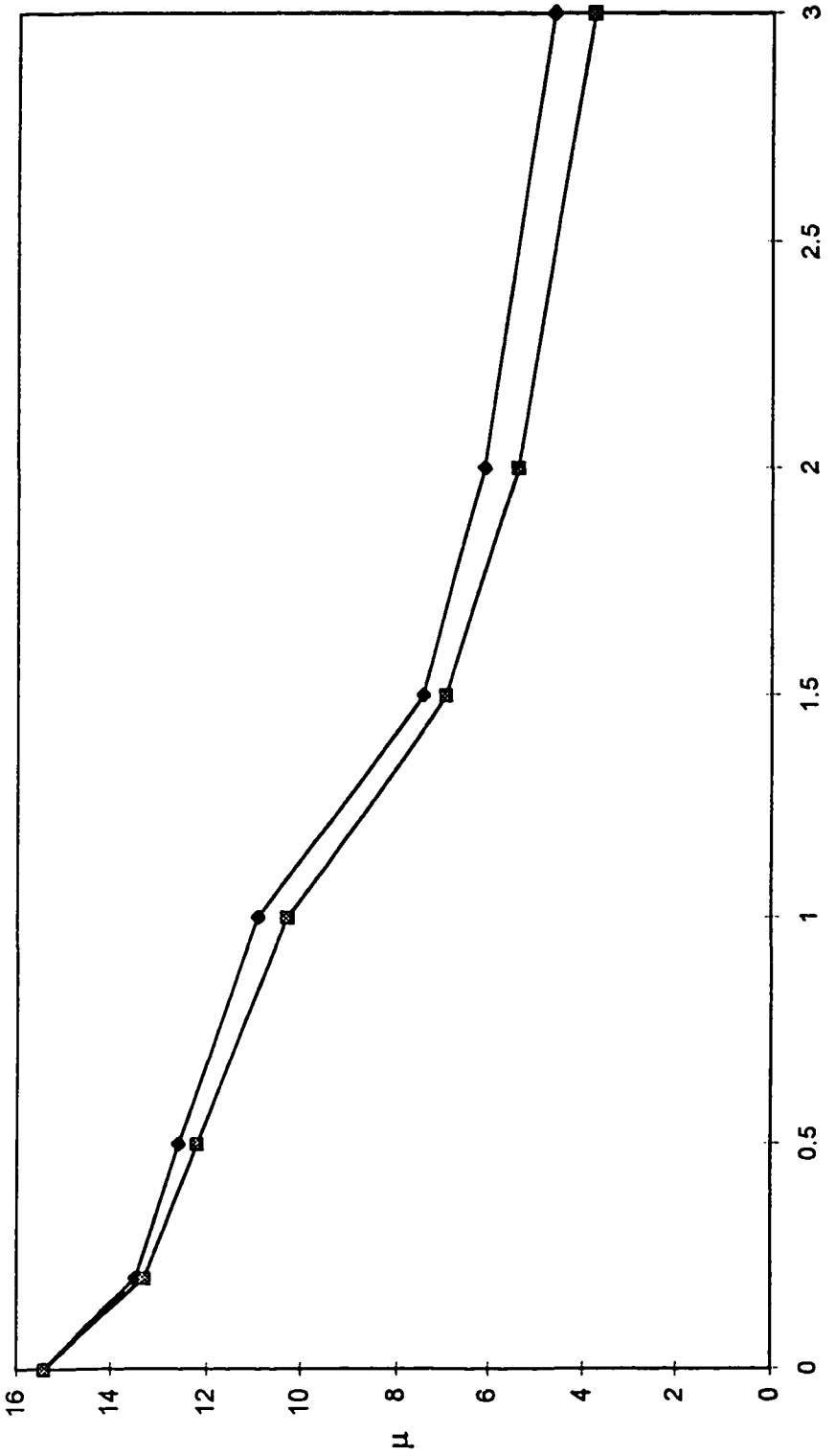

Fig. 2.7h. Mobilities (10^{-5} cm^2 S^{-1} V^{-1}) of Dns-DL-Threonine(upper line: L; lower line: D) vs. the concentration of Q-CD (mM). The experimental conditions are in Table 2.2.

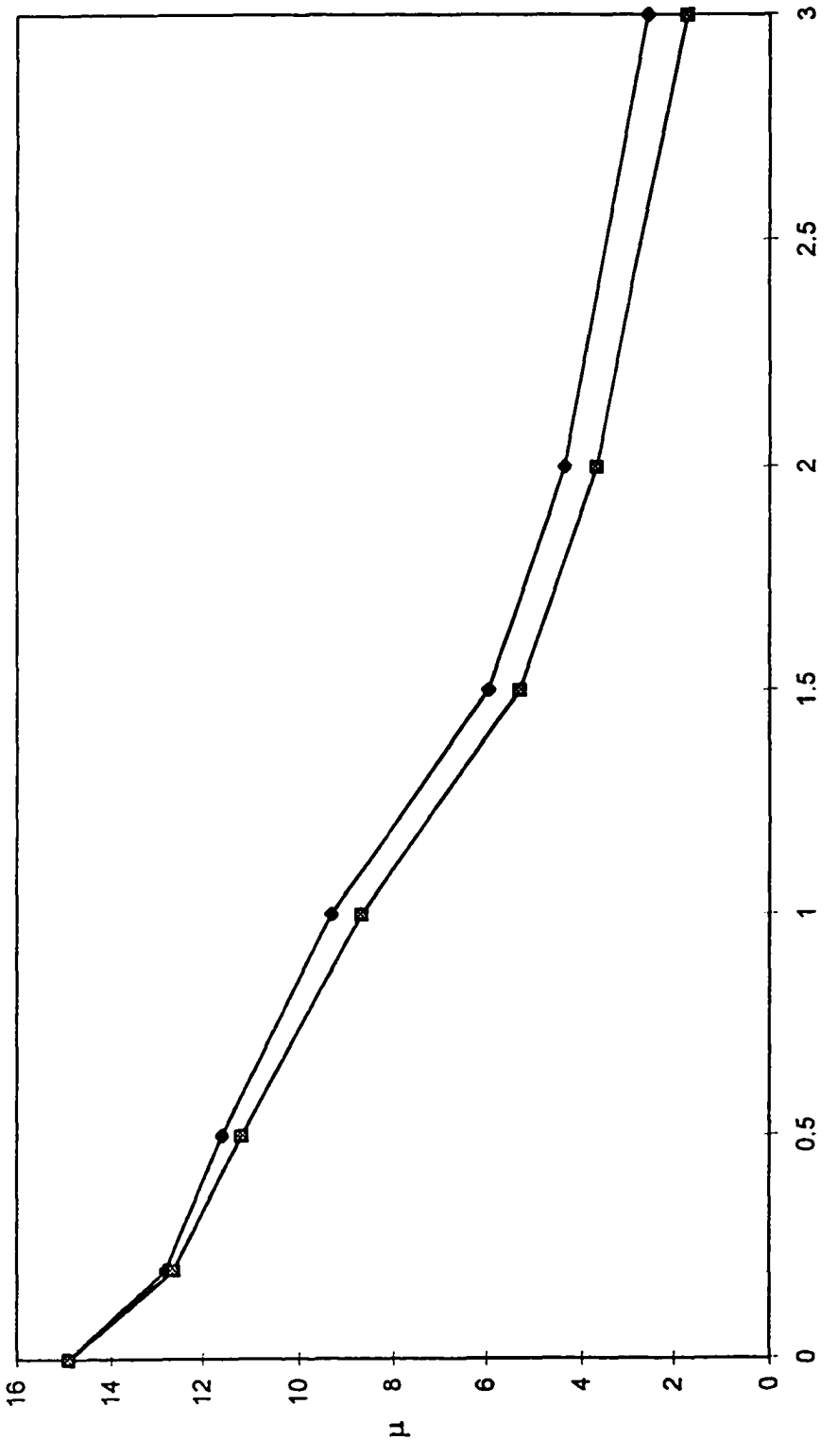

Fig. 2.7i. Mobilities (10^{-5} cm^2 S^{-1} V^{-1}) of Dns-DL-Valine(upper line: L; lower line: D) vs. the concentration of Q-CD (mM). The experimental conditions are in Table 2.2.

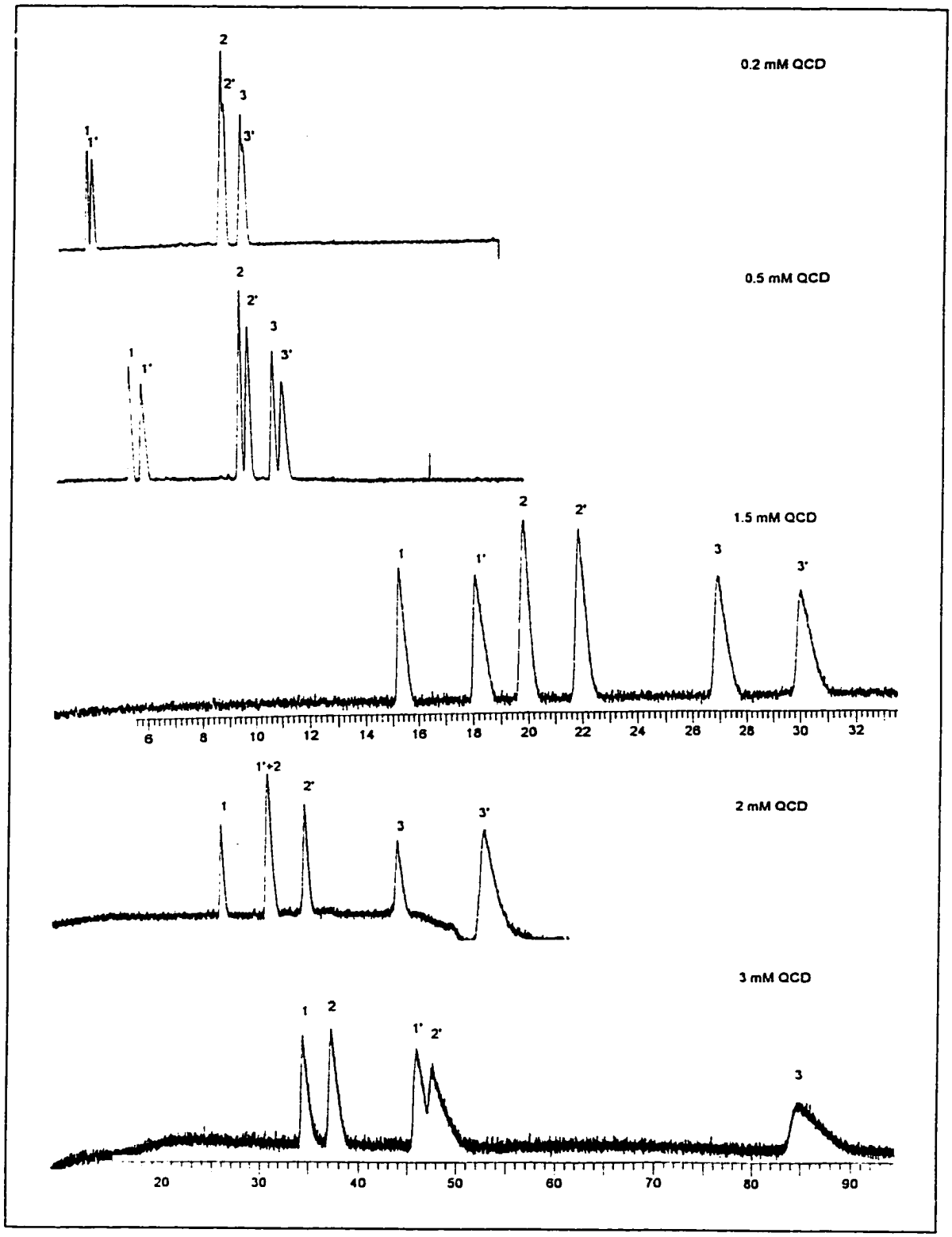

Fig. 2.8a. Separation of enantiomers of Asp, Abu and Norval. The concentration of Q-CD is printed on each electropherogram. Other conditions are listed in Table 2.2.

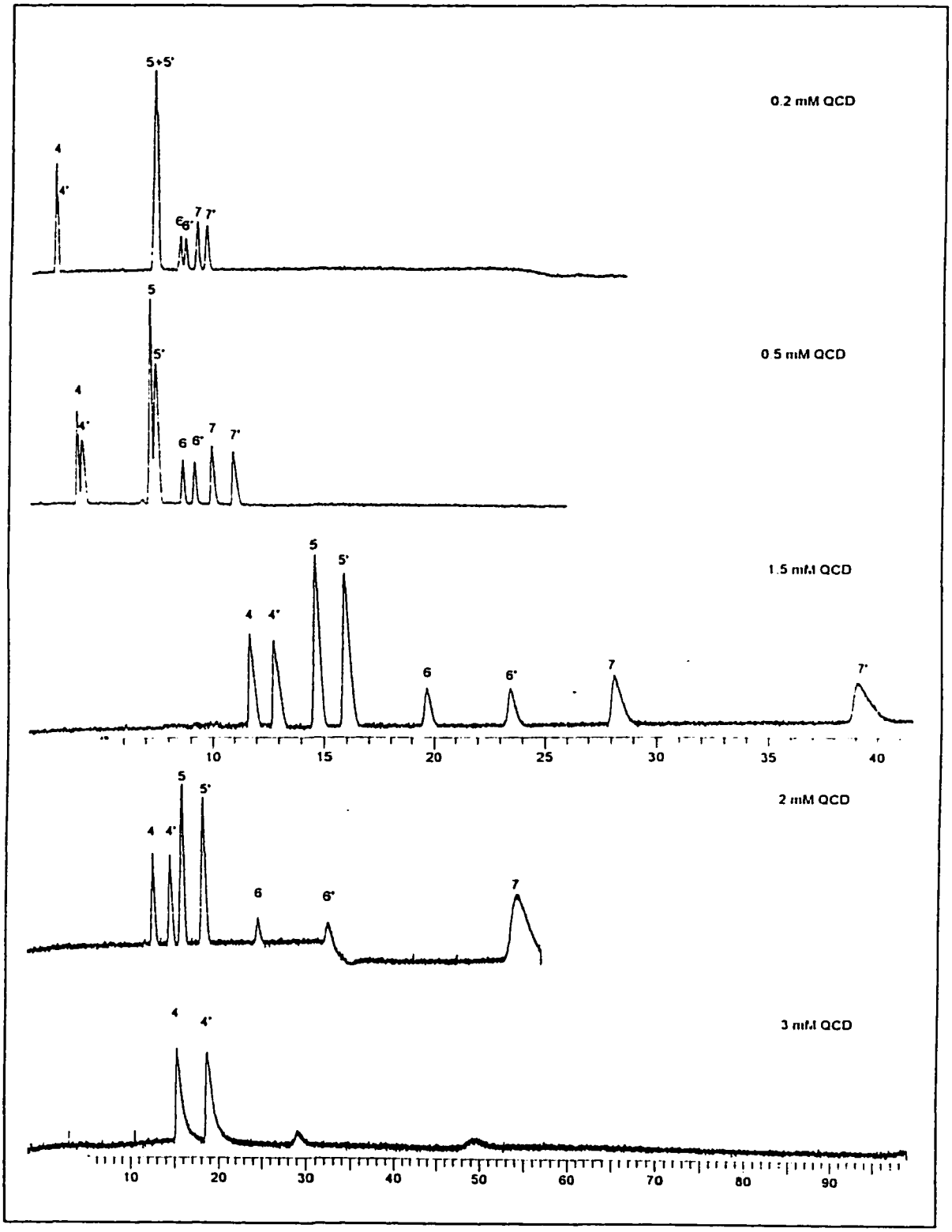

Fig. 2.8b. Separation of enantiomers of Glu, Ser, Met and Norleu. The concentration of Q-CD is printed on each electropherogram. Other conditions are listed in Table 2.2.

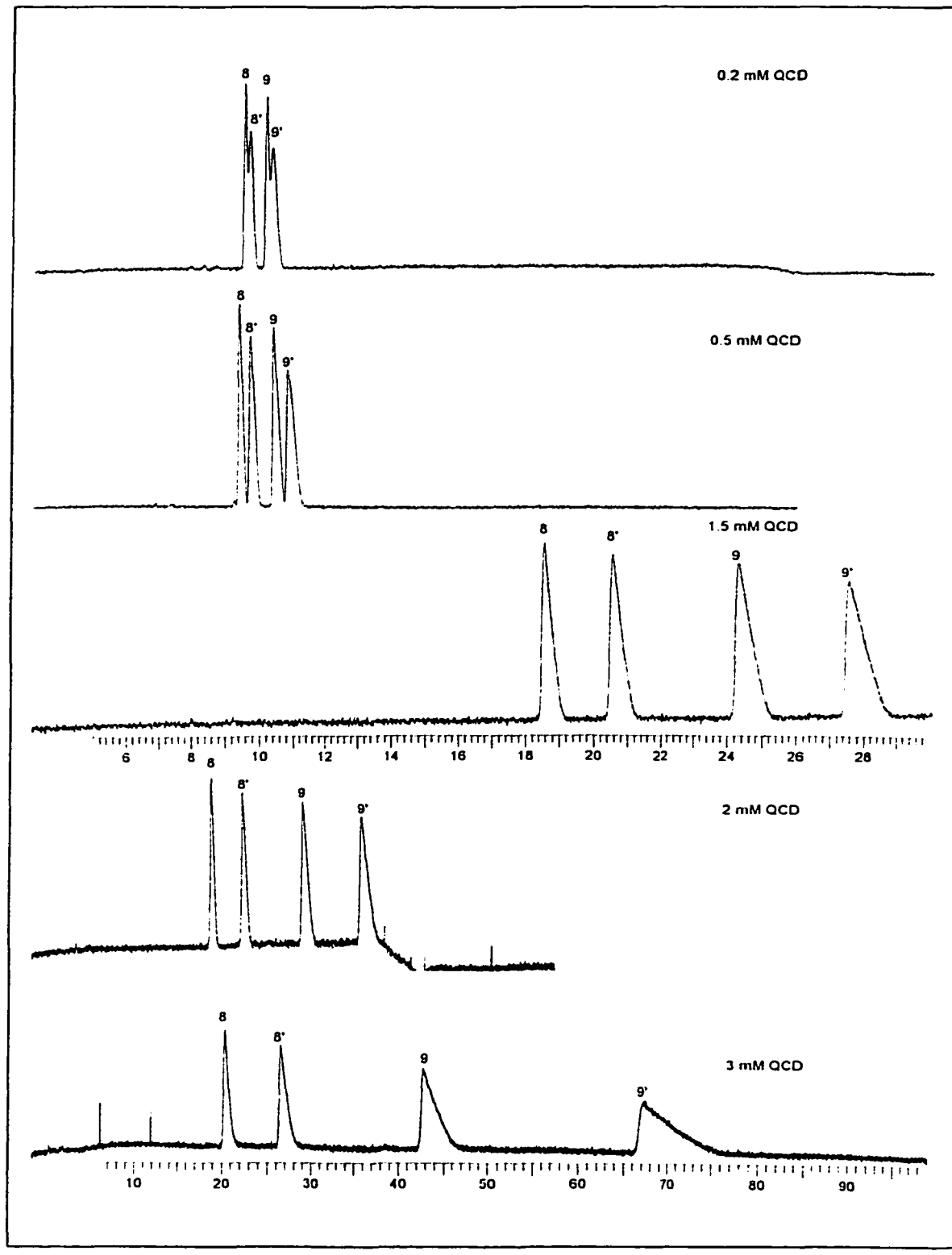

Fig. 2.8c. Separation of enantiomers of Thr and Val. The concentration of Q-CD is printed on each electropherogram. Other conditions are listed in Table 2.2.

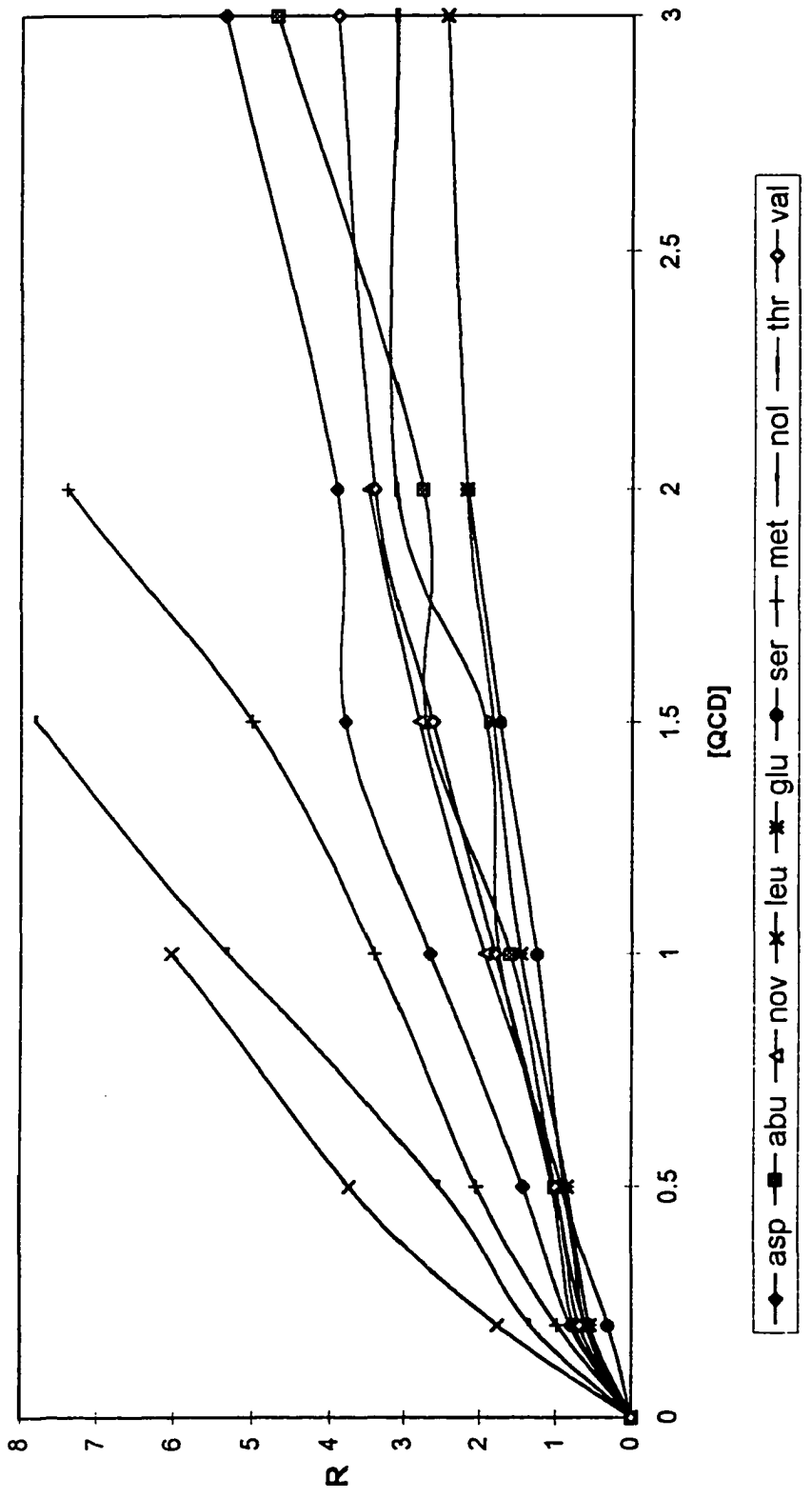

Fig. 2.9. Resolution of 10 Dns-DL-AA enantiomers as a function of the concentration of Q-CD. Conditions are listed in Table 2.2.

Secondly, the lack of electroosmotic flow improves the resolution. From the definition of CE resolution given by Terabe *et al.* [98],

$$R_S = \left(\frac{V}{32D}\right)^{\frac{1}{2}} \cdot \left(\frac{l}{L}\right)^{\frac{1}{2}} \cdot \frac{\Delta\mu_{ep}}{(\bar{\mu}_{ep} + \mu_{eo})^{\frac{1}{2}}} \qquad (32)$$

where V is the voltage, D is the solute diffusion coefficient, L is the total capillary length, l is the effective capillary length, $\Delta\mu_{ep}$ is the electrophoretic mobility difference, μ_{ep} is the mean electrophoretic mobility, and μ_{eo} is the electroosmotic mobility. Usually μ_{eo} is several times larger than μ_{ep}, so that it behaves as the principal factor in the denominator of the third term. Eliminating the electroosmotic flow enhances the resolution. In addition, the counterflow mode provides good contact between the enantiomers and the chiral selector to obtain the best possible chiral discrimination. The separation of Dns-DL-AA enantiomers is depicted schematically in Fig. 2.10.

As summarized in section 2.4, the theory of Wren and Rowe used the mobility difference to measure the separation, while Rawjee and Vigh prefer mobility ratio. Both mobility difference and ratio have the advantage of neglecting some complicating factors such as band broadening due to diffusion, and injection and detector length [94], which influence the resolution significantly. The plot of the mobility difference of Dns-DL-AAs vs. [Q-CD] is given in Fig. 2.11a. Three pairs of Dns-DL-AA (Asp, Glu and Norleu) show the trend that Wren and Rowe predicted, with the maximum mobility difference of

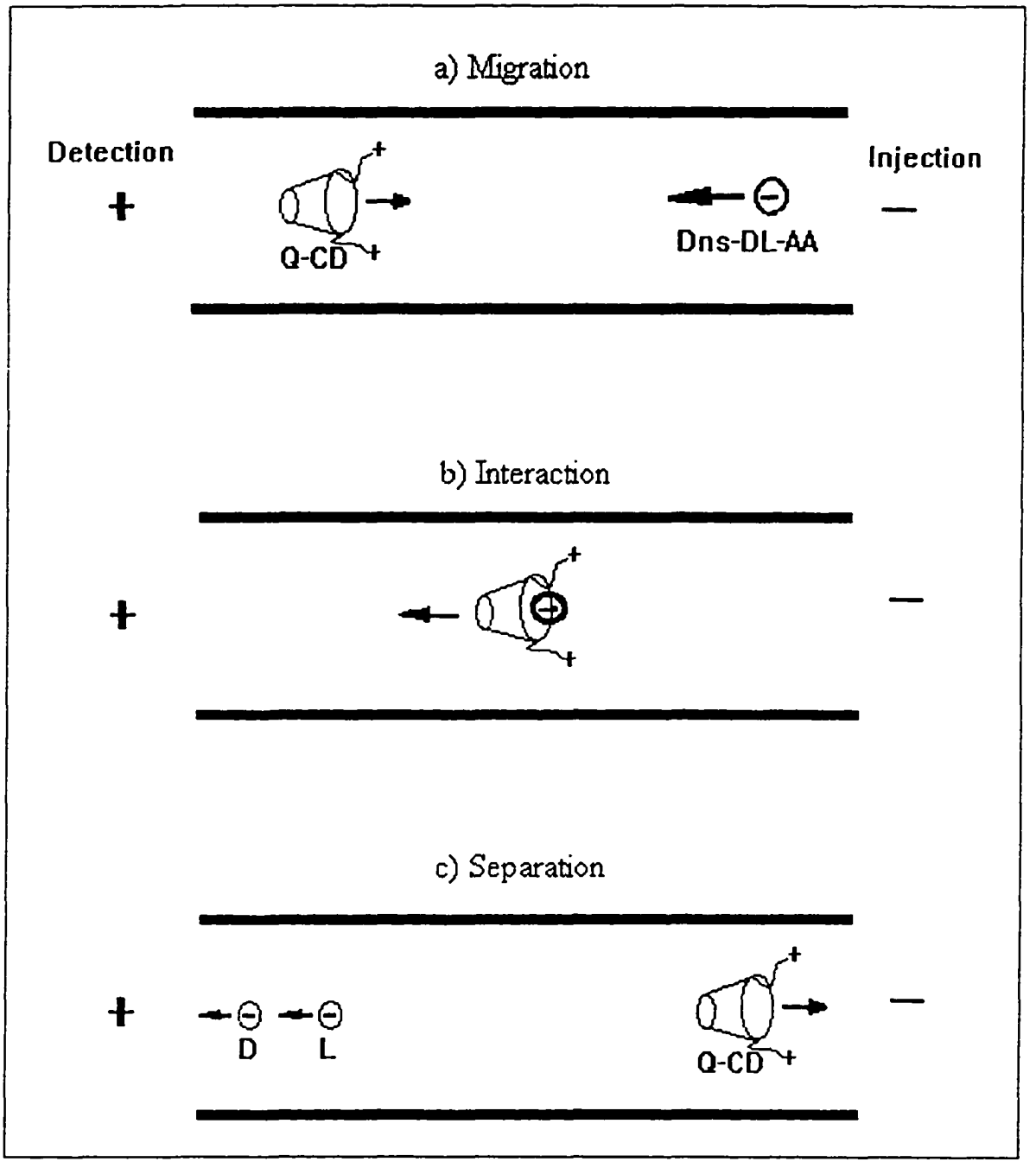

Fig. 2.10. The schematic showing of separating dansyl amino acid enantiomers by using Q-CD in a coated capillary.

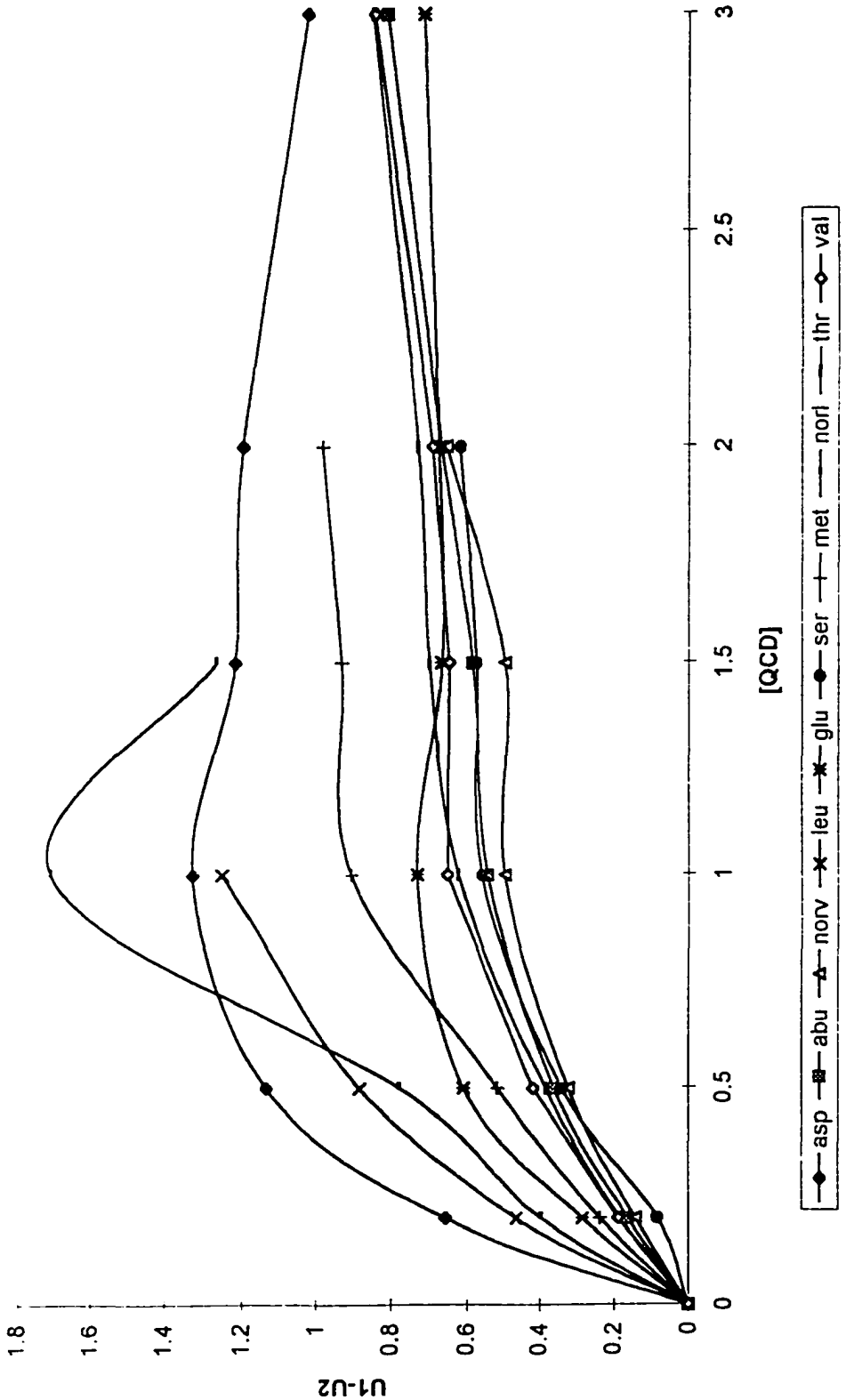

Fig. 2.11a. Mobility difference of 10 Dns-DL-AAs as a function of the concentration of Q-CD. Conditions are listed in Table 2.2.

enantiomer pairs at about 1 mM Q-CD. For all the other Dns-DL-AAs, the mobility difference increases rapidly up to the concentration of Q-CD of 1 mM, and then becomes nearly constant. In Fig. 2.11b, we plot the mobility ratio of enantiomers, $A_{D/L}$ as a function of [Q-CD], which results in a similar trend with resolution plot. Therefore we think that mobility ratio reflects the degree of separation better than mobility difference, since the latter more depends on the magnitude of the mobility.

According to equation (31), the binding constant and electrophoretic mobility of enantiomer-QCD complex of a single enantiomer can be determined from plotting apparent electrophoretic mobility of the enantiomer as a function of the part in the parenthesis (symbolized by X), if we know the binding ratio, n. Unfortunately, as mentioned in the experimental section, the instrument only allows a maximum run time of 100 minutes for each run. We could not gather enough data set for most of the Dns-DL-AA enantiomers separated to make the plots, because of the strong binding between the enantiomers and Q-CD, which makes the enantiomers move at very slow velocities.

Although the mole ratios of interaction between the enantiomers and Q-CD and the binding contants could not be obtained mathematically, the chiral resolution of different Dns-DL-AAs still gave us useful information of the molecular interactions during the chiral separations. Phe and Trp did not elute in 100 min with [Q-CD] = 0.5 mM, and

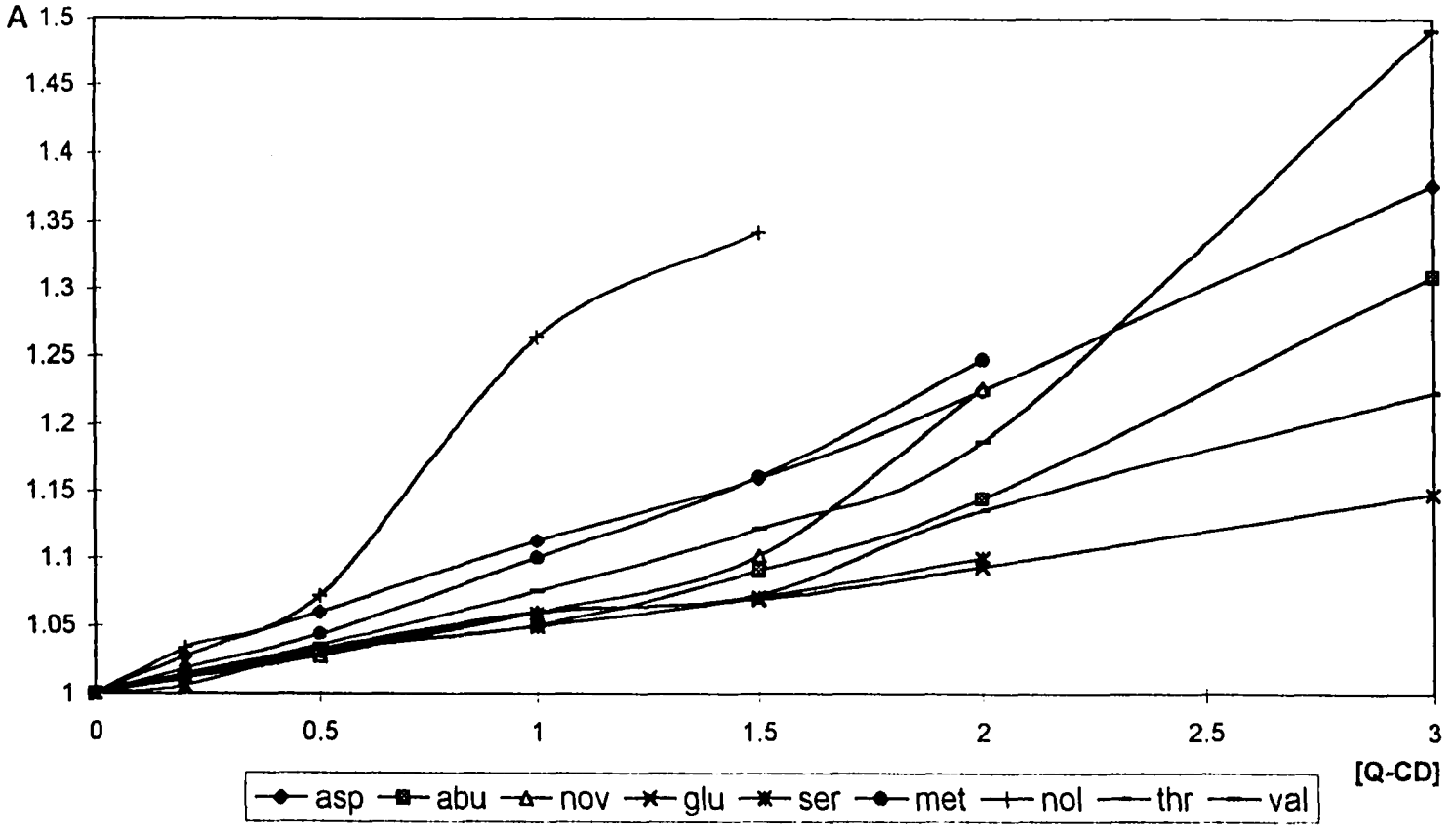

Fig. 2.11b. Mobility ratio of 10 Dns-DL-AA enantiomers as a function of the concentraiton of Q-CD. Conditions are listed in Table 2.2.

only one of the enantiomers of Leu eluted in 100 min with [Q-CD] = 1.5 mM. Norleu enantiomers, with a butyl chain, were better separated than those of Norval, which has a propyl chain. By studying the molecular structures of the Dns-DL-AAs (refer to Table 2.1), we notice that all of the compounds better separated by Q-CD possess a relatively large nonpolar group on the α-carbon, such as an aromatic group or a bulky alkyl chain, while other Dns-DL-AAs studied do not. As a result, they experience high chiral recognition even with quite low concentrations of Q-CD. The electropherograms of Leu in various buffers are given in Fig 2.12, and those of Phe and Trp are given in Fig. 2.13. All of the enantiomeric pairs are baseline resolved at [Q-CD] as low as 0.2 mM. Their extra binding must originate from these nonpolar groups, which are capable of hydrophobic interactions with the CD. The hydrophobic attraction between bulky non-polar dansyl group and the hydrophobic cone of cyclodextrin has been recognized by Grinberg and Karger *et al.* [75], and they also proposed that the interaction between a dansyl amino acid enantiomer and native β-CD is on a 1:1 basis. In our experiment, if the secondary hydrophobic interaction is responsible for extra binding and chiral selectivity of dansyl amino acids, this interaction has to take place with another Q-CD molecule since the hydrophobic cavity of the first Q-CD is occupied by the dansyl group. Therefore we believe that a single dansyl amino acid enantiomer interacts with two molecules of Q-CD simultaneously. This theory that a single solute molecule interacts with more than one molecule of cyclodextrin derivatives is not new. Armstrong *et al.* [100] gave evidence for a single 4-nitroaniline complexing with two β-CDs, and suggested that binding of a single molecule to two β-CDs or CD derivatives is possibly

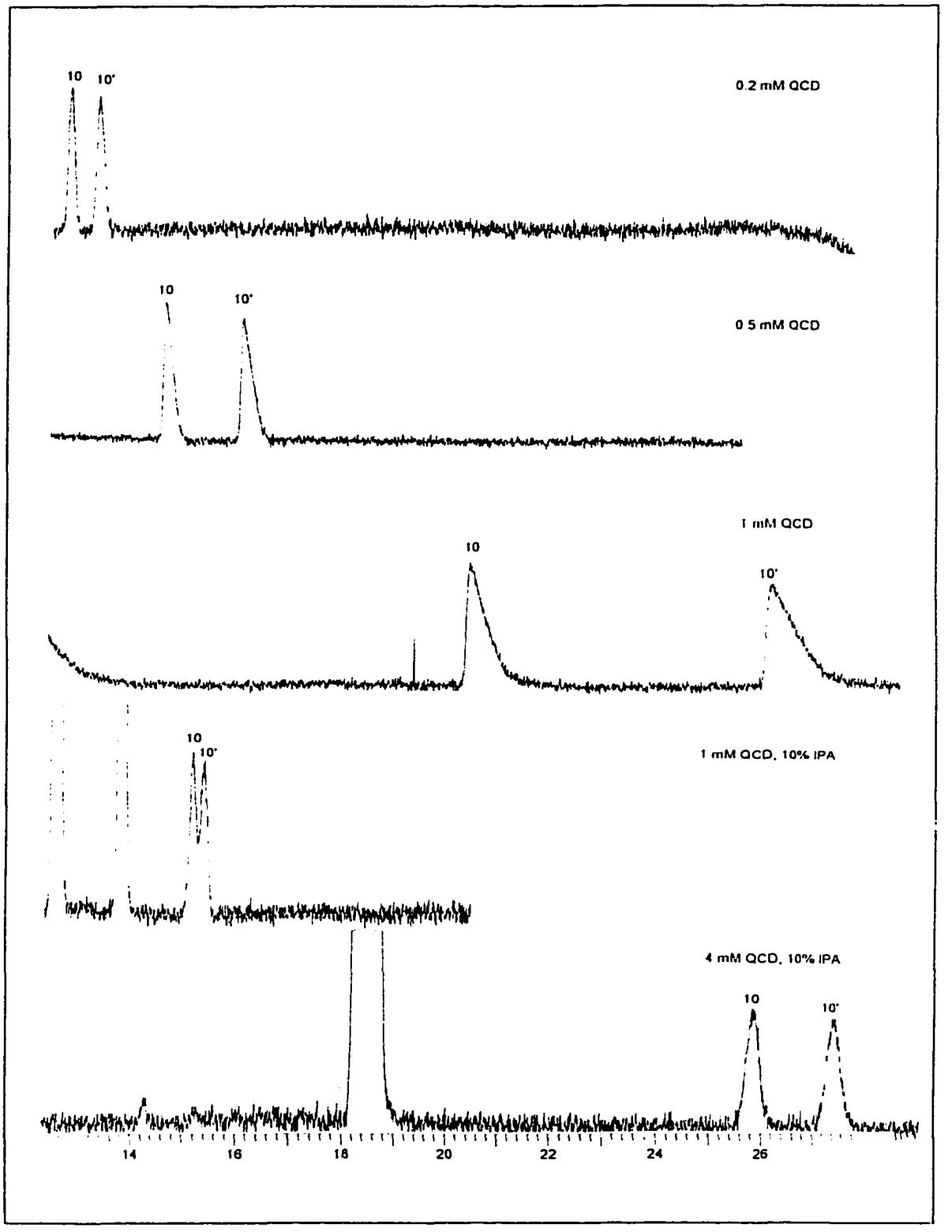

Fig. 2.12. Separation of enantiomers of Leu. The concentrations of Q-CD and organic modifier are printed on each electropherogram. Other conditions are listed in Table 2.2.

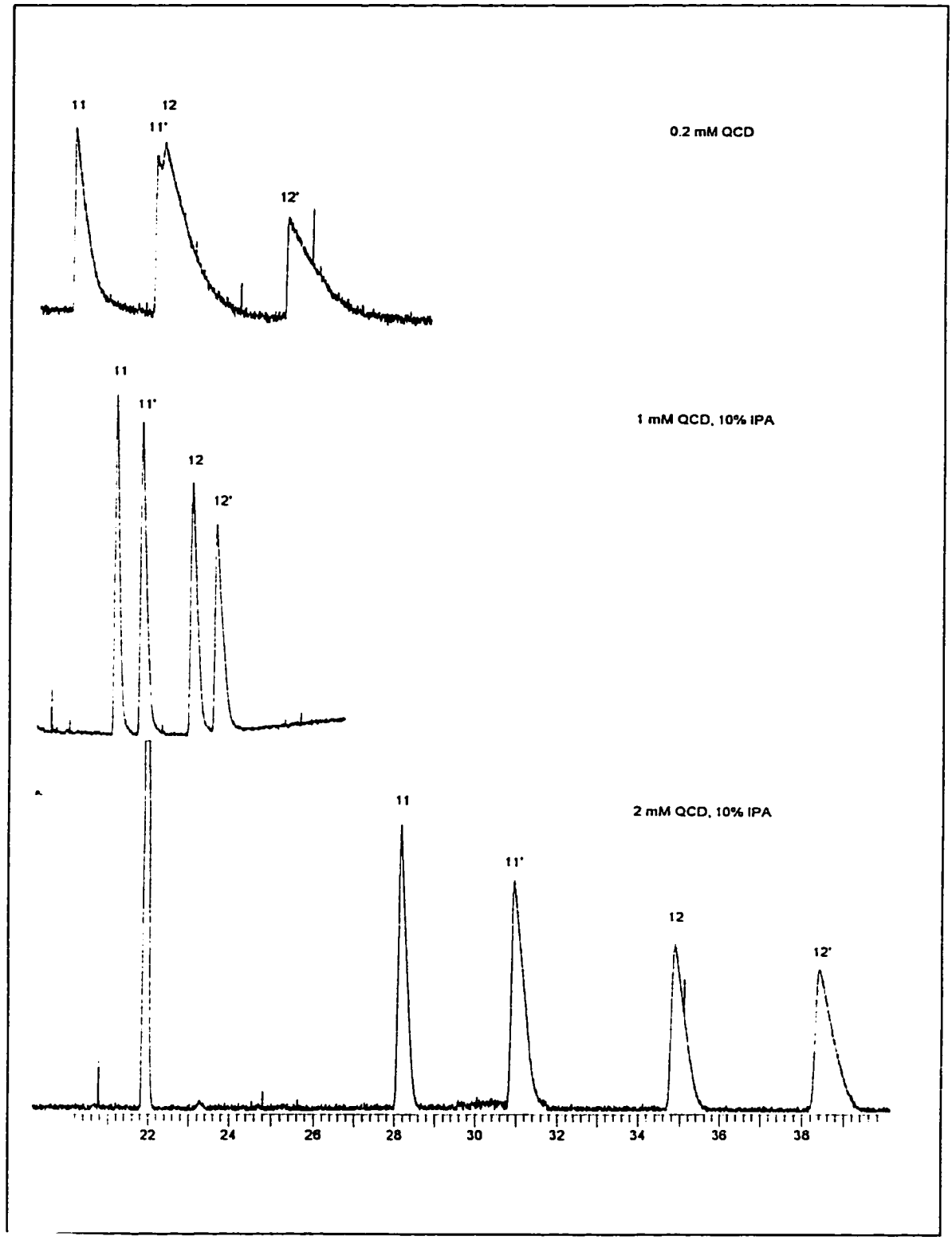

Fig. 2.13. Separation of enantiomers of Phe and Trp. The concentrations of Q-CD and organic modifier are printed on each electropherogram. Other conditions are listed in Table 2.2.

more general than has been recognized. A proposed schematic molecular interaction between Dns-DL-Phenylaniline (Phe) and Q-CD is depicted in Fig. 2.14, in which the dansyl group fits into the cone of a Q-CD, while the carboxylate group interacts with the quaternary ammonium group of the same Q-CD. A secondary hydrophobic interaction occurs between its benzyl group and the cone of a second Q-CD. This secondary hydrophobic interaction might take place even if the group is not as hydrophobic as an aromatic group. Again, Norleu enantiomers, with a butyl chain, were better separated than those of Norval, which has a propyl chain. When the functional groups on the α–carbon of a Dns-DL-AA are not hydrophobic, such as the cases with Asp and Glu, this secondary hydrophobic interaction probably does not occur.

Another functional group-related molecular interaction is that stronger binding of enantiomers to Q-CD does not necessarily guarantee better chiral selectivity. Glu and Asp have two carboxyl groups, which provides stronger static attraction to Q-CD; these enantiomers were not baseline resolved until [Q-CD] reached 1 mM. Norleu, Leu, Phe and Trp, all of which have one carboxylate group, had baseline resolution at [Q-CD] = 0.2 mM. In addition, the hydroxyl group on a Dns-DL-AA does not seem to provide any extra chiral selectivity.

2.5.2. Effect of organic modifiers

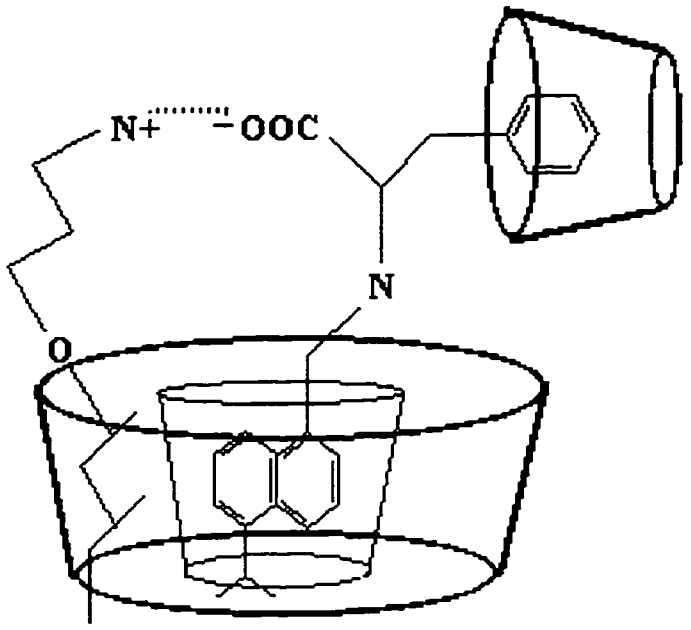

Fig. 2.14. Proposed molecular interaction between Q-CD and Dns-DL-Phenylalanine.

In the separation of Dns-DL-AAs, the addition of organic modifiers had dramatic effects on two important aspects of chiral separation: resolution and peak shape.

Resolution

The effect of different organic modifiers on chiral separation in capillary electrophoresis has been exploited by several groups of researchers [80,87,101,102]. Among them Fanali [102] used 40 mM β-CD to separate the enantiomers of the β–blocker propranolol, and found that adding methanol to the buffer could strongly enhance the resolution. Goodall *et al.* [87] separated tioconazole enantiomers using a β-CD. They found that in the range of 0-15% (v/v) of organic modifiers in the buffer, increasing the concentration of acetone caused twice the decrease of the host-guest binding constant in comparison to methanol. The model of Wren and Rowe [80] predicted that organic modifiers such as methanol and acetone should decrease the resolution when the concentration of the chiral selector ([β-CD]) is lower than the optimum concentration ($[\beta\text{-CD}]_{opt}$), while the resolution will increase when $[\beta\text{-CD}] > [\beta\text{-CD}]_{opt}$.

In our study, two different organic modifiers, methanol and isopropyl alcohol (IPA) were used. The electropherograms of Dns-DL-AAs with no organic modifier, 10% methanol, or 10% IPA in the presence of 1 mM of Q-CD are given in Fig. 2.15a-c. The resolution of all the Dns-DL-AAs decreases with addition of either of the organic modifiers, but IPA

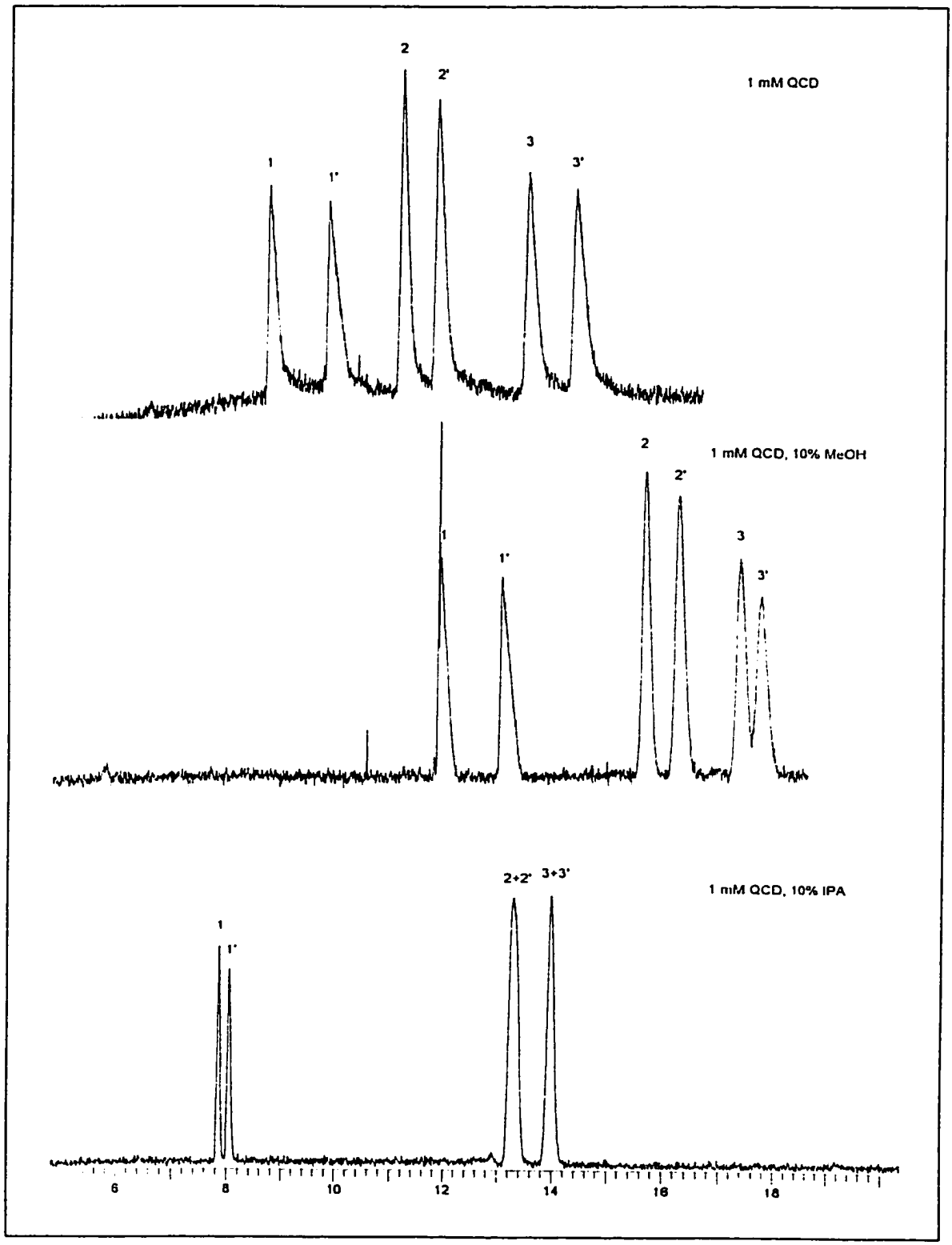

Fig. 2.15a. The effect of organic modifiers for the separation of Asp, Abu and Norval enantiomers. The concentrations of Q-CD and organic modifier are printed on each electropherogram. Other conditions are listed in Table 2.2.

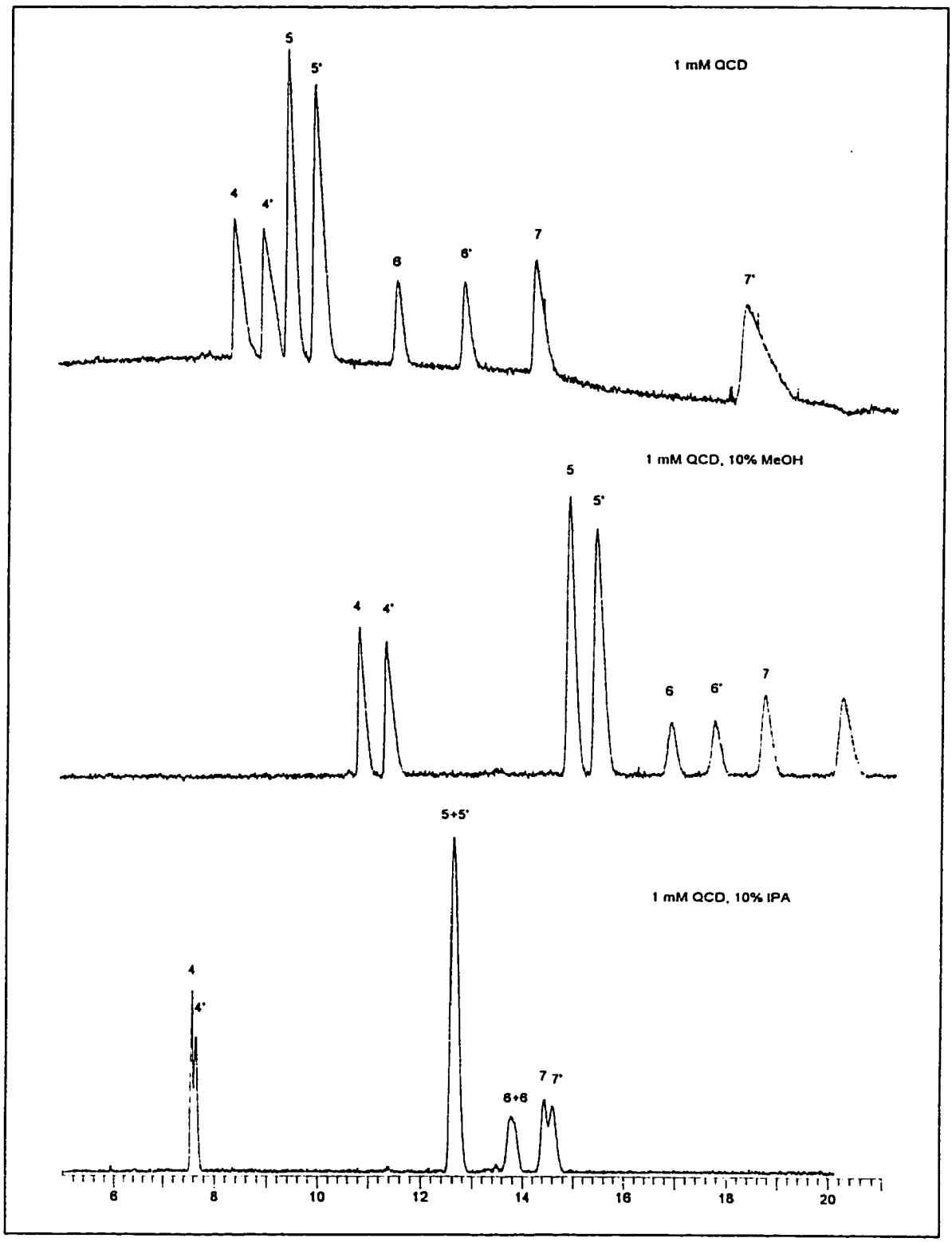

Fig. 2.15b. The effect of organic modifiers for the separation of Glu, Ser, Met and Norleu enantiomers. The concentrations of Q-CD and organic modifier are printed on each electropherogram. Other conditions are listed in Table 2.2.

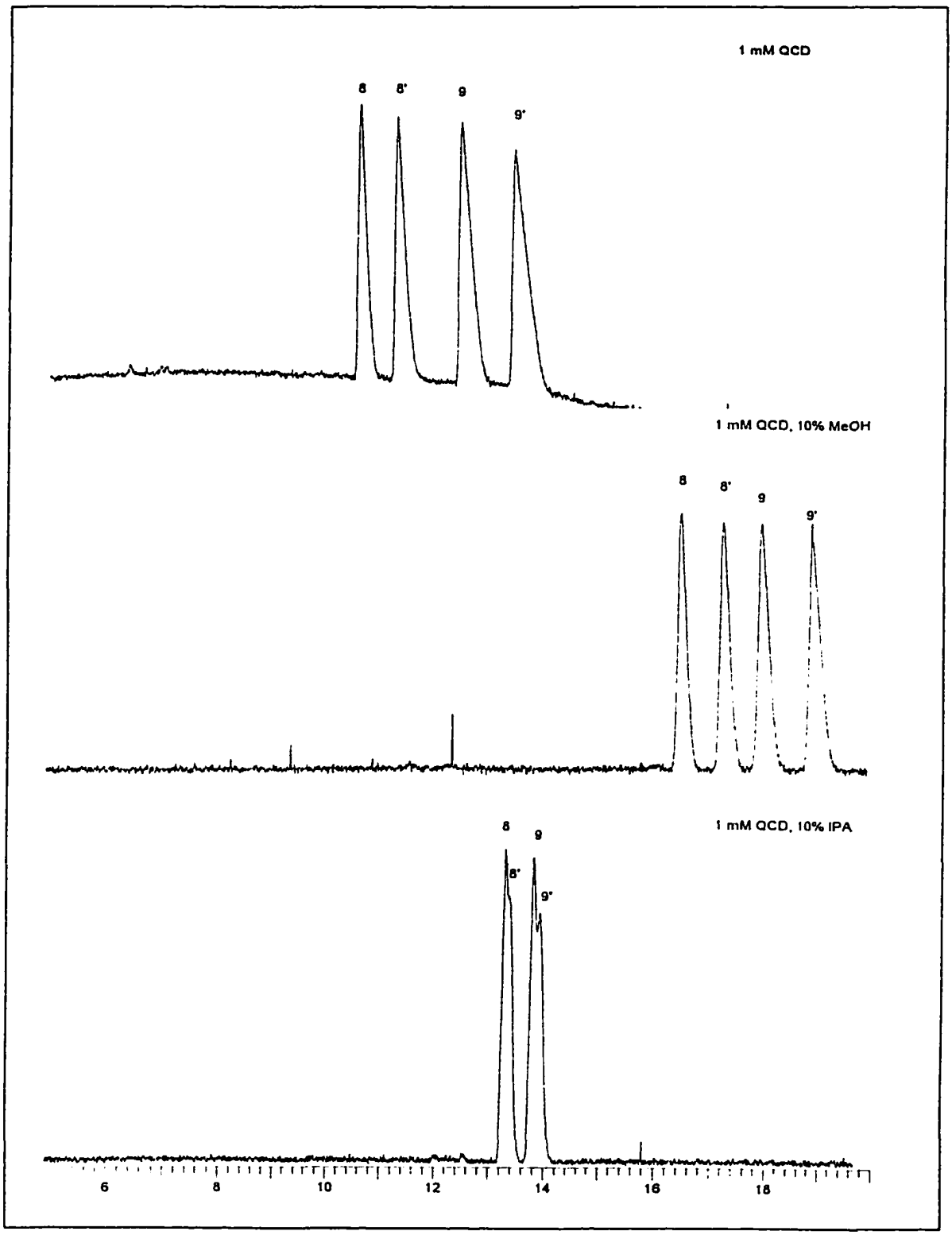

Fig. 2.15c. The effect of organic modifiers for the separation of Thr and Val enantiomers. The concentrations of Q-CD and organic modifier are printed on each electropherogram. Other conditions are listed in Table 2.2.

obviously has a much stronger effect than methanol. The binding between Dns-DL-AAs and Q-CD decreases since organic modifiers loosen the hydrophobic interaction between Dns-DL-AAs and Q-CD. IPA is a more hydrophobic solvent than methanol, so it is capable of reducing the binding interaction to a greater extent than methanol. With further increase in the amount of IPA added, chiral resolution deteriorated quickly, as shown in Fig. 2.16. 20% IPA in a buffer with 0.5 mM of Q-CD leaves the three Dns-DL-AAs completely unresolved.

Peak shape

The electropherograms in Fig. 2.8 show most of the peaks have some tailing. Several groups [103-105] have studied peak asymmetry, including fronting and tailing in capillary electrophoresis. One cause of tailing has been recognized as electromigration dispersion, which results from a sample zone that has mobility lower than that of the carrier constituents. This results in a concentration distribution that is sharp at the front and tailing at the rear. Another cause of tailing is adsorption of analytes on the capillary surface, which presumably should not happen to our coated capillary. Recently Gebauer and Bocek [106] developed a mathematical model of zone migration in a capillary to explain the causes of peak asymmetry. In our study, the peak shape was remarkably improved by adding organic modifier. Figs. 2.17a-c gives the electropherograms of Dns-DL-AAs in a series of buffers of several of concentration of Q-CD and 10% IPA. All the

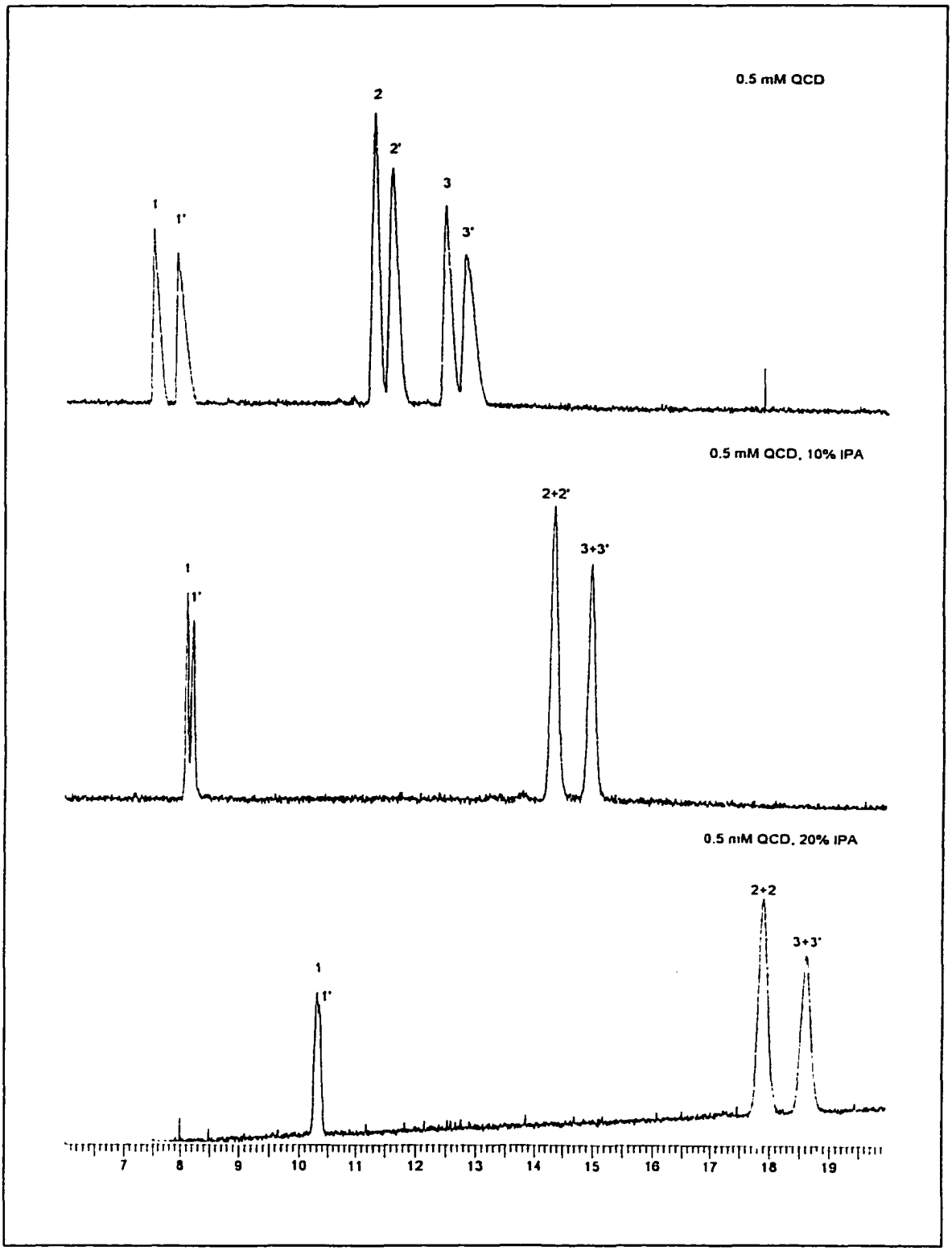

Fig. 2.16. The effect of increase of organic modifier concentration for the separation of Asp, Abu and Norval enantiomers. The concentrations of Q-CD and organic modifier are printed on each electropherogram. Other conditions are listed in Table 2.2.

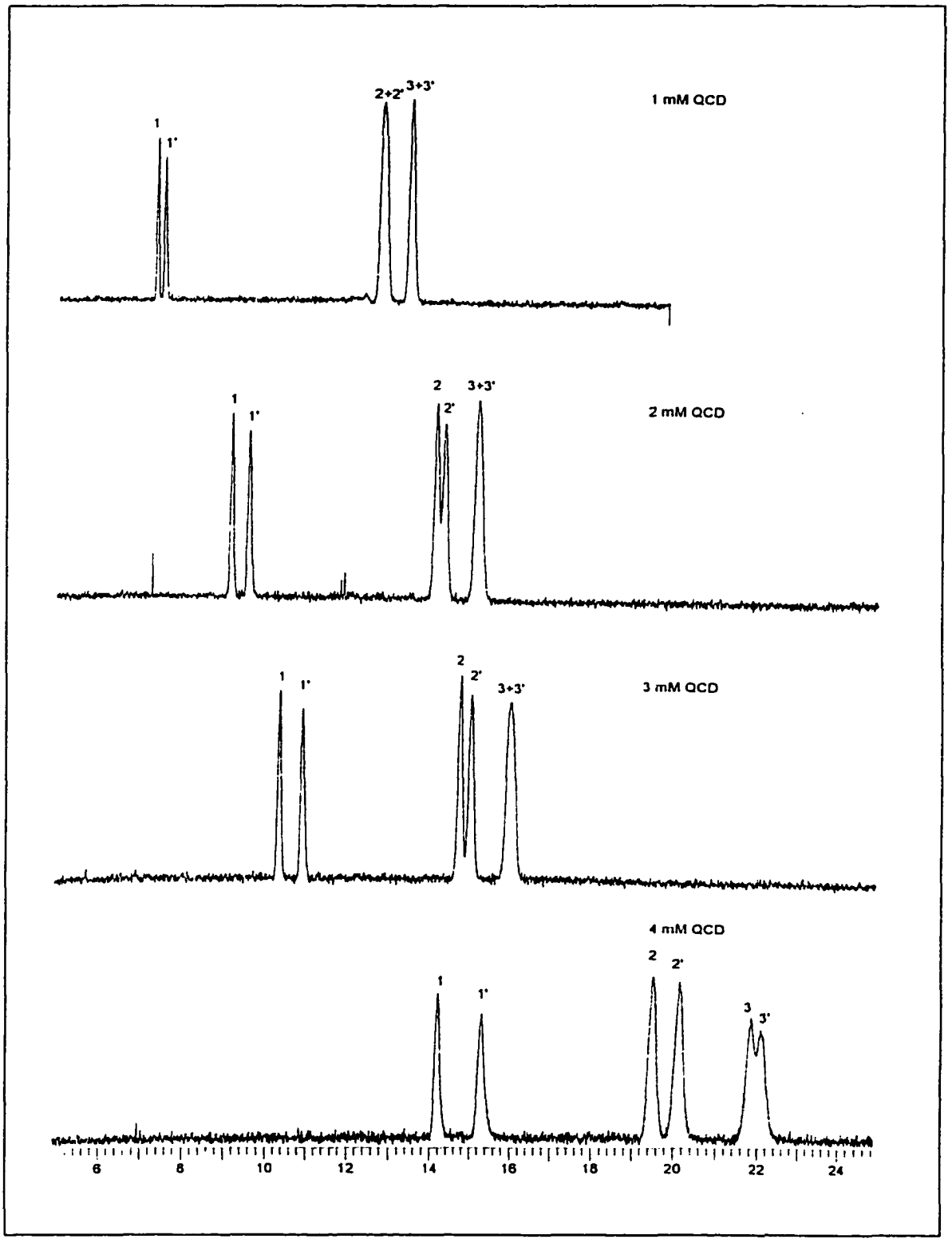

Fig. 2.17a. Separation of Asp, Abu and Nov enantiomers with 10% IPA in the buffer. The concentration of Q-CD is printed on each electropherogram. Other conditions are listed in Table 2.2.

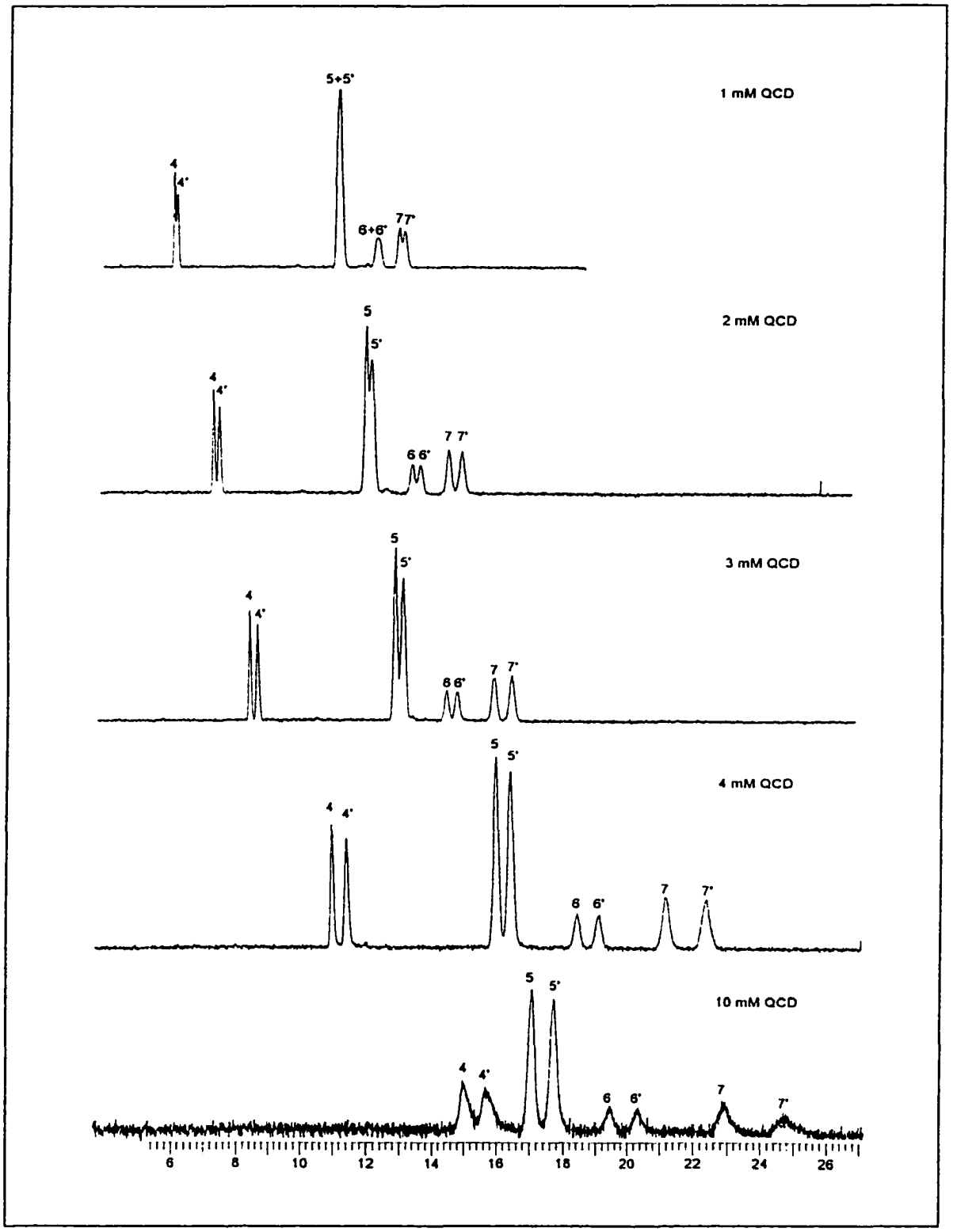

Fig. 2.17b. Separation of Glu, Ser, Met and Nol enantiomers with 10% IPA in the buffer. The concentration of Q-CD is printed on each electropherogram. Other conditions are listed in Table 2.2.

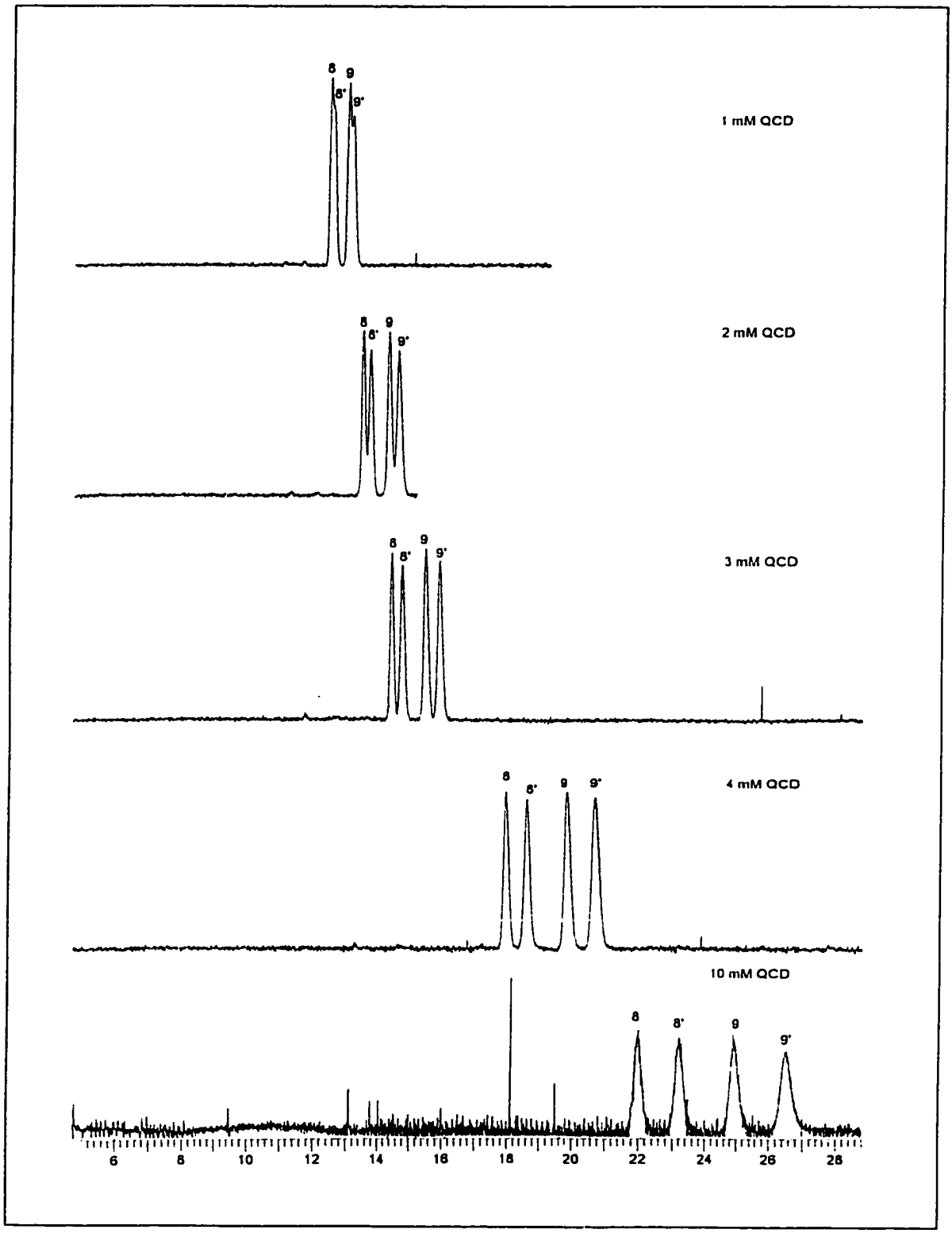

Fig. 2.17c. Separation of Thr and Val enantiomers with 10% IPA in the buffer. The concentration of Q-CD is printed on each electropherogram. Other conditions are listed in Table 2.2.

peaks appear symmetrical. Peak tailing is eliminated. The same occurs in Fig. 2.13, where severe tailing of Phe and Trp occur even with the concentration of Q-CD as low as 0.2 mM. After adding 10% IPA into the buffer with 1 mM of Q-CD, nearly symmetrical peaks are obtained for both Phe and Trp.

2.5.3. Effect of temperature

In Figs. 2.18a-c, the electropherograms show the effect of temperature on the separation in the range of 25 °C to 40 °C. Increasing the temperature shortens the migration time of the analytes because of the decrease in buffer viscosity, and the loser binding between the Q-CD and the enantiomers. Resolution of the enantiomers declines with increase in temperature. Fanali *et al.* [107] observed same effect of temperature on migration and chiral resolution of some sympathomimetic drugs, namely norepinephrine and epinephrine. Goodall *et al.* [88] demonstrated that the binding constants of trioconasole enantiomers decreased with increasing temperature in the range of 17 - 40 °C. The decrease in chiral selectivity can be ascribed to the shorter time spent by the analytes into the CD cavity and to a modification of thermodynamic parameters. As mentioned in section 2.4, enantiomers D and L undergo dynamic equilibrium with chiral selector C in solution.

$$D + C \xleftrightarrow{K_D} DC \qquad G^o_{f,DC} = - RT \ln K_D \qquad (33)$$

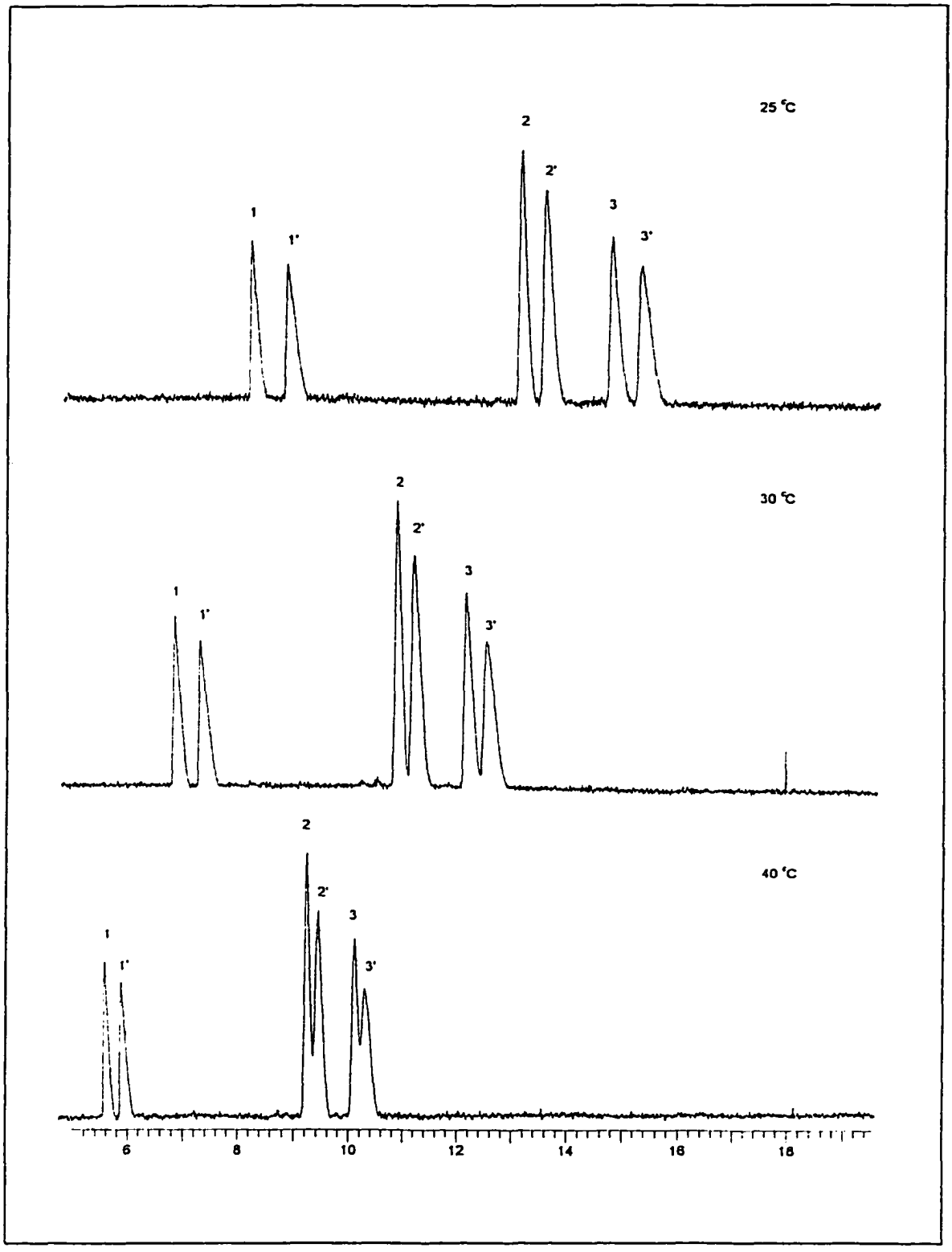

Fig. 2.18a. The effect of temperature on the separation of Asp, Abu and Nov enantiomers. The temperature is printed on each electropherogram. [Q-CD] = 0.5 mM. Other conditions are listed in Table 2.2.

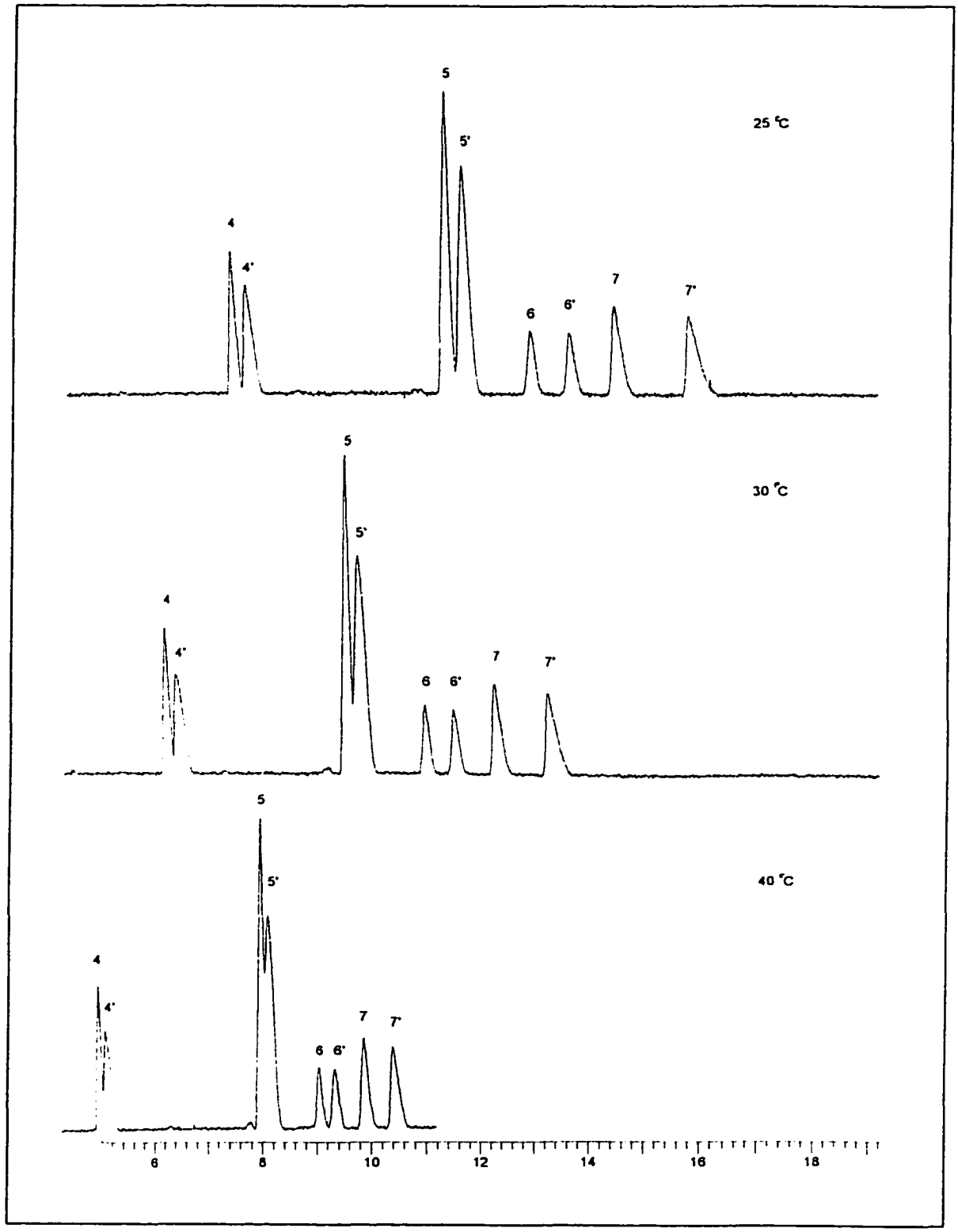

Fig. 2.18b. The effect of temperature on the separation of Glu, Ser, Met and Nol enantiomers. The temperature is printed on each electropherogram. [Q-CD] = 0.5 mM. Other conditions are listed in Table 2.2.

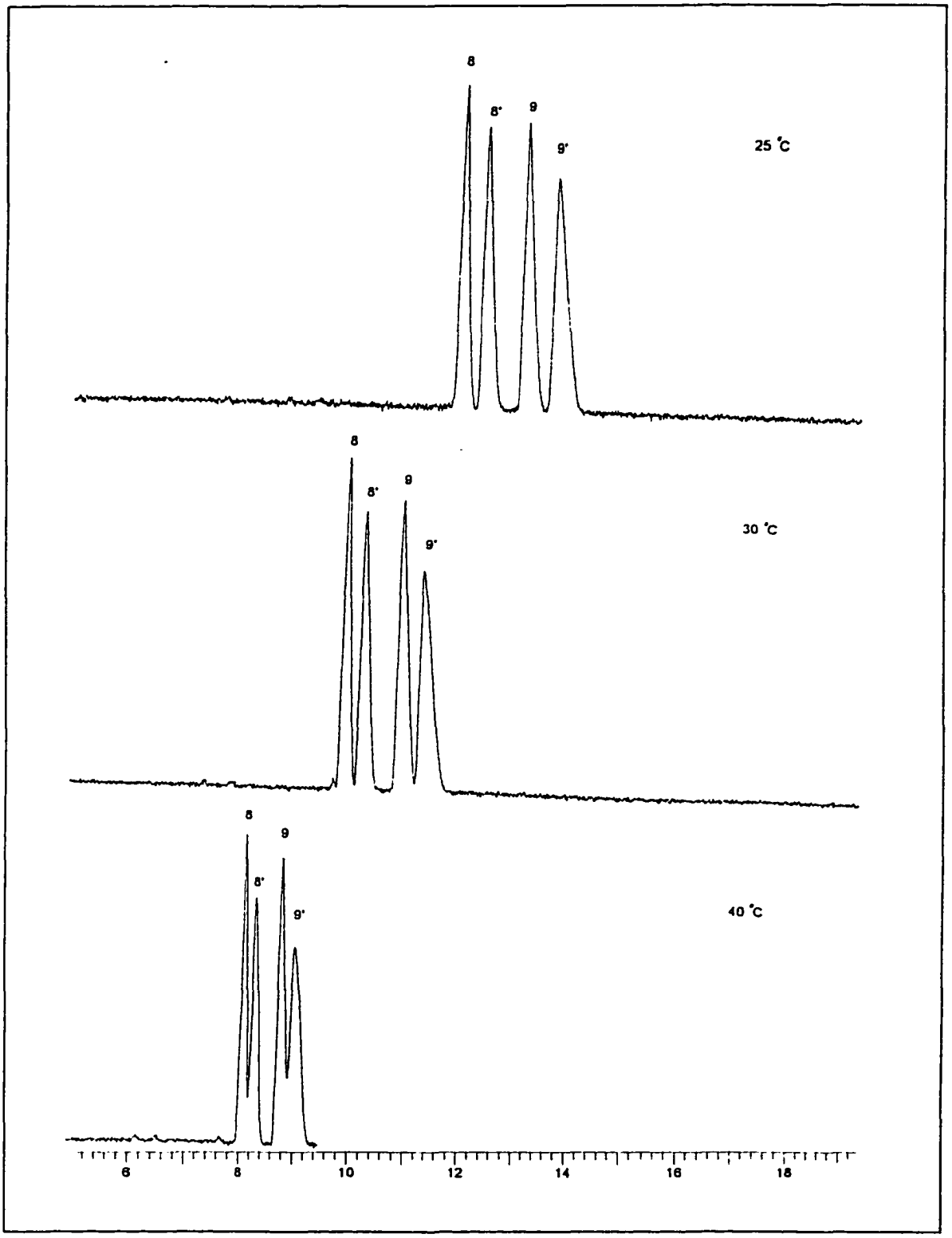

Fig. 2.18c. The effect of temperature on the separation of Thr and Val enantiomers. The temperature is printed on each electropherogram. [Q-CD] = 0.5 mM. Other conditions are listed in Table 2.2.

$$L + C \xleftrightarrow{K_L} LC \qquad G^o_{f,LC} = - RT \ln K_L \qquad (34)$$

where $\Delta G^o_{f,DC}$ and $\Delta G^o_{f,DC}$ are the standard free energy changes for the formation of the two enantiomer-chiral selector complexes. Taking the difference, one has:

$$\Delta\Delta G^o_f = \Delta G^o_{f,DC} - \Delta G^o_{f,LC} = -RT \ln (K_D/K_L) \qquad (35)$$

Since K_D/K_L can be used to represent chiral selectivity, it can be represented by A, the mobility ratio of the enantiomers. Combining eqn. (35) with the Gibbs-Helmholz equation:

$$\Delta\Delta G^o = \Delta\Delta H^o - T\Delta\Delta S^o, \qquad (36)$$

we can have that

$$\ln A = - \Delta\Delta H^o_f / R \cdot 1/T + \Delta\Delta S^o_f/R \qquad (37)$$

Therefore $\ln A$ is proportional to $1/T$. Fig. 2.19 shows that our data matches this linear relationship. Moreover, when $\Delta\Delta G^o_f = 0$ due to the enthalpy-entropy conpensation, no enantiomeric separation will occur. The temperature at which this occur is defined as the isoenantioselective temperature:

$$T_{iso} = \Delta\Delta H^o_f/\Delta\Delta S^o_f \qquad (38)$$

T_{iso} has been well documented in chiral separations by GC [108,109] and HPLC [110,111], but less mentioned in CE. The separation of enantiomers below T_{iso} is enthalpy controlled where as above T_{iso} the separation is entropy controlled. In our study,

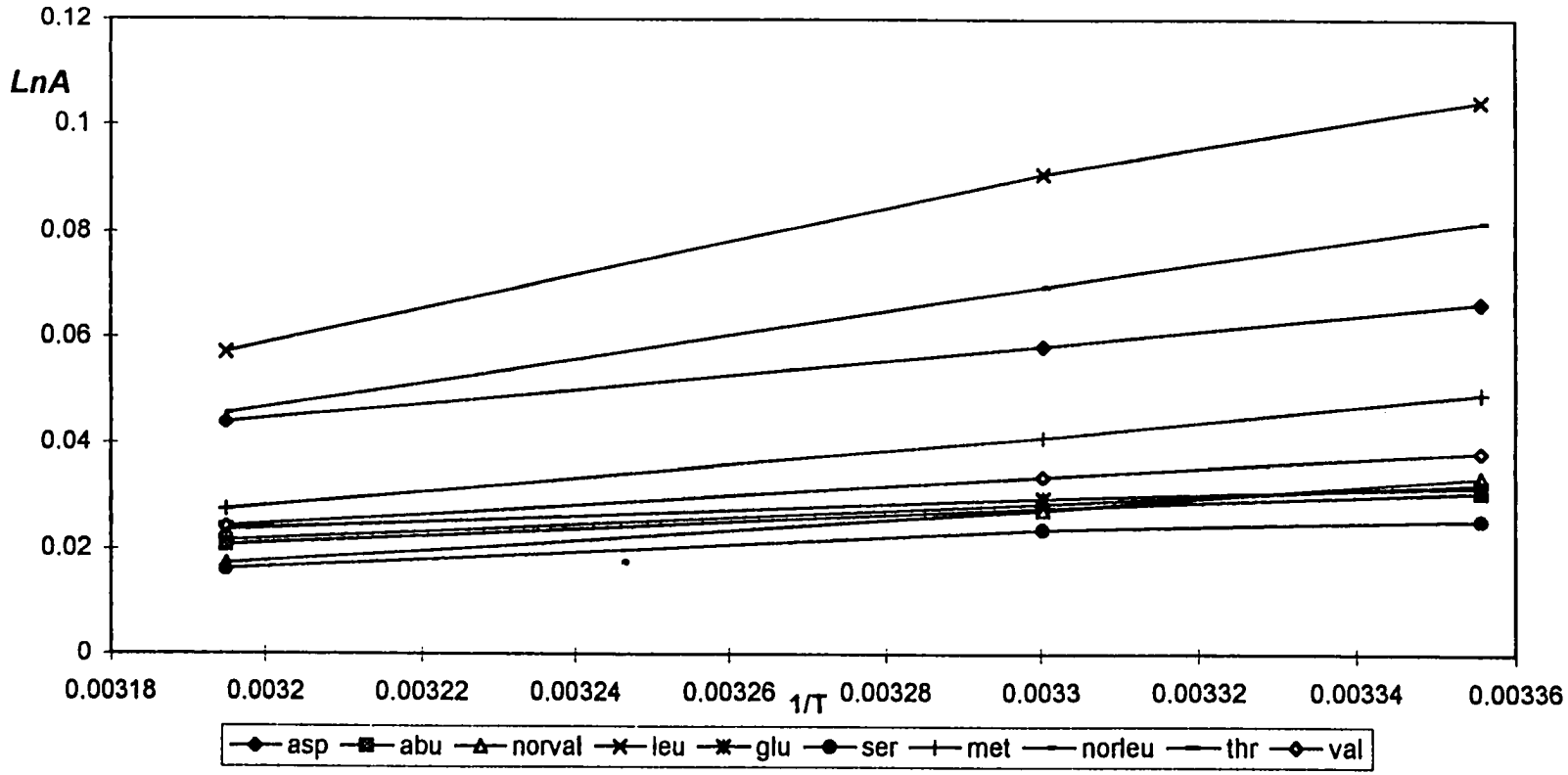

Fig. 2.19. *LnA*(mobility ratio) of 10 Dns-DL-AA enantiomers as a function of the reciprocal of temperature (°K). [Q-CD] = 0.5 mM. Other conditions are listed in Table 2.2.

the enantiomers of Dns-DL-AAs were less separated with increasing temperature. The separations are enthalpy controlled.

2.5.4. Effect of field strength

The driving force behind the migration of ions in CE is the electric field strength applied across the capillary. Jorgenson and Lukas stated that longitudinal diffusion is the only dispersion factor in CE, since EOF produces a flat front flow [28,112,113]. They obtained a linear relationship between the plate number and the applied voltage. But theoretical plate numbers are proportional to the voltage only when the current is low, because high current from the elevated voltage generates non-dissipatable Joule heating, which causes a differential thermal profile across the capillary. As a result the flat front flow becomes distorted. The separation efficiency will be damaged due to the differential diffusion caused by Joule heating.

In our study, electroosmotic flow is absent due to the coating on the capillary. Figs. 2.20a-c shows the electropherograms of Dns-DL-AAs over the applied voltage range of 10 - 20 kV. Fig. 2.21 are plots of resolution of the enantiomers as a function of the applied voltage over the same range. The resolution of enantiomers was not obviously influenced by increasing the applied voltage. Equation (32) shows suggests that increasing the

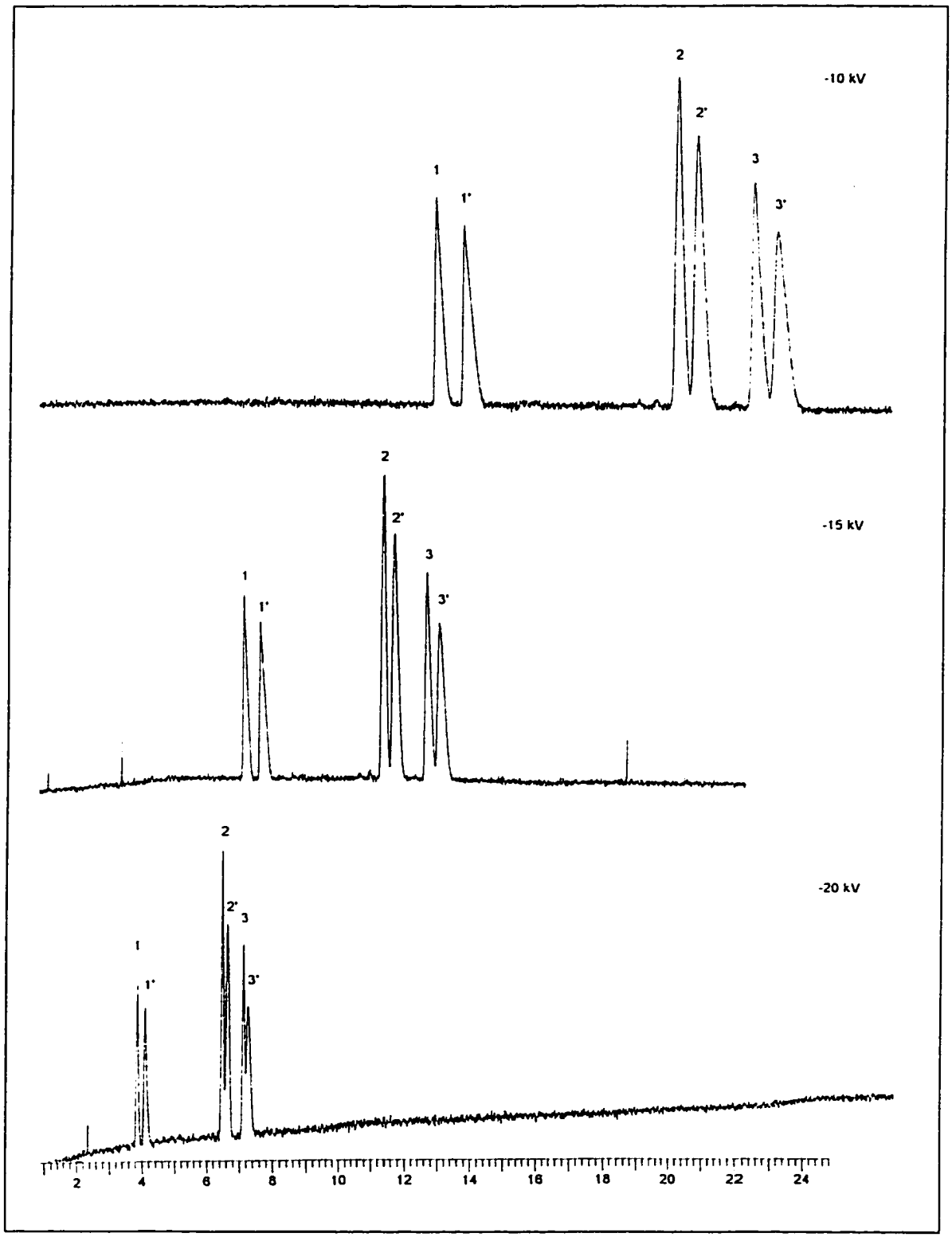

Fig. 2.20a. The effect of applied voltage on the separation of Asp, Abu and Nov enantiomers. The applied voltage is printed on each electropherogram. [Q-CD] = 0.5 mM. Other conditions are listed in Table 2.2.

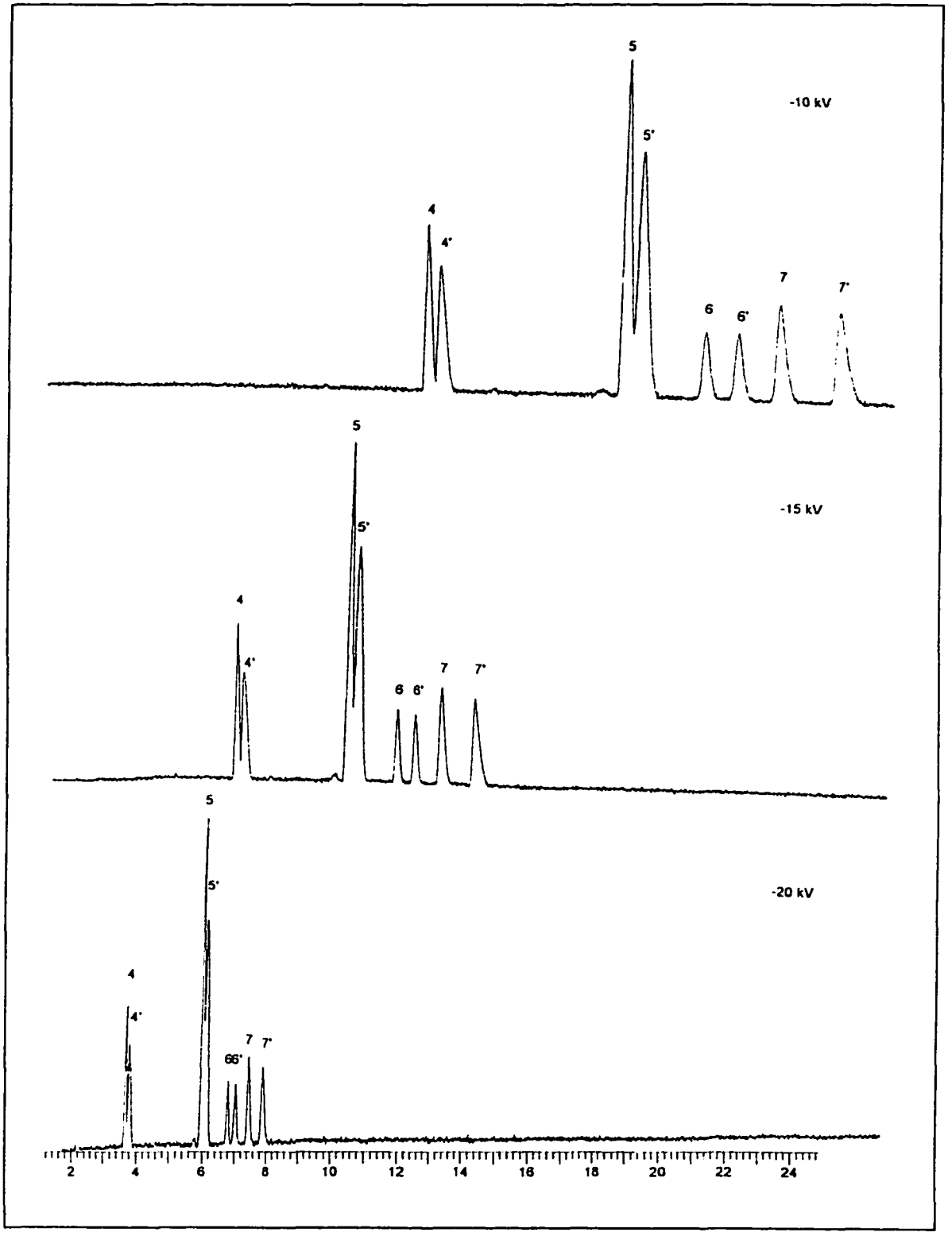

Fig. 2.20b. The effect of applied voltage on the separation of Glu, Ser, Met and Nol enantiomers. The applied voltage is printed on each electropherogram. [Q-CD] = 0.5 mM. Other conditions are listed in Table 2.2.

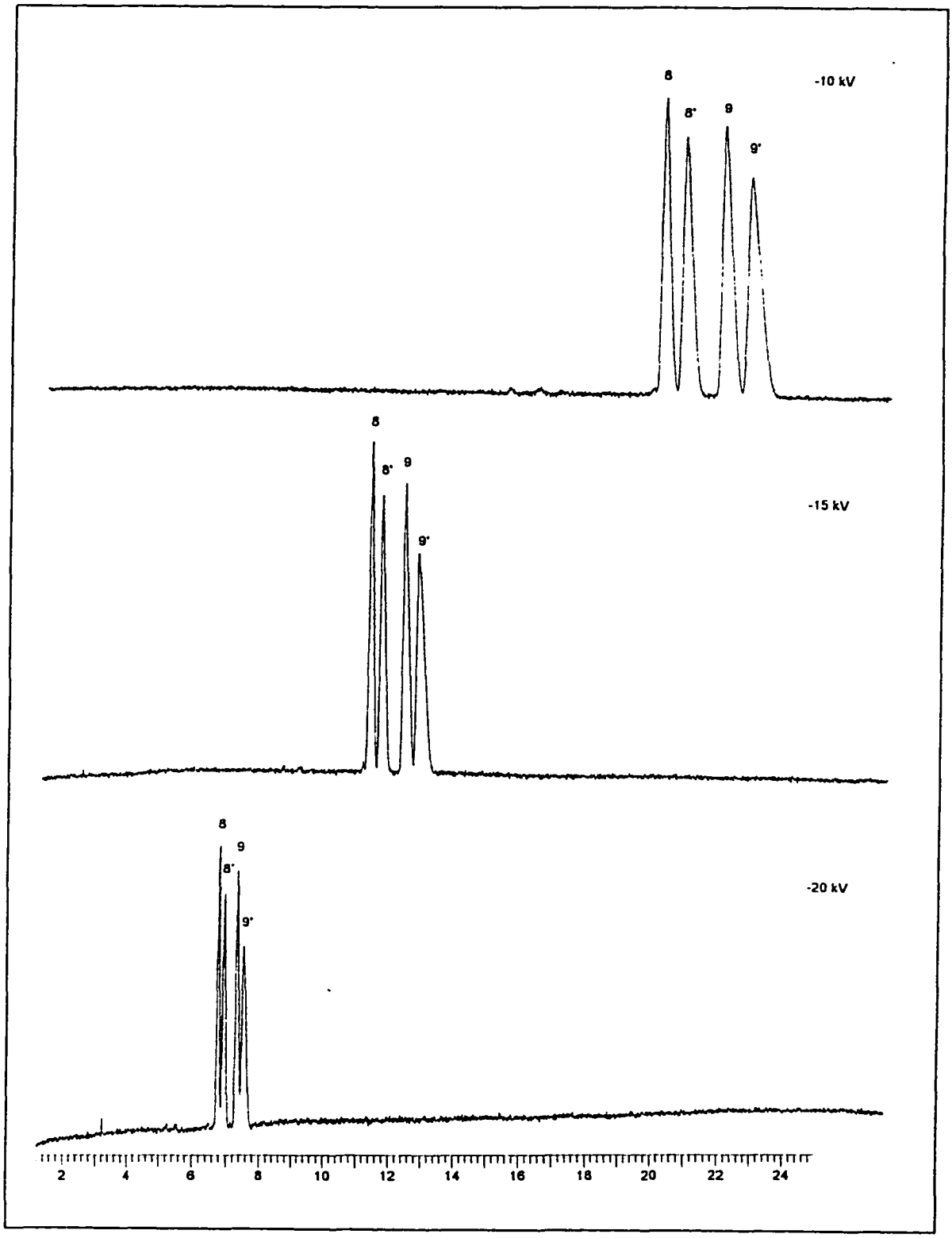

Fig. 2.20c. The effect of applied voltage on the separation of Thr and Val enantiomers. The applied voltage is printed on each electropherogram. [Q-CD] = 0.5 mM. Other conditions are listed in Table 2.2.

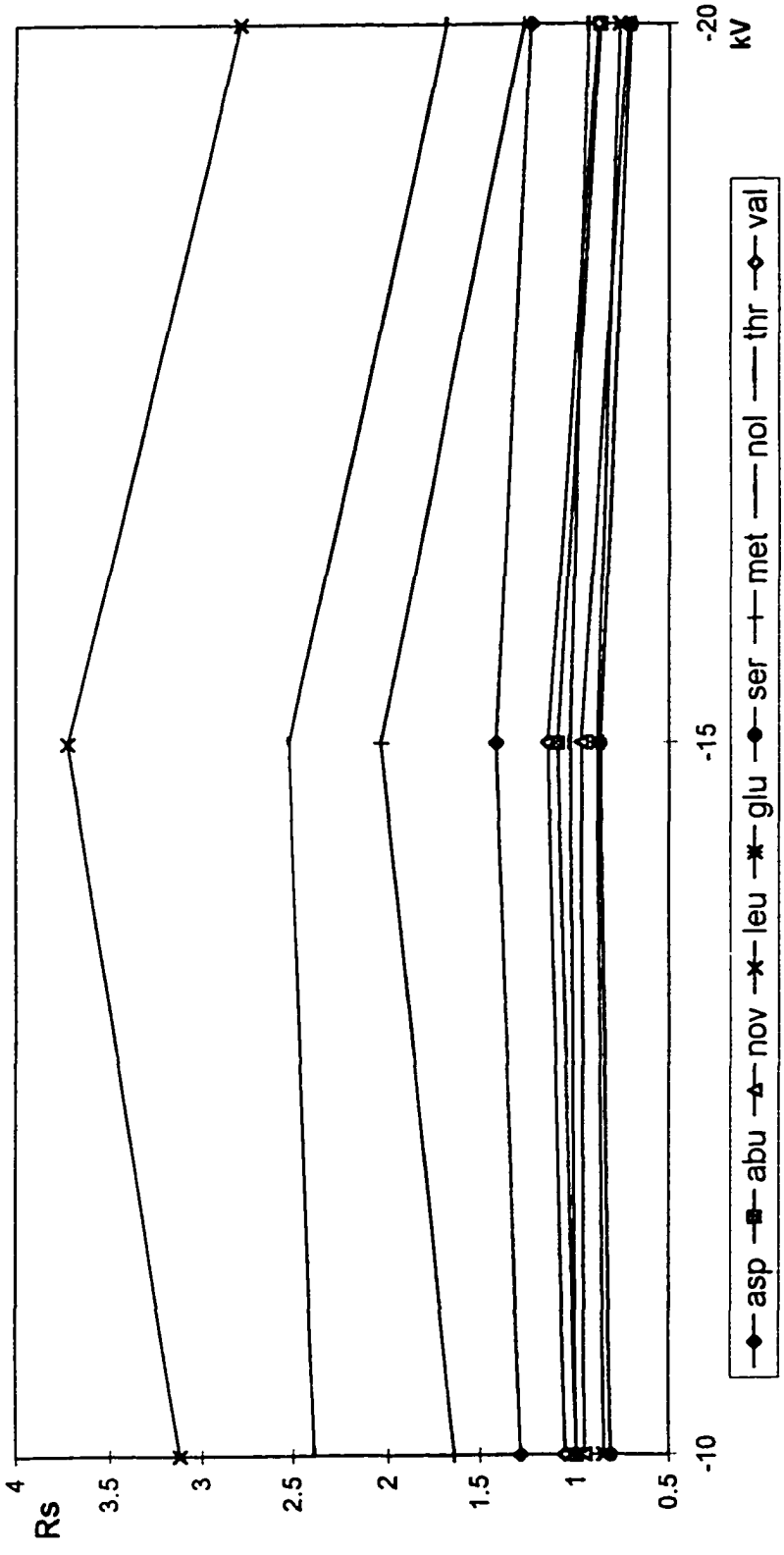

Fig. 2.21. The effect of the applied voltage on the resolution of 10 Dns-*DL*-*AA* enantiomers.

voltage is not very effective for improving resolution. To double the resolution, the voltage must be quadrupled. Ballou *et al.* [114] showed that efficiency and resolution are largely independent of the applied voltage when the capillary is efficiently thermostated. Although the joule heating has not evidently occurred with applied voltage of 20 kV in our study, we expect joule heating limitations will be quickly approached with further increase in the voltage.

2.5.5. Effect of the buffer pH

The model of Rawjee and Vigh for weak acid analytes predicted that good chiral resolution can be obtained only in the vicinity of the pK_a, which was supported by the separation of ibuprofen using native β-CD [83]. Fig. 2.22 shows the electropherograms of Dns-DL-AAs at pH 5 (30 mM of acetate buffer) and 7 (30 mM of phosphate buffer). At both pHs, all the Dns-DL-AAs behave as anions and migrate anodically. The migration times, resolution and peak shapes of all the enantiomers are comparable.

2.6. Counterflow capillary electrophoresis with the partial-filling method

2.6.1. Introduction

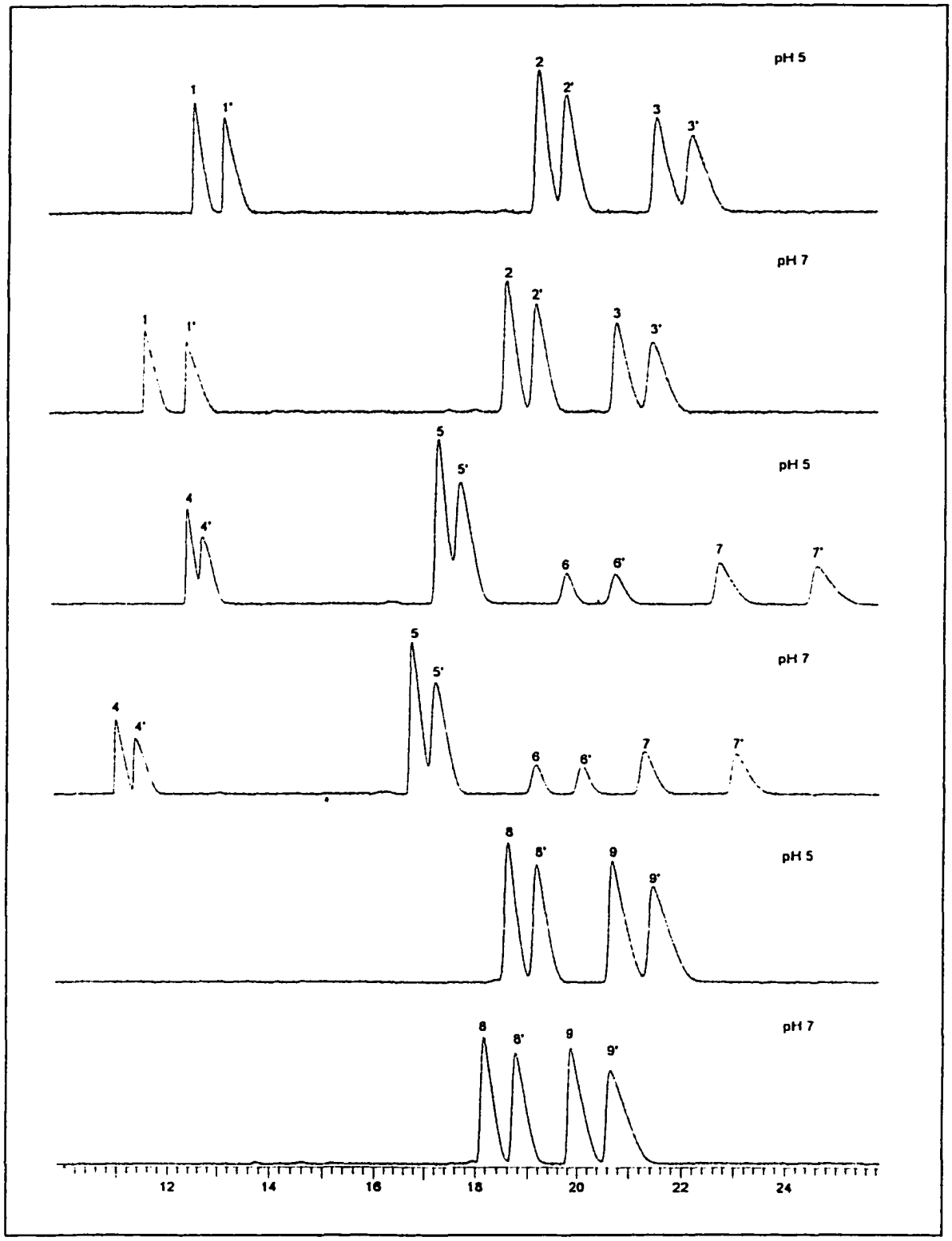

Fig. 2.22. The effect of buffer pH on the separation of Dns-DL-AA enantiomers. The buffer pH is printed on each electropherogram. pH 5 buffer contains 30 mM acetate, while pH 7 buffer contains 30 mM phosphate. [Q-CD] = 1 mM. Other conditions are listed in Table 2.2.

As shown, high chiral recognition has been achieved by using the counterflow mode in a coated capillary, in which the analytes injected migrate in the opposite direction to a constant electrophoretic flow of the chiral selector. All of the experiments above were performed in a "conventional" CE mode, which means that the buffer flowing between detection and injection side buffer reservoirs had identical composition (chiral selector in phosphate buffer solution). During the separations, the detection side (anode in our experiment) buffer reservoir constantly provides the chiral selector (Q-CD), which migrates across the capillary to injection side buffer reservoir (cathode). The analytes (Dns-DL-AAs) experience a dynamic equilibrium with the chiral selector continuously during their migration from the injection to detection. This method has certain advantages such that the system is simple, easy to control, and relatively reproducible. There are two major disadvantages for this method. First, a certain amount of chiral selector is necessary to make a series of buffers with various concentrations of additives during the methods development. Normally each buffer reservoir requires about 10 mL of buffer solution, but only several nL of it flows through the capillary and participates in the interaction with the analytes injected. First, use of a specialty chiral selector available only in limited amount could precludes study of that selector. Second, certain chiral selectors might interfere with some detection methods since the chiral selector is constantly flowing through the detection cell. No matter what kind of detection method is chosen, a noninterference detection background is always prefered. For instance, a UV absorbing chiral selector might be precluded if UV detection are required.

To find an alternative solution to these potential problems of CE chiral separations, an unconventional CE method, called "partial-filling method", was investigated. A schematic representation of this method is given in Fig. 2.23. The capillary is initially filled with selector-free buffer. Then, part or all of this is displaced by buffer containing chiral selector. Both injection and detection buffer reservoirs contain only selector-free buffer. Next, the analytes (Dns-DL-AAs) are injected immediately in the usual fashion, followed by application the high voltage across the capillary. Under the electric field, the zone of negatively charged analytes moves towards the detection end (anode), and the positively charged Q-CD moves away from detection end towards the injection end (cathode). The molecular interaction between Q-CD and the analytes takes place while they cross each other in the capillary. The detection window will be free of selector while the analytes pass through. Using a similar technique, Ward *et al.* [115] obtained baseline resolution of the enantiomers of seven nonsteroidal anti-inflammatory drugs and three dansyl amino acids using 2 mM vancomycin. Tanaka and Terabe [116] used chiral proteins to separate basic racemates using what they called "partial separation zone technique". Nelson and Lee [117] used partial-filling MEKC coupled with electrospray mass spectrometry detection to eliminate the potential mass spectral interference from high molecular weight surfactants such as sodium dodecyl sulfate (SDS). In these cases, the separated zone of the analytes and chiral selector or surfactant generated by the partial-filling method eliminated the potential interference of either SDS on mass spectral background or vancomycin on UV detection. In our study, several pairs of Dns-DL-AAs

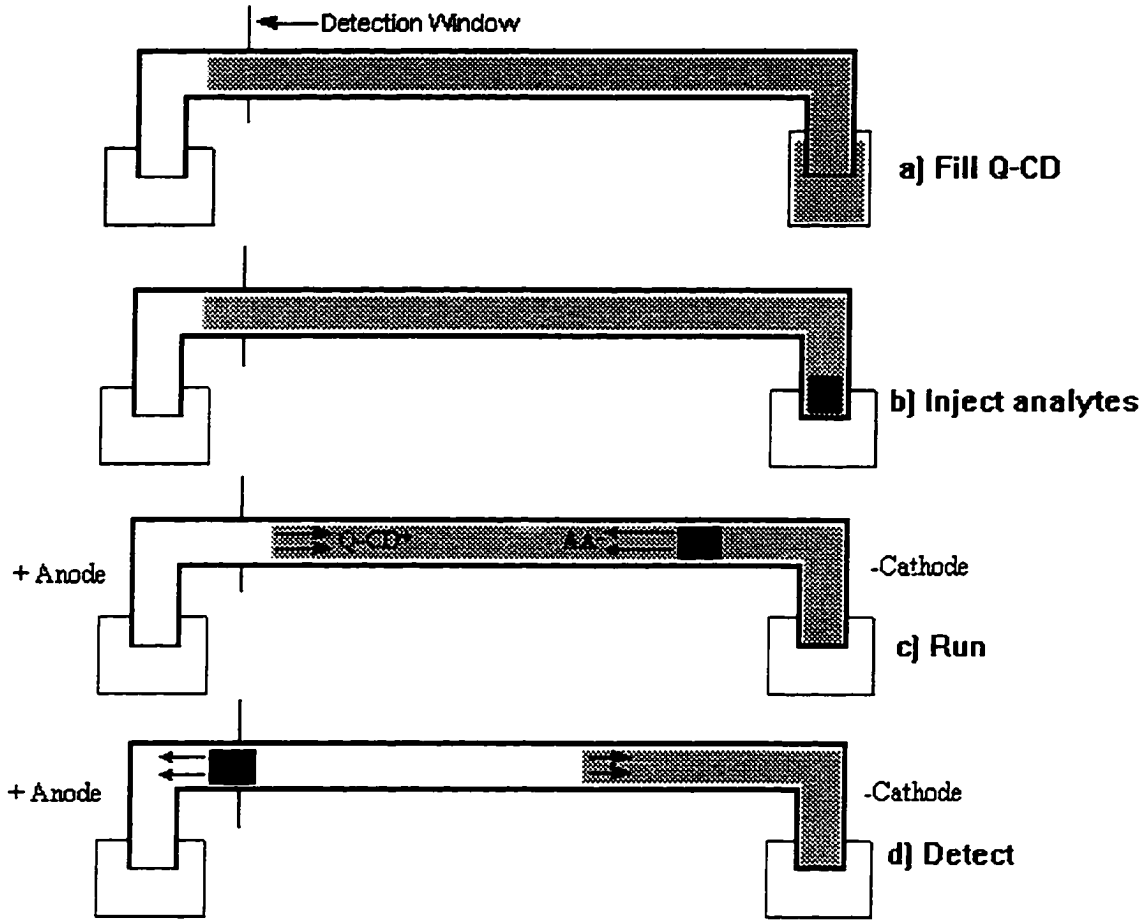

Fig.2.23. Schematic description of partial-filling method.

were separated by this partial-filling method with a coated capillary partially filled to various lengths with Q-CD-containing buffer. Some theoretical aspects of this method are discussed.

2.6.2. Theory

As illustrated in Fig. 2.23, the molecular interaction between Q-CD and enantiomers, which results in chiral separation, occurs only within the length of the moving Q-CD band (l_Q).

$$A^- + nQCD^+ \xleftrightarrow{K_A} A^-(QCD^+)_n \qquad (39)$$

where A^- stands for an analyte and K_A is the binding constant between the analyte and Q-CD. The retention times of an analyte can be expressed as the sum of the times spent in the Q-CD band and in the buffer,

$$t_A = (l-l_Q)/v_{AB} + l_Q/v_{AQ} \qquad (40)$$

Where l is the effective length of the capillary, l_Q is the length of the capillary filled by Q-CD buffer, v_{AB} is the electrophoretic velocity of the analyte in the buffer solution, and v_{AQ} is the electrophoretic velocity of the analyte in the moving Q-CD band. While v_{AB} can be determined experimentally, v_{AQ} can be expressed as:

$$v_{AQ} = v_{AB}\alpha_A + v_Q\alpha_{AQ} \quad (41)$$

$$= v_{AB}\,(1/1+K_A[QCD^+]^n) + v_Q(K_A[QCD^+]^n/(1+K_A\,[QCD^+]^n) \quad (42)$$

where α_A and α_A stand for the mole fraction of uncomplexed analyte and complexed analyte respectively, and v_Q stands for the electrophoretic velocity of Q-CD. Rearranging equation (42),

$$v_{AQ}=(\,1/1+K_A[QCD^+]^n)\,(v_{AB}+ v_Q K_A[QCD^+]^n). \quad (43)$$

Combining equation (40) and (43) and rearranging,

$$t_A = l_Q\left(\frac{1+K_A\left[QCD^+\right]^n}{v_{AB}+v_Q K_A\left[QCD^+\right]^n}-\frac{1}{v_{AB}}\right)+\frac{1}{v_{AB}} \quad (44)$$

The retention time of an analyte should be linear function of filing length, l_Q. Assigning $l_Q = fL$. Where f is the fraction of the length of the capillary filled with Q-CD buffer. The velocities can be substituted by mobilities using $v = \mu V/L$, where L is the total length of the capillary and V is applied voltage. Plugging these into equation (44), the retention time of an analyte is:

$$t_A = f\cdot\frac{L^2}{V}\left(\frac{1+K_A\left[QCD^+\right]^n}{\mu_{AB}+\mu_Q K_A\left[QCD^+\right]^n}-\frac{1}{\mu_{AB}}\right)+\frac{Ll}{\mu_{AB}V} \quad (45)$$

Equation (42) shows that the retention time of an analyte should be linearly proportional to the fraction of the capillary length filled with Q-CD buffer, f.

The chiral selectivity can be measured by mobility ratio of enantiomers ($A_{D/L}$),

$$A_{D/L} = \mu_D/\mu_L = v_D/v_L = t_L/t_D. \quad (46)$$

A cumbersome equation will be generated if equation (45) is inserted. Alternatively, the definition of resolution, $R_S = 2\Delta t/(W_D+W_L)$, may be used with equation (45) to describe the degree of separation without considering the effect of diffusion. Then Δt should increase linearly with increasing f.

2.6.3. Experimental section

The flow rate of the Q-CD solution using vacuum injection is calculated as follows. First an analyte solution is injected and driven towards the detector by applying a vacuum of 20 mm Hg at the detection side with no applied voltage. The retention time of the analyte is measured. The flow rate is obtained by dividing the effective length of the capillary by the retention time. In our study, the measured flow rate is 78.7 cm/min using a vacuum of 20-mm Hg in a 44-cm long, 50 μm id capillary. This enables calculation of the time required to inject any length of Q-CD solution. The separation of 5 Dns-DL-AAs using 1.5 mM Q-CD was examined with filling times from 0.2 to 1 min (corresponding to about half to total length of the capillary). Other experimental conditions are same as

described in Table 2.2.

2.6.4. Results and Discussion

The electropherograms of Dns-DL-AAs separated by the partial-filling method are given in Figs. 2.24a,b. The migration time of the enantiomers increased with increase of the filling time. Fig. 2.25 illustrates the retention time of enantiomers as a function of *f*, which is calculated as follow:

$$f = l_{QCD}/L = 78.6t_{QCD}/44 = 1.17t_{QCD} \qquad (44)$$

where t_{QCD} is Q-CD buffer filling time, L is the length of the capillary, and l is the effective length. In Fig. 2.26 is a plot of retention time difference of enantiomers as a function of *f*. The results support the theory in section 2.5.2. With increasing length of filled Q-CD buffer, the retention times of Dns-DL-AAs increased linearly, and the chiral resolution is improved until Q-CD buffer occupies the whole capillary.

The use of partial-filling method has several advantages over the conventional mode of capillary electrophoresis in the application of chiral separation. Since no chiral selector is present in either side of the buffer, only a minute amount of chiral selector is needed to complete the separation. It enables the use of expensive or specially synthesized

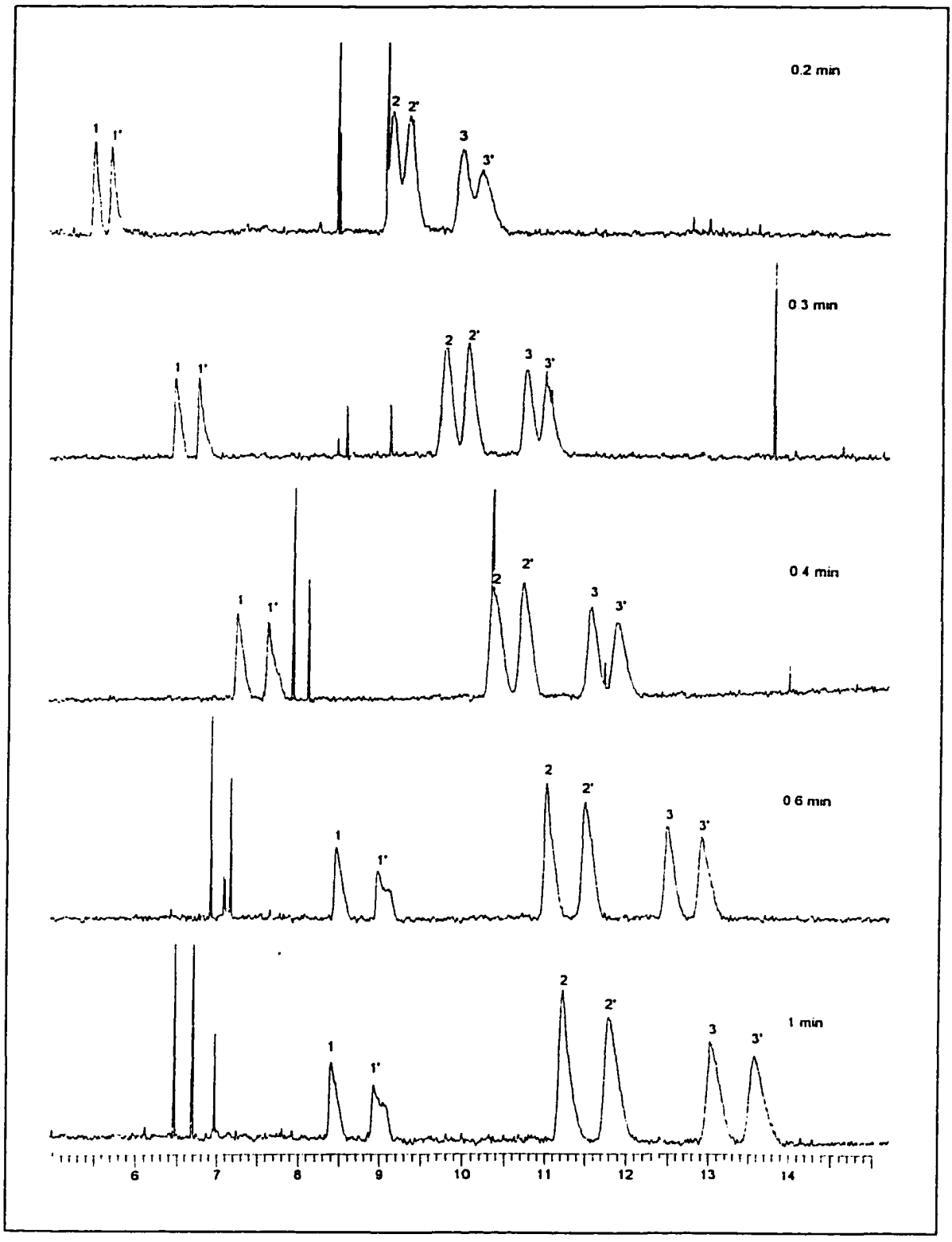

Fig. 2.24a. The separation of Asp, Abu and Norval enantiomers by the method of capillary partially filled with chiral selector. Filling time is printed on each electropherogram. [Q-CD] = 1.5 mM. Capillary is 44 cm total length with 23.5 effective length between detection and injection. Other conditions are listed in Table 2.2.

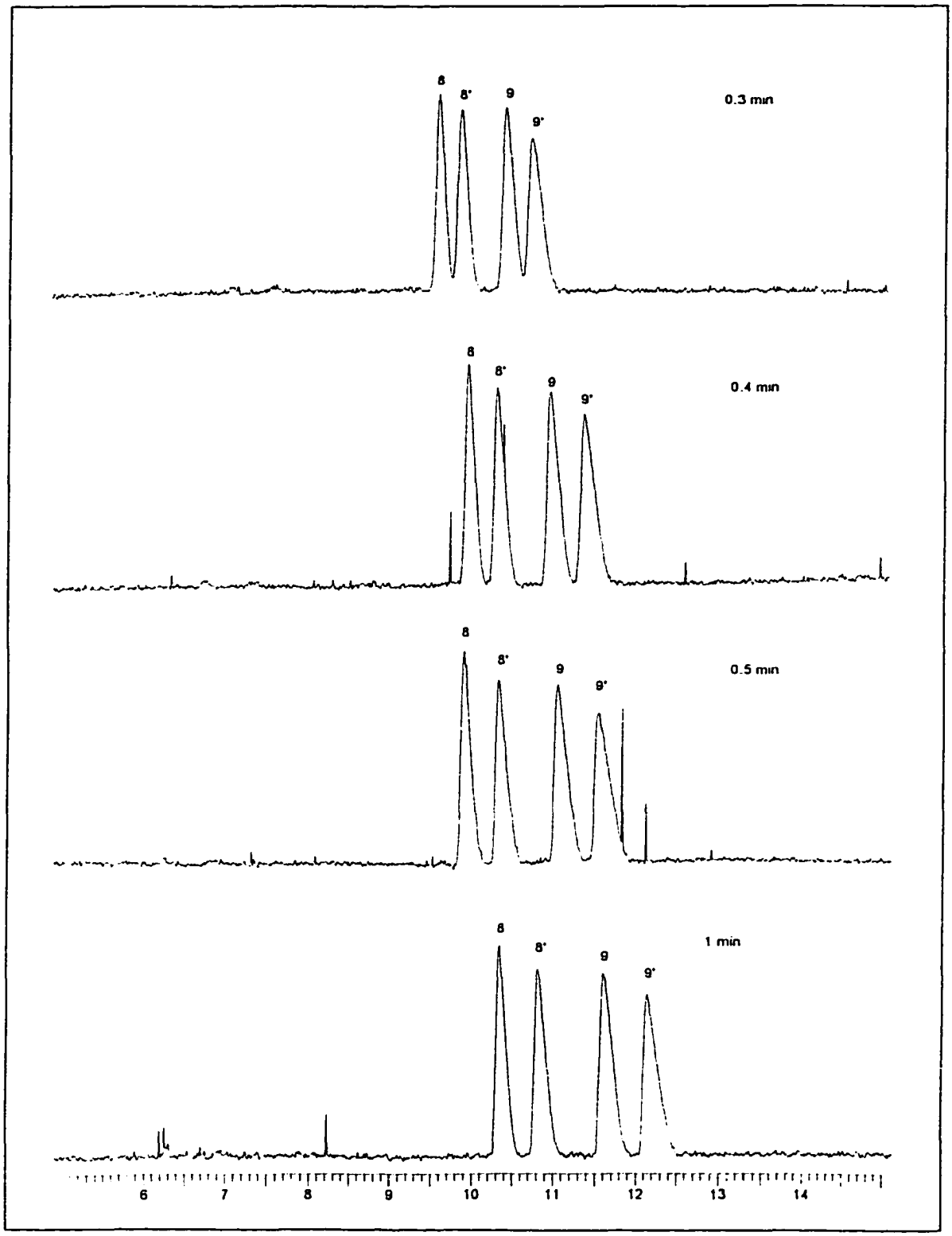

Fig. 2.24b. The separation of Thr and Val enantiomers by the method of capillary partially filled with chiral selector. All conditions are the same as Fig. 2.24a.

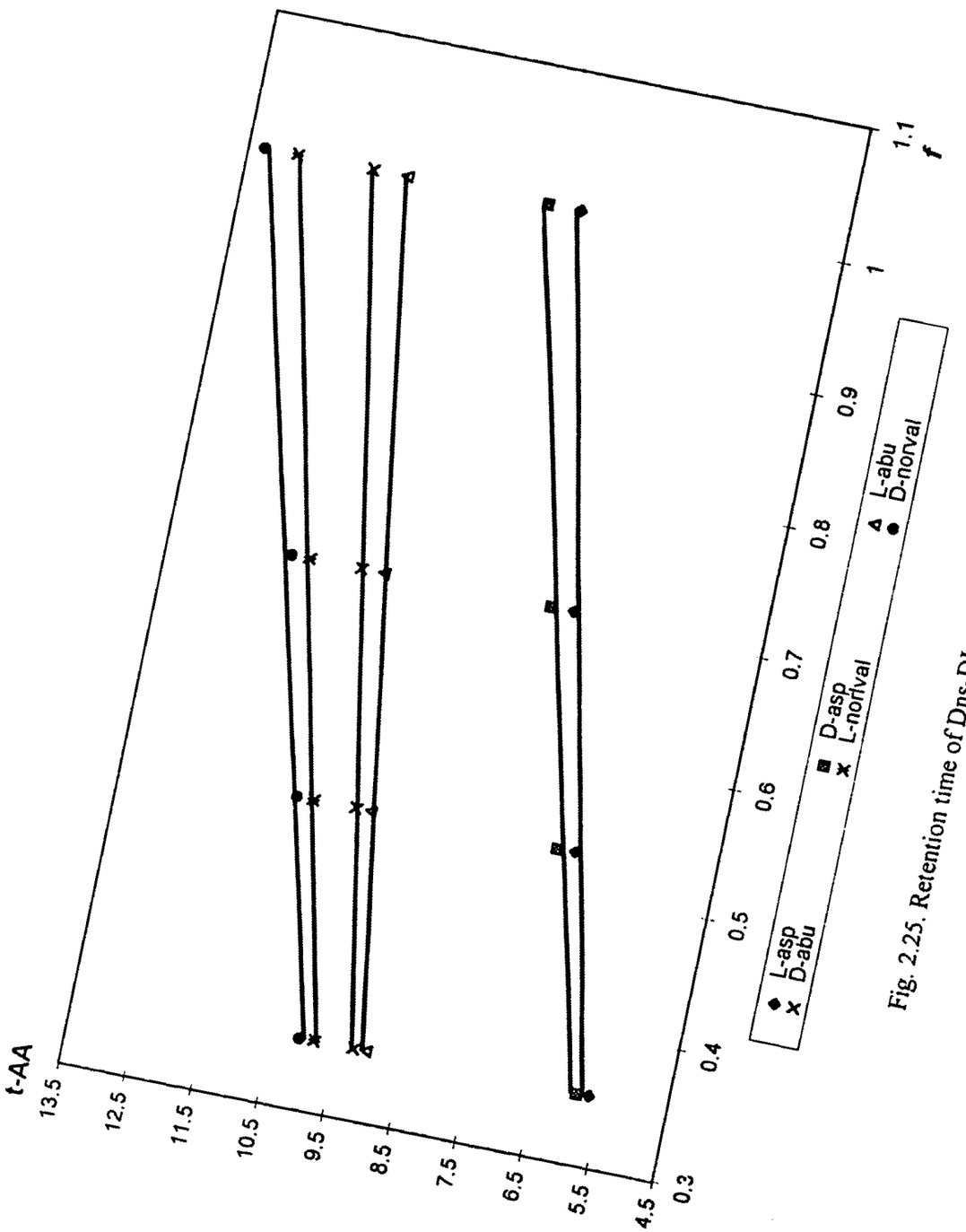

Fig. 2.25. Retention time of Dns-DL-AAs as a fuction of f.

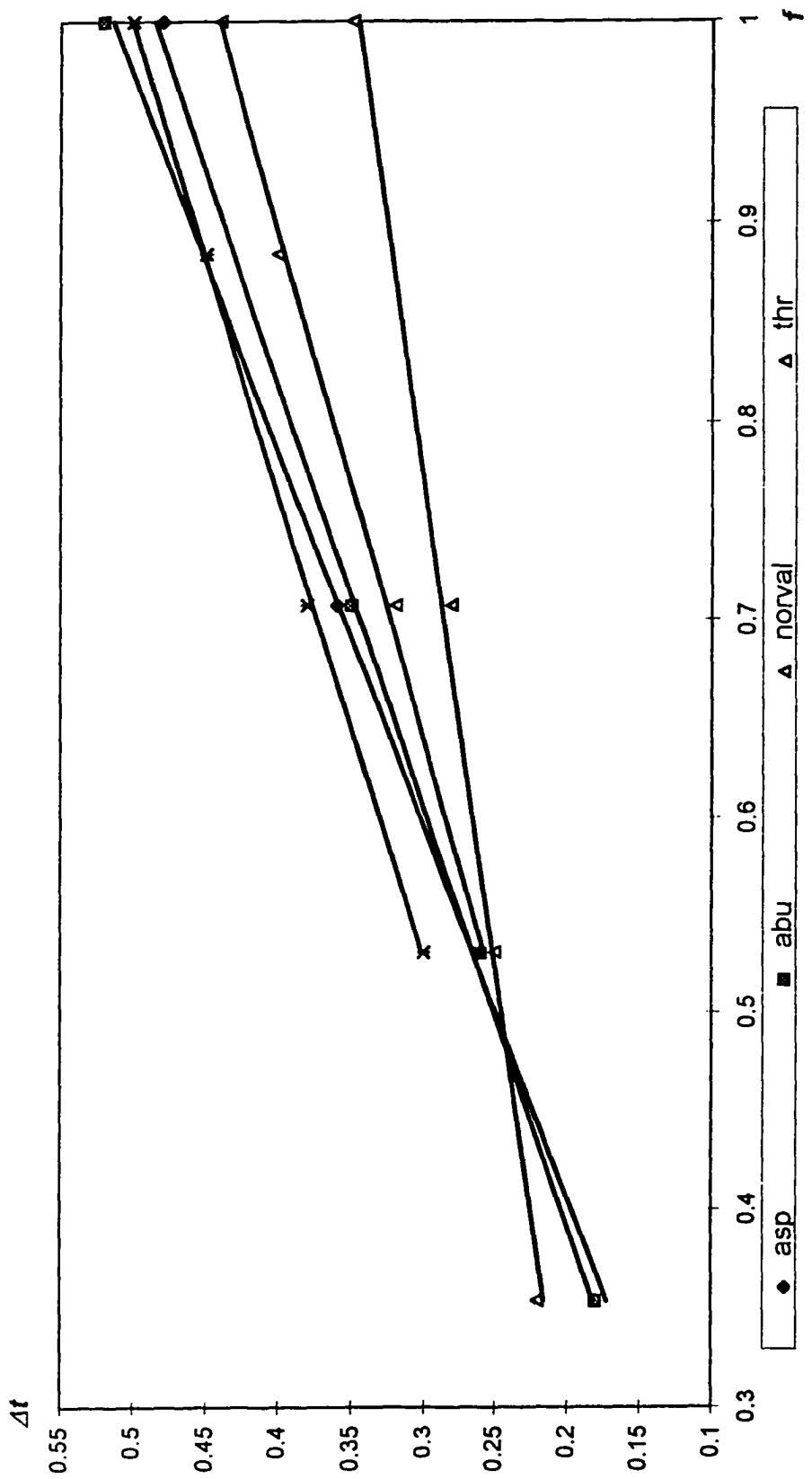

Fig. 2.26. The retention time difference (Δt) of enantiomers as a function of f.
All conditions are the same as Fig. 2.24a.

compounds available in a very limited amount. Since chiral selector in capillary travels to the injection side upon applying the voltage, the detection window is clear when the enantiomers arrive. This feature is valuable for various CE detection modes, most of which require clean background for sensitive detection.

2.7. Conclusions

Cationic quaternary ammonium β-cyclodextrin shows significantly better chiral selectivity than native β-cyclodextrins or neutral cyclodextrin derivatives for separation of anionic enantiomers such as the dansyl amino acids used in our study. All twelve Dns-DL-AAs showed baseline resolution at concentration of Q-CD as low as 0.2 - 1 mM. Electrostatic attraction between the Q-CD and solutes not only provided stronger binding but also contributed one of the points of molecular interaction necessary to achieve successful chiral recognition. Using a coated capillary totally suppressed the electroosmotic flow, and enabled true counterflow in a capillary, which provides the good contact between anionic enantiomers and cationic chiral selectors.

Adding organic modifiers to the buffer reduced the hydrophobic interaction between analytes and Q-CD, and consequently reduced the resolution of the enantiomers. However organic modifiers improved the peak shape. Peak tailing was completely

eliminated in the presence of 10% isopropyl alcohol in the buffer. Temperature and applied voltage also had dramatic effects on the separation. Increasing temperature had a purely negative effect on the resolution of the enantiomers of Dns-DL-AAs, since the separation temperatures were below their isoenantioselective temperatures. Increasing the applied voltage is not a very good way of improving the resolution. High voltage could lead to Joule heating, which would severely damage the separation. In addition, changing buffer pH from 5 to 7 had no noticeable effect on either the mobility or resolution of the enantiomers.

Counterflow capillary electrophoresis with the partial-filling method provides an unconventional way for chiral separations. This approach needs only a tiny amount of chiral selector to accomplish a separation because no chiral selector is present in the background electrolyte. The separated moving zone of the analytes and chiral selector eliminate the potential detection interference by chiral selector.

References

Part one

1. Pizzi, A., Holzforschung, 1993, 47, 53.
2. Pizzi, A., Holzforschung, 1993, 47, 343.
3. Gibert Jr., F.I.; Minn, C.E.; Duncan, R.C., Archiv. Environ. Contamin. Toxicity, 1990, 19, 603.
4. ASTM D 1625-71. 1995 Annual Book of ASTM Standards, Vol. 04.10, Wood. American Society for Testing and Materials, Philadelphia, PA 19103.
5. Ganapati, P. N.; Nagabhushanam, R., J. Timb. Dry. Preserv. Ass. India. 1964, 10 (1), 13.
6. Sanders, J. G.; Window, H. L., Estuar. Coast. Mar. Sci. 1980, 10, 555.
7. IARC. IARC Mongr. Eval. Carcinog. Risk Chem.Humans. 1980, 23, 39.
8. USEPA. Ambient Water Quality Criteria For Chromium. 1988, Springfield, VA.
9. AARC Team Inc., Engineering Services, 346 Broadway, NY. Report, "Nott Ave. Pier, Long Island City, NY: Condition Survey of Pier for Structural Integrity", Feb. 1997.
10. Kovalevich, M., President, AARC Team Inc., Private Communication.
11. Information Pamphlet, Recycling, Dept. of Goverment Relations and Science Policy, ACS, Washington, DC 20036.
12. Technology Transfer Manual-Plastic Collection and Sortation. Piscataway, NJ: Center for Plastics Recycling Research, 1988.

13. Hegberg, B.A.; Brenniman, R; Hallenbeck, W.H., Mixed Plastics Recycling Technology, Noyes Data Corp., Boston, 1992.

14. Kellis, A. M.; Solomon, K. R., J. Arch. Environ. Contam. Toxicol. 1995, 28, 134.

15. Weis P.; Weis, J. S.; Greenberg, A.; Nosker, T., J. Arch. Environ. Contam. Toxicol. 1992, 22, 99.

16. Lyman, J.; Fleming, R.H. Composition of Sea Water., J. Marine Res., 3, 1940, 134.

17. Mahoney, J. Professor, Manhattan College, Private Communication.

18. Van Nostrand Reinhold Encyclopedia of Chemistry, 4th ed. 1984, NewYork.

19. Ainsworth, S., J. Chem. Eng. News. Jan. 1994, 34.

20. McGraw-Hill Encyclopedia of Chemistry, 2nd ed. 1993, McGraw-Hill, New York.

21. Rowell, R., Chemistry of Solid Wood. ACS, 1984, 57.

22. Hillis, W.E., Ed, Wood Extractives, VCH, New York, 1962.

23. Ullmann's Encyclopedia of Industrial Chemistry, 5rd Ed. VCH, New York, 1995.

24. Merck Index, 11th ed.

25. Fawell, J.K.; Hunt, S., Environ. Toxicol., Organic Pollutants. Ellis Horwood Ltd., London, 1988.

26. Cherian, P. V.; Sharma, M. N.; Cherian, C. J., J. Ind. Acad. Wood Sci. 1979, 10, 31.

27. Hegarty, B. M.; Curran, P. W., J. Inst. Wood Sci. 1986, 10, 245.

Part Two

1. Anon..,C&EN, 1990 (March 19), 38.
2. Innes, I.R.; Nickersen, M. in Goodman L.S.; Gilman, A. (Edrs), The Pharmacological Basis of Therapeutics, MacMillan, New York, NY, 1970, p. 477.
3. Vermeulen, N.P.E.; Koppele, J. M. te; Wainer, I.W. (Edrs) Drug Stereochemistry, Marcel Dekker, New York, 1993, p. 245.
4. Stinson, S.C. C&EN, 1992 (Sept. 28), 46.
5. Debowski, J.; Sybilska, D. Jurczak, J., J. Chromatogr., 282, 1983, 83.
6. Blaschke, G., J. Liq. Chromatogr., 9, 1986, 341.
7. Dou, L.; Zeng J.N.; Gerochi, M.P.; Stuting, H.H. J. Chromatogr., 679, 1994, 367.
8. Maas, B.; Dietrich, A.; Mosandl, A. J. Microcolumn Sepn., 8, 1996, 47.
9. Feibush, B.; Woolley, C.L.; Mani, V., Anal. Chem., 65, 1993, 1130.
10. Duncan, J.D., J. Liq. Chromatogr., 13, 1990, 2737.
11. Duncan, J.D.; Armstrong, D.W.; Stalcup, A.M., J. Liq. Chromatogr., 13, 1990, 1091.
12. Garcia, K.E.; Medvedovici, A.; Sandra, P., J. Liq. Chromatogr., 19, 1996, 569.
13. Stingham, R,W.; Blackwell, J., A. Anal. Chem., 69, 1997, 1414.
14. Macaudiere, P.; Caude, M.; Rosset, R., J. Chromatogr. Sci., 27, 1989, 583.
15. Pirkle, W.H.; Welch, C.J., J. Chromatogr., 731, 1996, 322.
16. Schleimer, M.; Pirkle, W.H.; Schurig, V., J. Chromatogr. A, 679, 1994, 23.

17. Pirkle, W.H.; Terfloth, G.J., J. Chromatogr. A, 704, 1995, 269.

18. Villani, C.; Pirkle, W.H., J. Chromatogr., 693, 1995, 63.

19. Amstrong D.W.; Faulkner J.R.J.; Han, S.M., J. Chromatogr. A, 452, 1994, 367.

20. Armstrong, D.W.; Zukowski, J., J. Chromatogr. A, 666, 1994, 445.

21. Reid, G.L.; Wall, W.T.; Armstrong, D.W., J. Chromatogr., 633, 1993, 143.

22. Armstrong, D.W.; Chang, C.-D.; Lee, S.H., J. Chromatogr., 539, 1991, 83.

23. Stalcup, A.M.; Change, S.-C.; Armstrong, D.W., J. Chromatogr., 513, 1990, 181.

24. Karger, B.L.; Cohen, A.S.; Guttman, A., J. Chromatogr., 492, 1989, 585.

25. Deyl, Z.; Stuzinsky, R., J. Chromatogr., 569, 1991, 63.

26. Kuhn, W.G.; Monning, C., A. Anal. Chem., 64, 1992, 389A.

27. Mikker, F.E.P.; Everaerts, F.M.; Verheggen, P.E.M., J. Chromatogr., 169, 1979, 11.

28. Jorgenson, J.W.; Lukacs, K.D., Anal. Chem., 53, 1981, 1298.

29. Weinberger, R., Practical Capillary Electrophoresis, 1993, Academic Press, New York.

30. Terabe, S.; Otsuka, K.; Ichikama, K.; Tsuchiya, A.; Ando, T., Anal. Chem., 56, 1984, 111.

31. Terabe, S.; Otsuka, K.; A.; Ando, T., Anal. Chem., 57, 1985, 834.

32. Everaerts, F.M.; Beckers, J.L.; Verheggen, Th.P.E.M., Isotachophoresis: Theory, Instrumentation and Applications, 1976, Elsevier Scientific Publishing, Amsterdam.

33. Bocek, P.; Deml, M.; Gebauer, P.; Dolnik, V., Analytical Isotachophoresis, 1988, VCH, New York.

34. Cohen, A.S.; Karger, B.L., J. Chromatogr., 397, 1987, 409.

35. Tsuji, K., J. Chromatogr., 550, 1991, 823.

36. Hjerten, S.; Zhu, M.D., J. Chromatogr., 346, 1985, 265.

37. Mazzeo, J.R.; Krull, I.S., Anal. Chem., 63, 1991, 2852.

38. Li, S.; Purdy, W.C., Chem. Rev., 92, 1992, 1457.

39. Fanali, S., J. Chromatogr., 474, 1989, 441.

40. Nardi, A.; Ossicini, L.; Fanali, S., Chirality, 4, 1992, 56.

41. Belder, D.; Schomburg, G., J. High Resolut. Chromatogr., 15, 1992, 686.

42. Quang, C.; Khaledi, G., J. High Resolut. Chromatogr., 17,1994, 99.

43. Heuermann, M.; Blaschke, G., J. Chromatogr,. 648, 1993, 267.

44. Smith, N.W., J. Chromatogr., 652, 1993, 259.

45. Schmitt, T.; Engelhardt, H., J. High Resolut. Chromatogr., 16, 1993, 525.

46. Schmitt, T.; Engelhardt, H., Chromatographia. 37, 1993, 475.

47. Nardi, A.; Eliseev, A.; Bocek, P.; Fanali, S., J. Chromatogr., 638, 1993, 247.

48. Armstrong, D.W; Tang, Y.; Ward, T.; Nichols, M., Anal. Chem., 65, 1993, 1114.

49. Mayer, S.; Schurig, V., J. High Resolut. Chromatogr., 15, 1992, 129.

50. Mayer, S.; Schurig, V., J. Liq. Chromatogr., 16, 1993, 915.

51. Gassman E.; Kuo, J.E.; Zare, R.N., Science, 230, 813.

52. Gozel, P.; Gassman E.; Michelsen, H.; Zare, R.N., Anal. Chem., 59, 1987, 44.

53. Davankov, V.A.; Rogozhin, S.V., J. Chromatogr., 60, 1971, 280.

54. Cohen, A.S.; Paulus, A.; Karger, B.L., Chromatographia, 24, 1987, 15.

55. Nishi, H., J. Chromatogr. A, 735, 1996, 57.

56. Kuhn, R; Stoechlin, F.; Erni, F., Chromatographia, 33, 1992, 32.

57. Hohne, E; Krauss, G-J.; Gubitz, G., J. High Resolut. Chromatogr. 15,1992, 698.

58. Allenmark, S; Andersson, S. Molecular Interaction in Bioseparations, 1993, Plenum Press, New York, p. 179.

59. Valtcheva,L.; Mohammad, J.; Petterson, G.; Hjerten, S., J. Chromatogr., 638, 1993, 263.

60. Birnbaum, S.; Nilsson, S., Anal. Chem., 64, 1992, 2872.

61. Ward, T.J., Anal. Chem., 66, 1994, 633A.

62. Armstrong, D.W.; Rundlett, K; Reid, G.L., Anal. Chem., 66, 1994, 1690.

63. Soini, H.; Teikkola, M.L.; Novotny, M.V., J. Chromatogr., 608, 1992, 265.

64. Terabe, S.; Otsuka, K.; Ando, T., J. Chromatogr., 1985, 332, 211.

65. Gahm, K-H.; Chang, L.W.; Armstrong, D.W., J. Chromatogr. A., 759, 1997, 149.

66. Terabe, S., Trends Anal. Chem. 8, 1989, 129

67. Nardi, A.; Eliseev, A.; Bocek, P.; Fanali, S., J. Chromatogr., 638, 1993, 247.

68. Lelievre F.; Gareil P.; Jardy A., Anal. Chem., 69, 1997, 385.

69. Hjerten, S., J. Chromatogr., 347,1985, 191.

70. Janini, G.M.; Issaq. H. J., J. Chromatogr. A, 657, 1994, 419.

71. Chirari, M.; Nesi, M., Electrophoresis, 15, 1994, 177.

72. Novotny, M.V., Anal. Chem., 62, 1990, 2478.

73. Yoshnaga, M.; Tsanaka, M., J. Chromatogr. A, 679, 1994, 359.

74. Yoshnaga, M.; Tsanaka, M., J. Chromatogr. A, 710, 1995, 331.

75. Guttman, A.; Paulus, A.; Cohen, A.S.; Grinberg, N.; Karger, B.L., J. Chromatogr., 488, 1988, 41.

76. Armstrong, D.W.; Gasper, M.P.; Rundlett, K.L., J. Chromatogr. A, 689, 1995, 285.

77. Sun, P.; Wu, N.; Barker, G.; Hartwick, R.A., J. Chromatogr. A, 648, 1993, 475.

78. Sundin, N.G.; Dowling, T.M.; Grinberg, N.; Bicker, G., J. Microcolumn Sepn, 8, 1996, 323.

79. Wren, S.A.; Rowe, R.C., J. Chromatogr., 603, 1992, 235.

80. Wren, S.A.; Rowe, R.C., J. Chromatogr., 609, 1992, 363.

81. Wren, S.A.; Rowe, R.C., J. Chromatogr., 635, 1993, 113.

82. Wren, S.A., J. Chromatogr., 636, 1993, 57.

83. Wren, S.A.; Rowe, R.C.; Payne, R.S., Electrophoresis, 15, 1994, 804.

84. Penn, S.G.; Liu G., Bergstrom E.T.; Goodall, D.M.; Loran, J.S., J. Chromatogr., 680, 1994, 147.

85. Penn, S.G.; Bergstrom E.T.; Goodall, D.M.; Loran, J.S., Anal. Chem., 66, 1994, 2866.

86. Piperaki, S.; Penn, S.G.; Goodall, D.M., J. Chromatogr.,700, 1995, 59.

87. Ferguson, P.D.; Goodall, D.M.; Loran, J.S., J. Chromatogr., 745, 1996, 25.

88. Penn, S.G.; Bergstrom E.T.; Knights, I.; Liu G.; Ruddick, A. Goodall, D.M., J.

Phys. Chem., 99, 1995, 3875.

89. Rawjee, Y.Y.; Staerk, D.U.; Vigh, G., J. Chromatogr., 652, 1993, 291.

90. Rawjee, Y.Y.; Williams, R.L.; Vigh, G., J. Chromatogr., 652, 1993, 233.

91. Rawjee, Y.Y.; Williams, R.L.; Vigh, G., J. Chromatogr., 680, 1994, 599.

92. Baumy, P.; Morin, P.; Dreux, M; Viaud, M.C.; Boye, S.; Guillaumet, G., J. Chromatogr. A, 707, 1995, 311.

93. Shibukawa, A.; Lloyd, D.K.; Wainer, I.W., Chromatographia, 5, 1993, 419.

94. Valko, I.E., Billiet, H.A.H., Frank, J., Luyben, K.C.A.M., Chromatographia, 38, 1994, 730.

95. Penn, S.G.; Goodall, D.M.; Loran, J.S.J., J. Chromatogr., 636, 1993, 149.

96. Fanali, S.; Bocek, P., Electrophoresis, 17, 1996, 1921.

97. Armstrong, D.W.; DeMond, W., J. Chromatogr. Sci., 22, 1984, 411.

98. Terabe, S.; Yashima, T.; Tanaka, N.; Araki, M., Anal. Chem., 60, 1988, 1673.

99. Huang, X; Coleman F.; Zare, R. N., J. Chromatogr., 480, 1989, 95.

100. Armstrong, D.W.; Ward, T.J; Armstrong, R.D.; Beesley, T.E., Science, 232, 1986, 113.

101. Fanali, S., J. Chromatogr., 545, 1991, 437.

102. Fanali, S.; Aturki, Z., J. Chromatogr., 694, 1995, 297.

103. Mikkers, F.E.P.; Everaerts, F.M.; Verhegeen, T.P.E.M., J. Chromatogr.,169, 1979, 1.

104. Thormann, W., Electrophoresis, 4, 1983, 383.

105. Beckers, J. Electrophoresis, 16, 1995, 1987.

106. Gebauer, P.; Bocek, P., Anal. Chem., 69, 1997, 1557.

107. Schutzner, W.; Fanali, S., Electrophoresis, 13, 1992, 687.

108. Schurig V.; Link, R., in Stevenson, D.; Wilson, I.D. (Edrs), Chiral Separation, Plenum Press, New York, 1988.

109. Schurig V.; Link, R.; Ossig, J., Angew. Chem. Int. Ed., 289, 1989, 194.

110. Smith, R.J.; Taylor, D.R.; Wilkins, S.M., J. Chromatogr., 697, 1995, 591.

111. Cabrera, K.; Lubda, D., J. Chromatogr. A, 666, 1994, 433.

112. Jorgenson, J.W.; Lukacs, K.D., J. Chromatogr. A, 218, 1981, 209.

113. Jorgenson, J.W.; Lukacs, K.D., Science, 222, 1983, 266.

114. Peterson, S.L.; Ballou, N., Anal. Chem., 64, 1992, 1676.

115. Ward. T.J.; Dann III, C.; Brown, A., Chirality, 8, 1996, 77.

116. Takada, Y.; Terabe, S., J. Chromatogr. A, 694, 1995, 277.

117. Nelson, W.M.; Lee, C.S., Anal. Chem., 68, 1996, 3265.

IMAGE EVALUATION TEST TARGET (QA-3)

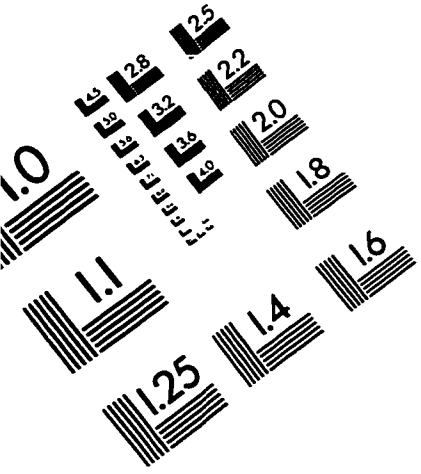

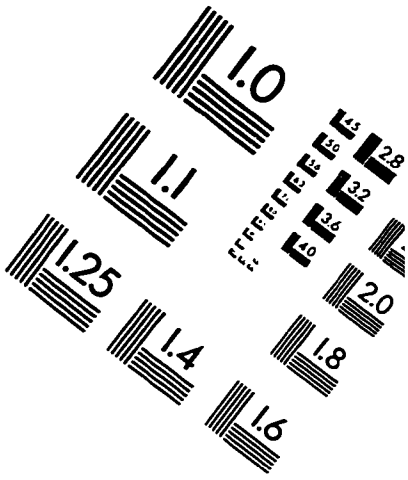

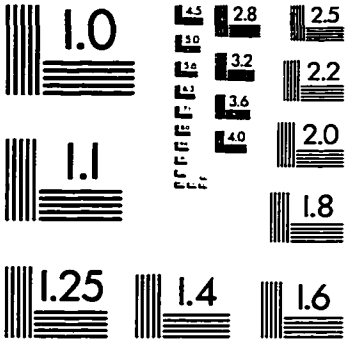

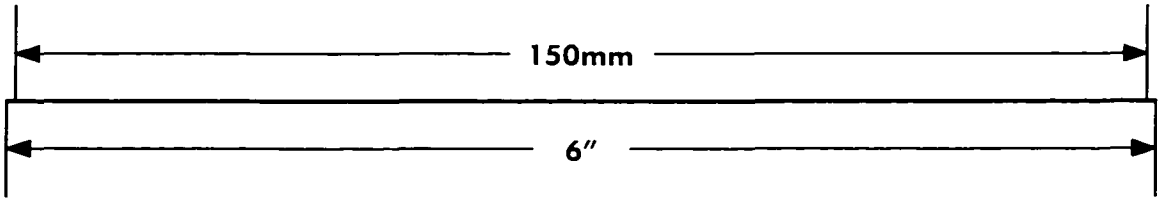

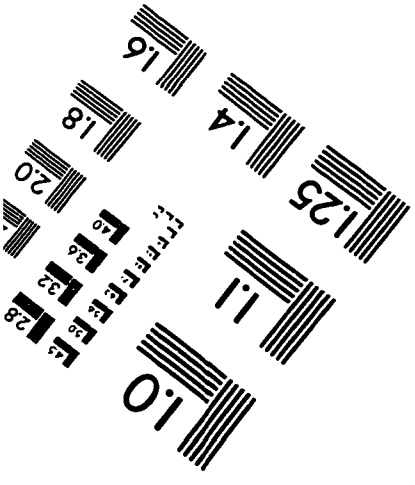

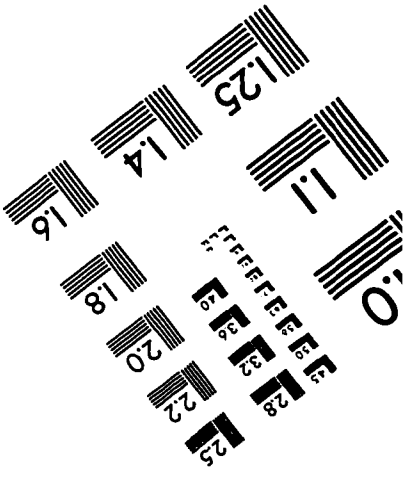

APPLIED IMAGE, Inc
1653 East Main Street
Rochester, NY 14609 USA
Phone: 716/482-0300
Fax: 716/288-5989